

FJSRL-TR-89-0004

FRANK J. SEILER RESEARCH LABORATORY

A Fundamental
Electrochemical Investigation
of Bromoaluminate and
Mixed Chloro-Bromoaluminate
Room Temperature
Molten Salt Systems

Jeffrey A. Boon,
John S. Wilkes
and John A. Lanning

DTIC
ELECTE
APR 25 1989
S D CG D

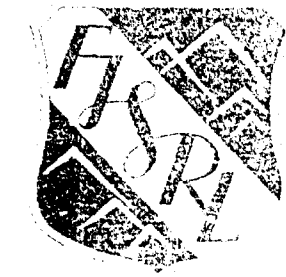
APPROVED FOR PUBLIC RELEASE;
DISTRIBUTION UNLIMITED.

March 1989

AIR FORCE SYSTEMS COMMAND

UNITED STATES AIR FORCE

089 4 25 158



AD-A207 119



FJSRL-TR-89-0004

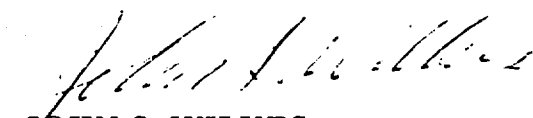
This document was prepared by the Electrochemistry Division, Directorate of Chemical Sciences, Frank J. Seiler Research Laboratory, United States Air Force Academy, CO. The reserach was conducted under Project Work Unit number 2303-F2-10, Dr John S. Wilkes was the project officer.

When US Government drawings, specifications, or other data are used for any purpose other than a definitely related government procurement operation, the government thereby incurs no responsibility nor any obligation whatsoever, and the fact that the government may have formulated, furnished or in any way supplied the said drawings, specifications or other data is not to be regarded by implication or otherwise, as in any manner licensing the holder or any other person or corporation or conveying any rights or permission to manufacture, use or sell any patented invention that may in any way be related thereto.


Inquiries concerning the technical content of this document should be addressed to the Frank J. Seiler Research Laboratory (AFSC), FJSRL/NC, USAF Academy, Colorado Springs, CO 80840-6528. Phone AC 719-472-2655.

This report has been reviewed by the Commander and is releasable to the National Technical Information Service (NTIS). At NTIS, it will be available to the general public, including foreign nations.

This technical report has been reviewed and is approved for publication.


JOHN S. WILKES
Project Scientist


STEPHEN W. LANDER, Lt Col, USAF
Director, Chemical Sciences


KENNETH E. SIEGENTHALER, Lt Col, USAF
Chief Scientist

Copies of this report should not be returned unless return is required by security considerations, contractual obligations, or notice on a specific document.

Printed in the United States of America. Qualified requestors may obtain additional copies from the Defense Documentation Center. All others should apply to:

National Technical Information Service
6285 Port Royal Road
Springfield VA 22161

Unclassified

SECURITY CLASSIFICATION OF THIS PAGE

REPORT DOCUMENTATION PAGE

Form Approved
OMB No. 0704-0188

1a. REPORT SECURITY CLASSIFICATION Unclassified			1b. RESTRICTIVE MARKINGS	
2a. SECURITY CLASSIFICATION AUTHORITY			3. DISTRIBUTION/AVAILABILITY OF REPORT Distribution unlimited Approved for public release	
2b. DECLASSIFICATION/DOWNGRADING SCHEDULE				
4. PERFORMING ORGANIZATION REPORT NUMBER(S) FJSRL-TR-89-0004			5. MONITORING ORGANIZATION REPORT NUMBER(S)	
6a. NAME OF PERFORMING ORGANIZATION Frank J. Seiler Research Lab	6b. OFFICE SYMBOL (If applicable) FJSRL/NC	7a. NAME OF MONITORING ORGANIZATION		
6c. ADDRESS (City, State, and ZIP Code) USAF Academy Colorado 80840-6528		7b. ADDRESS (City, State, and ZIP Code)		
8a. NAME OF FUNDING/SPONSORING ORGANIZATION Air Force Office of Scientific Research	8b. OFFICE SYMBOL (If applicable) AFOSR	9. PROCUREMENT INSTRUMENT IDENTIFICATION NUMBER		
8c. ADDRESS (City, State, and ZIP Code) Bldg 410 Bolling AFB DC 20332		10. SOURCE OF FUNDING NUMBERS		
		PROGRAM ELEMENT NO 61102F	PROJECT NO. 2303	TASK NO. F2
		WORK UNIT ACCESSION NO. 10		
11. TITLE (Include Security Classification) A Fundamental Electrochemical Investigation of Bromoaluminate and Mixed Chloro-Bromoaluminate Room Temperature Molten Salt Systems (Unclassified)				
12. PERSONAL AUTHOR(S) Jeffrey A. Boon, John S. Wilkes and John A. Lanning				
13a. TYPE OF REPORT Technical Report	13b. TIME COVERED FROM Jan 87 TO Aug 88	14. DATE OF REPORT (Year, Month, Day) 1989/March	15. PAGE COUNT 104	
16. SUPPLEMENTARY NOTATION				
17. COSATI CODES			18. SUBJECT TERMS (Continue on reverse if necessary and identify by block number)	
FIELD	GROUP	SUB-GROUP		
10	02		Molten Salt ; Electrochemistry ; Molten salt ;	
07	04		Bromine ; Mixed salts ; (K) ; active fuel cells ;	
			Bromoaluminate ;	
19. ABSTRACT (Continue on reverse if necessary and identify by block number)				
<p>In this project, the chemical and electrochemical properties of the bromoaluminate molten salt system were determined. With knowledge of the bromide system, the chemical and electrochemical properties of the mixed chloro-bromoaluminate molten salt system were determined, allowing further work on the applicability of these systems as electrolytes in high density electrical storage devices.</p> <p>The qualitative electrochemical behavior of the bromide and chloride systems were compared. The systems were found to behave similarly, but the basic bromide system had two oxidative processes, compared to the single process of the chloride system. The bromide system was also shown to have a smaller electrochemical voltage window. <i>Deposited</i></p> <p>The fundamental electrochemical parameters of the bromide species were determined for the basic bromide melt system. All of the parameters, except the diffusion coefficients, compared well with the literature values of the bromide species solvated in acetonitrile. The ionic properties of the molten salt system were shown to effect the (continued)</p>				
20. DISTRIBUTION/AVAILABILITY OF ABSTRACT <input checked="" type="checkbox"/> UNCLASSIFIED/UNLIMITED <input type="checkbox"/> SAME AS RPT <input type="checkbox"/> DTIC USERS			21. ABSTRACT SECURITY CLASSIFICATION Unclassified	
22a. NAME OF RESPONSIBLE INDIVIDUAL John S. Wilkes			22b. TELEPHONE (Include Area Code) (719)472-2655	22c. OFFICE SYMBOL FJSRL/NC

Unclassified

SECURITY CLASSIFICATION OF THIS PAGE

diffusion coefficients of the bromide species, and are approximately two orders of magnitude smaller in the melt than in acetonitrile. The bromine formed by the oxidation of bromide was shown to react with bromide to form tribromide. The rate and equilibrium constant of the reaction were investigated and discussed. Although neither parameter was explicitly determined, both should be considered when performing electrochemical experiments in melts containing bromide.

Finally, a preliminary investigation of the mixed melt system was performed. When MEIB or MEIC was added to a chloride or bromide melt respectively, the expected results were obtained. It was observed, however, that a minor addition of MEIB to a chloride melt dramatically increased the peak current for the oxidation of the chloride. ²⁷Al NMR showed the halides of the tetrahaloaluminate species were in exchange.

Unclassified

SECURITY CLASSIFICATION OF THIS PAGE

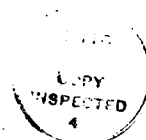
A FUNDAMENTAL ELECTROCHEMICAL INVESTIGATION OF
BROMOALUMINATE AND MIXED CHLORO-BROMOALUMINATE
ROOM TEMPERATURE MOLTEN SALT SYSTEMS

Jeffrey A. Boon and John S. Wilkes
Frank J. Seiler Research Laboratory
USAF Academy, CO 80840-6528

John A. Lanning
University of Colorado at Denver
Denver, CO 80204

March 1989

FJSRL-TR-89-0004



Accession For	
NTIS CRA&I	<input checked="checked" type="checkbox"/>
DTIC TAB	<input type="checkbox"/>
Unannounced	<input type="checkbox"/>
Justification	
By	
Distribution /	
Availability Codes	
Dist	Avail and/or Special
A-1	

ABSTRACT

In this project, the chemical and electrochemical properties of the bromoaluminate molten salt system were determined. With knowledge of the bromide system, the chemical and electrochemical properties of the mixed chloro-bromoaluminate molten salt system were determined, allowing further work on the applicability of these systems as electrolytes in high density electrical storage devices.

The qualitative electrochemical behavior of the bromide and chloride systems were compared. The systems were found to behave similarly, but the basic bromide system had two oxidative processes, compared to the single process of the chloride system. The bromide system was also shown to have a smaller electrochemical voltage window.

The fundamental electrochemical parameters of the bromide species were determined for the basic bromide melt system. All of the parameters, except the diffusion coefficients, compared well with the literature values of the bromide species solvated in acetonitrile. The ionic properties of the molten salt system were shown to effect the diffusion coefficients of the bromide species, and are approximately two orders of magnitude smaller in the melt than in acetonitrile. The bromine formed by the oxidation of bromide was shown to react with bromide to form tribromide. The rate and equilibrium constant of the reaction were investigated and discussed. Although neither parameter was explicitly determined, both should be considered when performing electrochemical experiments in melts containing bromide.

Finally, a preliminary investigation of the mixed melt system was performed. When MEIB or MEIC was added to a chloride or bromide melt respectively, the expected results were obtained. It was observed, however, that a minor addition of MEIB to a chloride melt dramatically increased the peak current for the oxidation of the chloride. ^{27}Al NMR showed the halides of the tetrahaloaluminate species were in exchange.

ACKNOWLEDGEMENTS

The authors wish to acknowledge the invaluable assistance of John L. Pflug, and Fred C. Kibler.

CONTENTS

CHAPTER	PAGE
1. INTRODUCTION	1
History of Molten Salts	1
History of Non-Aqueous Bromide Research	2
Analytical Problem Definition	3
2. CHEMICAL BACKGROUND	5
Synthesis and Purification of Reagents	5
Molten Salt Definitions	8
Synthesis of the Molten Salts	10
Physical Properties	14
Summary	19
3. ELECTROCHEMICAL BACKGROUND	21
Description of Apparatus	21
Conventions	22
Reference Electrodes	22
Working Electrodes	24
4. DETERMINATION OF FUNDAMENTAL ELECTROCHEMICAL PARAMETERS	27
CV of Selected Melt Compositions	27
Formal Electrode Potentials	37
Number of Electrons Transferred	37
Chemical Additions	56
Diffusion Coefficients	57

CHAPTER	PAGE
Heterogeneous Rate Constant	64
5. DISCUSSION OF THE CHEMICAL PARAMETERS	75
Reaction Rate	75
Equilibrium Constant	76
Summary	88
BIBLIOGRAPHY	89
APPENDIX 1	92

TABLES

Table	PAGE
1. Coefficients for the Calculation of the Density.....	16
2. Coefficients for the Calculation of the Viscosity.....	16
3. Number of Electrons Transferred by RDLSV.....	41
4. n for the Transfer of Several Different Moles of Electroactive Species and Electrons.....	45
5. Summary of the Transfer Coefficient and the Number of Electrons Transferred.....	56
6. Diffusion Coefficient as a Function of the Melt Composition.....	61
7. Diffusion Coefficient as a Function of the Melt Composition.....	63
8. Heterogeneous Rate Constant as a Function of the Sweep Rate.....	69

FIGURES

Figure	PAGE
1. ^1H NMR of a Chloride Melt Before and After Chlorination.....	4
2. ^1H NMR and CV Showing Purity of MEIB.....	7
3. UV-VIS of Tetramethylammonium Tribromide.....	9
4. Anionic Composition Diagram.....	11
5. The CVs Showing Slow Acquisition of Equilibrium When AlBr_3 is Mixed With MEIB.....	13
6. Phase Diagrams of Bromide and Chloride Melts.....	15
7. Density Diagrams of Bromide and Chloride Melts.....	17
8. Viscosity Diagrams of Bromide and Chloride Melts.....	18
9. Density Coefficients and the Natural Log of the Viscosity as a Function of the melt Composition.....	20
10. Electrochemical Conventions.....	23
11. Reference Electrodes.....	25
12. Working Electrodes.....	26
13. The CVs of Neutral Melts.....	28
14. The CVs of a Bromide Melt at Slow and Fast Scan Rates.....	29
15. The CVs of Slightly Acidic Melts.....	31
16. The CVs of Fully Acidic Melts.....	33
17. The CVs of Slightly Basic Melts.....	34
18. The Peak Potentials and Limiting Currents as a Function of the Bromide Concentration.....	35
19. The CVs of Fully Basic Melts.....	36

Figure	PAGE
20. Formal Potential as a Function of Sweep Rate.....	38
21. CV as a Function of Sweep Rate.....	39
22. Potential as a Function of $\ln[(i_d-i)/i]$	42
23. $E_p-E_{p/2}$ as a Function of Sweep Rate.....	44
24. Tafel plots of an $N = 0.4883$ Bromide Melt.....	47
25. Tafel Plots of an $N = 0.4588$ Bromide Melt.....	48
26. UV-VIS Calibration Curves.....	51
27. Coulometric Cell	52
28. UV-VIS of an Aliquot Removed from the Coulometric Cell after Passing 35 Coulombs.....	53
29. Transference Numbers of the Anionic Constituents as a Function of the Melt Composition.....	55
30. Addition of Tetramethylammonium Tribromide to a Basic Bromide Melt.....	58
31. The Limiting Current as a Function of the Square Root of the Rotation Rate.....	60
32. The Current as a Function of the Square Root of the Inverse of Time.....	62
33. Proposed Structure of a Chloride Melt.....	65
34. Peak Separation as a Function of Bromide Concentration.....	67
35. Peak Separation as a Function of ψ	68
36. The Current and the Semiintegral as a Function of Time for an $N = 0.4600$ Bromide Melt.....	71
37. The Potential as a Function of $\ln[(m_\infty-m)/m]$	72
38. The $\ln(Q)$ as a Function of the Potential.....	74
39. The CV of an $N = 0.4900$ Bromide Melt at Various Scan Rates.....	77
40. Potentiometric Titration Curves.....	79
41. Addition of MEIB to a Chloride Melt.....	82

Figure	PAGE
42. Addition of Two Dissimilar Melts.....	84
43. ^{27}Al NMR of Several Compositions of Mixed Chloride-Bromide Melts.....	86
44. ^{27}Al NMR of a Mixed Melt at Various Temperatures.....	87

CHAPTER 1

INTRODUCTION

History of Molten Salts

In August 1948, Frank H. Hurley was awarded a patent for depositing aluminum from a molten salt bath made from ethyl pyridinium bromide and aluminum chloride.¹ This bath was unique because the molten salt was a liquid at room temperature. In 1951, Hurley and Wier improved the utility of the system by showing that not only aluminum, but a range of other metals including silver, copper, nickel, lead, and iron could efficiently be plated from the bath.² For approximately the next fifteen years, the electrochemical and physical properties of the bath were studied, and the ability to plate out metals, which had been added, in the form of a salt, to the bath, was improved.

In 1968, the Air Force, through the Air Force Office of Aerospace Research (AFOAR), began to investigate the feasibility of using this type of molten salt system as an electrolyte for high density energy storage applications.³ In 1978, John C. Nardi, Charles L. Hussey, and Lowell A. King developed a series of organic substrates including methyl-, ethyl-, propyl-, and butylpyridinium chlorides and patented the use of molten salts as battery electrolytes.⁴ There are several theoretical advantages of using a molten salt instead of a conventional aqueous system as an electrolyte.

Current molten salt systems are stable liquids over a much greater temperature range than aqueous systems. Conditions demanded by the military and encountered in space vary dramatically. Currently, military specifications require equipment to operate from -40 to +74 °C. Lovell Lawrence Jr., a space systems designer for the Mercury project, indicates, the equipment on earth orbiting satellites must be able to withstand temperatures ranging from -65 to +110 degrees centigrade.⁵ It is desirable to find a battery system which is operable in either extreme. Depending on the composition of the molten salt, liquid ranges from -90 to over +200 °C are possible. Compared to aqueous systems, which are liquid from approximately -20 to +120 °C, it is apparent the molten salt systems would be more appropriate than aqueous systems for space and military applications.

Molten salt systems are comprised totally of ionic species. Theoretically, all of the ions in a melt are capable of carrying a portion of the current in a cell. In aqueous systems, the water molecules, which are incapable of carrying current, are present only to solvate the ions which do carry charge. The weight of the water is, therefore, non-productive, and decreases the energy density of the cell. Since the molten salt is completely ionic, it is theoretically capable of obtaining a higher energy density than aqueous systems, making smaller and lighter cells possible. This will, in turn, allow for the production

of smaller and lighter vehicles, which are inherently more energy efficient.

Because water passivates aluminum electrodes, thereby decreasing the efficiency of the electrode, aluminum electrodes are impractical for use in aqueous battery systems. Lead is the principal battery electrode material used in aqueous battery systems today. Since the molten salt systems do not show a tendency to passivate aluminum electrodes, the molten salt systems allow for the use of an aluminum couple at an aluminum electrode. Changing to an aluminum electrode system will offer dramatic weight savings, with all of the inherent benefits explained above.

The use of aluminum as an electrode material not only increases the energy density of a battery by decreasing the weight of the cell, but also by increasing the theoretical power stored in the cell. The standard electrode potential of aluminum is higher than that of lead. This means the power inherent in an aluminum couple is greater than the power of a lead couple, so the energy density of a cell using an aluminum electrode will be greater than one using a lead electrode. By the same argument, the power available from an aluminum couple is higher than that available from a zinc couple, which is typically used in "dry cell" energy storage systems.

In 1981 the organic constituent of the molten salt was changed from the substituted pyridinium bromide to a disubstituted imidazolium chloride.⁶ Many of these systems were characterized, and it was found that melts made from 1-methyl-3-ethylimidazolium chloride (MEIC) and aluminum chloride had the characteristics most suitable for use as an electrolyte.⁷

History of Non-Aqueous Bromide Research

In the late 1950s, Alexander I. Popov and David H. Geske, published a series of papers dealing with the electrochemistry of halogen and mixed halogen systems. The sixteenth in this series investigated the electrochemistry of bromide and mixed iodo-, and chloro-bromide systems.⁸ Since that time, the use of electrochemistry, as a means of investigating non-aqueous bromide systems, has received considerable attention.

It is possible to monitor the progress of bromination reactions in organic chemistry by following the appearance or disappearance of the bromide oxidation wave. Desbene-Monvernay et al.⁹ used electrochemistry to observe the progress of the bromination of styrene with tribromide. The concentration of bromide was followed by rotating disk voltammetry. The limiting current of a species is proportional to the concentration of the species. As the concentration of the bromide decreased, the limiting currents also decreased until all of the bromide was consumed.

The fundamental work of Popov and Geske has also helped to illuminate the electrochemistry occurring in the Zinc-Bromine battery systems. In 1987 Adanuvor et al. studied the effects of the reaction of bromine with bromide to form tribromide on the electrochemical behavior of a bromine electrode.¹⁰ Mastragostino et al.¹¹ and Daniel J. Eustace¹² have studied the effect of complexing the bromine on the electrochemistry of a Zinc-Bromine battery.

Analytical Problem Definition

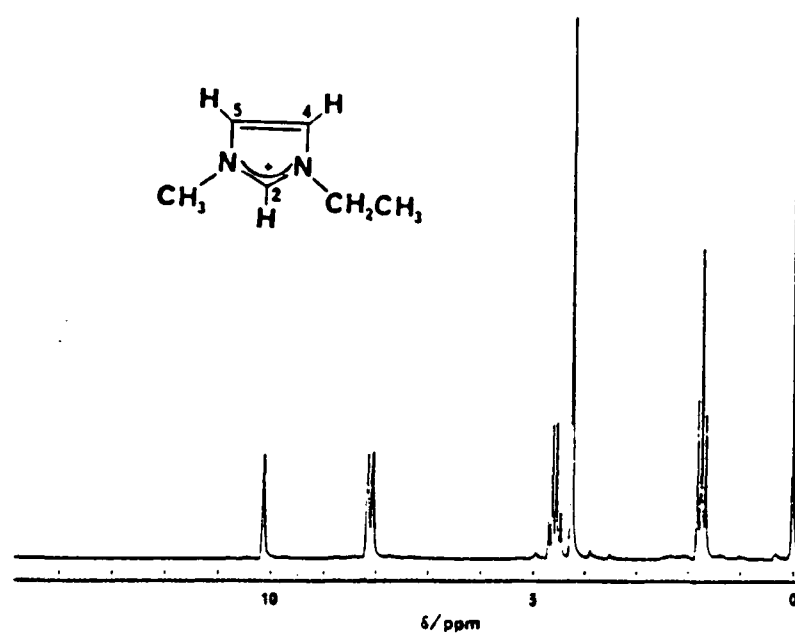
The most promising battery system to date, employing a molten salt electrolyte, has been the use of a reversible aluminum electrode as the cathode and a reversible chlorine electrode as the anode.¹³ Recent work at Frank J. Seiler Research Labs shows that molten salts made from MEIC and aluminum chloride tend to chlorinate the imidazolium cation in the presence of chlorine¹⁴, according to the reaction:

Figure 1 shows the proton NMR of an MEIC-aluminum chloride melt before and after bubbling chlorine through it at elevated temperatures for approximately 72 hours. The pair of singlets at approximately 8 ppm, which are due to the protons attached to the number 4 and 5 carbons, disappears as a result of their being exchanged for chlorines. A singlet appears at approximately 13 ppm which is due to the HCl formed during the chlorination reaction. The singlet at 10 ppm can be observed to break up into a series of three singlets, corresponding to zero, one, and two chlorine substitutions. This series of three singlets coalesces back into a singlet after the 4 and 5 positions are completely chlorinated.

The absorbances due to the two methyls and the ethyl protons are split into higher multiplets upon chlorination. Through integration, it is apparent the peak due to the proton in the 2 position (at 10 ppm) is less than half of its original intensity. This indicates the imidazolium ring is also chlorinating at the 2 position, albeit at a much slower rate.

The tendency of the imidazolium ring to chlorinate makes the use of the chlorine-chloride couple, in an MEIC-AlCl₃ melt electrolyte, impractical. Previous work at Seiler indicates the melts show no tendency towards bromination.¹⁴ The molten salt formed by combining 1-methyl-3-ethylimidazolium bromide (MEIB) with aluminum bromide (AlBr₃), though, tends to decay, through a process involving the autooxidation of bromide to tribromide, after several days. For these reasons it was suggested the most promising system might be to solvate bromine (or bromide) in an MEIC-AlCl₃ melt. To understand this system, the electrochemistry of the pure bromide system must be investigated. This information will help to understand the electrochemistry occurring in the mixed chloro-bromoaluminate system and will pave the way for future studies on the applicability of these systems as energy storage devices.

A)



B)

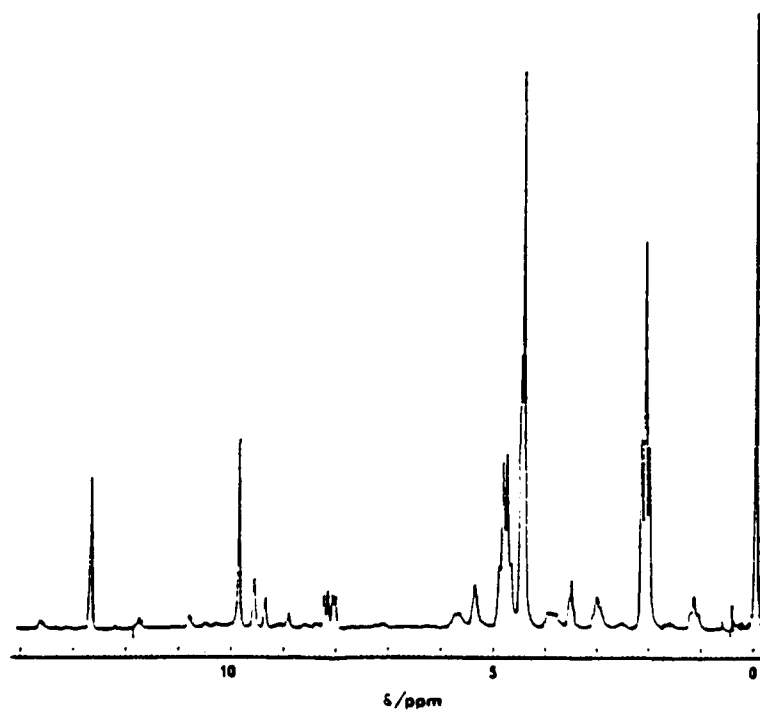


Figure 1. ¹H NMR of an N = 0.333 chloride melt A) before, and B) after chlorination.

CHAPTER 2

CHEMICAL BACKGROUND

Synthesis and Purification of Starting Materials

Acetonitrile. All of the acetonitrile (Fisher, Certified Reagent) used in these experiments was refluxed over anhydrous phosphorous pentoxide for at least two days before use. Nitrogen, which had been dried by passing through a "Dreirite" anhydrous calcium sulfate column, was continually flushed over the top of the still. The acetonitrile was removed at the time of use.

1-methylimidazole. The 1-methylimidazole (Fluka, Puriss) was vacuum refluxed over anhydrous barium oxide for at least two days before collecting by distillation.

1-methyl-3-ethylimidazolium bromide (MEIB). The 1-methyl-3-ethylimidazolium bromide was formed by the substitution reaction:

220 mL of 1-methylimidazole were combined with 250 mL of acetonitrile and 250 mL of ethyl bromide (J.T. Baker "Baker Analyzed") in a 2 liter round bottom flask. A Teflon stir bar was added to the reaction vessel and a condenser with a drying tube at the top was put on the reaction flask. The mixture was cooled with an ice bath for approximately 8 hours, to slow the reaction down, and then refluxed for four days while stirring.

500 mL of ethyl acetate (J.T. Baker, "Baker Analyzed" HPLC grade) were added to the reaction mixture and the flask was shaken continuously until all of the MEIB was recrystallized. The mother liquor was forced off through a glass tube by applying a pressure of nitrogen which had been dried with a "Dreirite" column. The MEIB was dissolved in 250 mL of acetonitrile and recrystallized with ethyl acetate, as above, for a total of five times. The resulting MEIB was washed with ethyl acetate a final time and dried under high vacuum for approximately 12 hours. The reaction flask was taken into the dry box, and the MEIB was transferred

to a brown glass bottle which had been dried for at least 12 hours and put into the dry box while still hot.

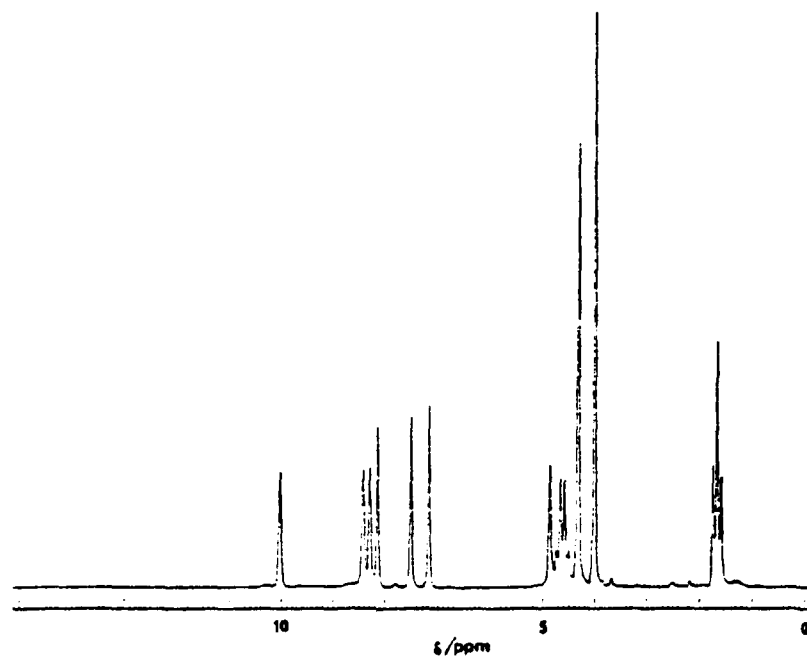
Since the recrystallization scheme does not remove any unreacted 1-methylimidazole, care was taken to allow the reaction to go to completion. The purity of the MEIB was determined by two methods. Figure 2 shows the ^1H NMR of a solution containing approximately equal parts of MEIB and 1-methylimidazole. The singlet at 3.7 ppm, the doublet centered at 7.0 ppm, and the singlet at 7.6 ppm are due to the 1-methylimidazole. The presence of protonic impurity (typically due to insufficient care being taken during the preparation of the MEIB, or through the absorption of water from the atmosphere of the dry box), in a melt made with the MEIB, was determined electrochemically. The cyclic voltammogram (CV) of a neutral or basic melt, which contained any protonic impurity, would show an irreversible reduction wave at approximately +0.100 V on a platinum electrode, when referenced against a chloride reference cell. The CV of a neutral bromide melt, containing protonic impurity, is shown in Figure 2. If there was any question whether the wave was due to the reduction of the proton, a CV of the same melt was run on a glassy carbon working electrode. Since a very high over potential is required to reduce protons at a glassy carbon electrode, the wave would disappear. Contaminated MEIC was removed from the dry box and recrystallized as described above.

1-methyl-3-ethylimidazolium chloride (MEIC). The MEIC was prepared by a modification of the method described by Levisky and Wilkes.¹⁵ 220 mL of 1-methylimidazole were combined with 200 mL of acetonitrile in a 750 mL pressure vessel. 250 mL of ethyl chloride were added to the solution by passing the ethyl chloride gas through a dry ice-isopropyl alcohol gas condenser. A stir bar was added to the reaction mixture and the vessel was sealed with a green neoprene stopper which was clamped in with a stopcock puller. The reaction mixture was warmed very gently on a hot plate while stirring. A blast shield was immediately placed around the reaction vessel and caution was exercised at all times due to the relatively high pressures involved. The reaction was allowed to proceed for two weeks. The reaction flask was removed from the hot plate, placed in an ice bath, and allowed to cool for approximately half an hour. The stopper was carefully removed from the reaction vessel, and the reaction mixture was transferred to a 2 liter round bottom flask, while streaming dry nitrogen over the mixture. The MEIC was purified and stored in the same method as described above for MEIB.

Aluminum bromide. The aluminum bromide was purified by distillation. A thirteen inch long, thick wall, glass tube, with a one inch inside diameter, was sealed on one end and a male 19/20 ground glass joint was put onto the other. Ten, three inch, aluminum wires, 1 mm in diameter, (Alfa Products, 99.999%) were put in the tube. 100 grams of aluminum bromide (Alpha, 98%) and 0.5 gram of sodium bromide were added to the tube. A gas inlet valve connected to a female 19/20 ground glass joint was used to seal the tube. The tube assembly was removed from the dry box and a vacuum was applied for fifteen minutes. The tube was flame sealed while still under a vacuum and annealed in an annealing furnace.

The cooled tube was hung vertically in a tube furnace which had a temperature gradient with the bottom of the furnace at 220 °C and the top at room temperature. All of the aluminum bromide was allowed to become

A)



B)

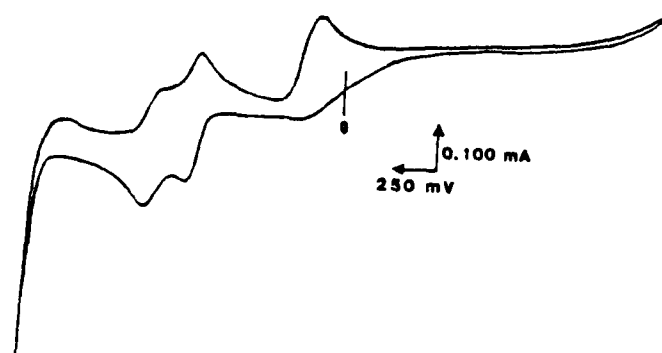


Figure 2. A) ^1H NMR of MEIB, and B) CV of an $N = 0.500$ bromide melt.

and remain molten for six hours. The tube was withdrawn from the tube furnace at a rate of approximately half an inch a week. The purified aluminum bromide condensed at the top of the tube, while the impurities remained at the bottom, as the tube was withdrawn.

The cooled tube was wrapped with aluminum foil and strapping tape in order to minimize the dissociation caused by ultraviolet light. When needed, the tubes were brought into the dry box, all of the tape and aluminum foil was removed, the tubes were scored on each end, wrapped in a cloth towel, and broken open. The aluminum bromide was collected and stored in a brown glass bottle which had been dried in the drying oven for 12 hours and transferred to the dry box while still hot.

During the later stages of the research, the aluminum bromide was purified by vacuum sublimation. The sublimation was done outside of the dry box, and after completion, the sublimator was brought into the dry box, where the purified aluminum bromide was collected. The aluminum bromide was sublimed three times before use. No discernible difference was observed between the aluminum bromide purified by distillation and that purified by sublimation.

Aluminum chloride. Aluminum chloride (Fluka, Puriss) was purified and stored as the aluminum bromide was above, except sodium chloride was substituted for sodium bromide, and the sealed tube was withdrawn from the tube furnace at a rate of approximately an inch an hour. The tube was not wrapped with aluminum foil and strapping tape, since the aluminum chloride showed no tendency to photodissociate.

Tetramethylammonium bromide. The tetramethylammonium bromide (J.T. Baker, Reagent grade) was recrystallized from 95% ethyl alcohol three times.

Tetramethylammonium tribromide. The tetramethylammonium tribromide was prepared by the method described by Chattaway and Hoyle.¹⁶ Nine grams of tetramethylammonium bromide were dissolved in 60 mL of 95% ethyl alcohol. Three mL (9.2 grams) of bromine were added to the solution, and the mixture was boiled down to a volume of approximately 25 mL. The mixture was allowed to cool, and the product was collected by vacuum filtration. The orange needle-like crystals were recrystallized from 25 mL of ethyl alcohol which had been saturated with bromine. This recrystallization procedure was repeated a total of three times. The melting point of the purified product was 119-120 °C, which compares well with the literature value of 118-119 °C.¹⁷ The resulting product was analyzed by spectrophotometry.

The UV-VIS spectra of the reaction product, bromine, and the tetramethylammonium bromide, as well as a mixture of bromine and the reaction product, were taken with methylene chloride as a solvent. All of the solutions were prepared immediately before the spectra were taken to minimize any dissociation which might occur. These spectra are shown in Figure 3. The spectra of the product compared well with the spectra attributed by Buckles et al. to the tribromide anion.¹⁸

Molten Salt Definitions

When the MEIB and the $AlBr_3$ are mixed, a set of dissolution reactions occur. As aluminum bromide is added to the MEIB, the MEIB is solvated

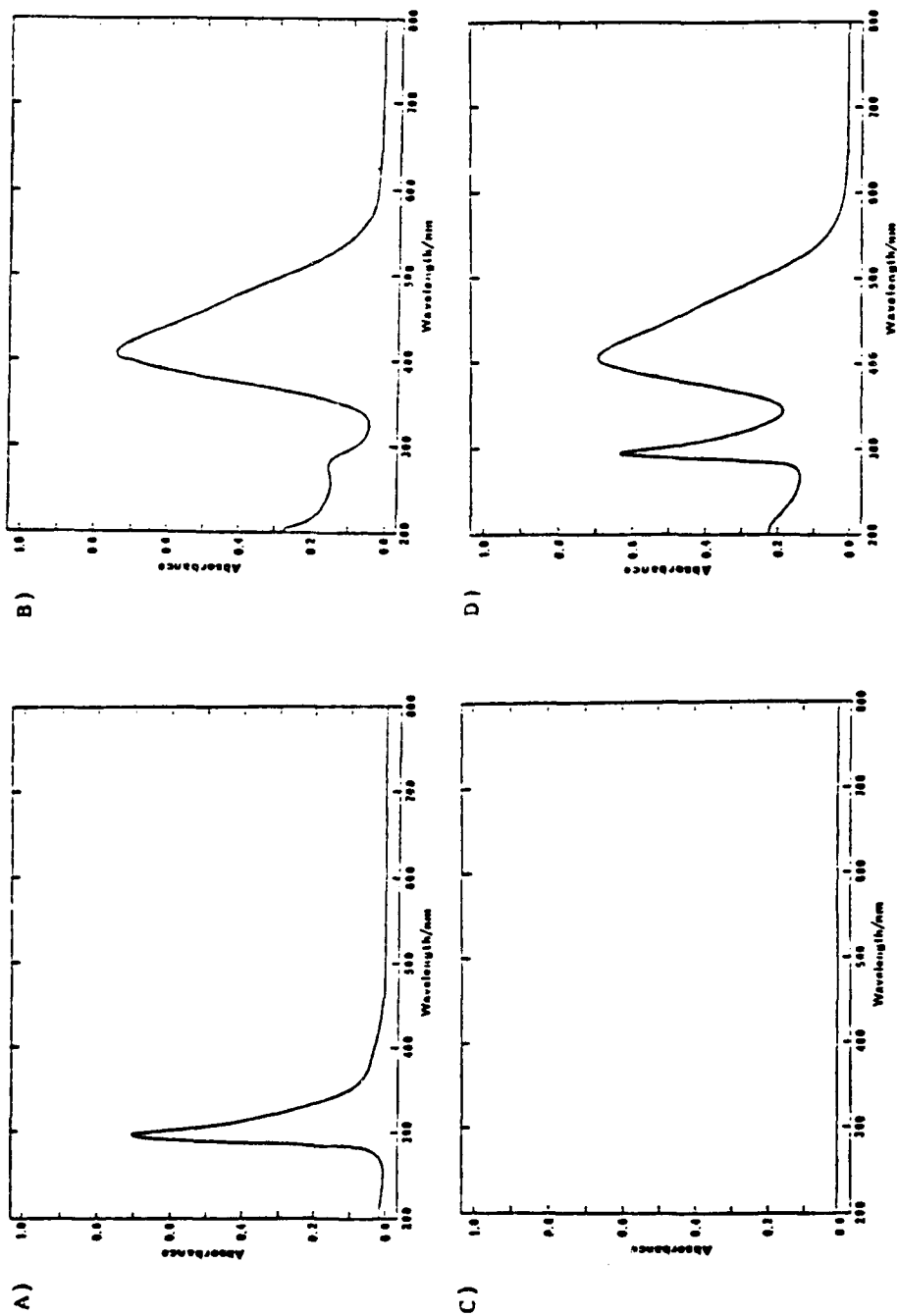
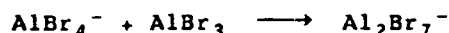


Figure 3. UV-VIS spectra of A) reaction product, B) bromine, C) tetramethyammonium bromide, and D) bromine plus the reaction product.

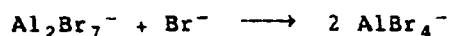
and the reaction:



occurs. As more aluminum bromide is added, all of the bromide is consumed, and the aluminum bromide begins to react with the tetrabromoaluminate by the reaction:



No unreacted aluminum bromide is present in any melt composition, so a term, called the apparent mole fraction of aluminum bromide (N), is introduced. The acid-base properties of the system are usually described by the reaction:



In a method completely analogous to the chloride system,¹⁹ where the anionic make up of the melt was calculated assuming the association reactions listed above proceed completely to the right. Figure 4 shows the anionic composition of the melt as a function of the apparent mole fraction of aluminum bromide. For the chloride system, the equilibrium constant of the acid-base reaction was found to be approximately 10^{16} ¹³, which suggests the previous assumption is justified. Although the formation constant of the AlBr_4^- was not determined in this work, bromoaluminate molten salts will be assumed to behave in a similar manner.

There are three compositions of particular interest in the working range ($0.33 \leq N \leq 0.66$) of a melt made from MEIB and aluminum bromide. At an apparent mole fraction equal to 0.33, the bromide and the tetrabromoaluminate are present in equal concentrations. At an apparent mole fraction equal to 0.50 the only anionic species present is the tetrabromoaluminate. At $N = 0.66$ the only anionic species present is the heptabromoaluminate. This allows for the selection of the species present and their concentration in any melt, by changing the amount of the inorganic salt added to the melt.

Two distinct regions, in the working range of the melts, are apparent from the composition diagram of the MEIB-aluminum bromide molten salt system, shown in Figure 4. Any melt with an apparent mole fraction of aluminum bromide less than 0.50 is called a "basic" melt. In these melts, the bromide ion acts as a Lewis base. Any melt with an apparent mole fraction of aluminum bromide greater than 0.50 is said to be an "acidic" melt, because the heptabromoaluminate acts as a Lewis acid. A melt with an apparent mole fraction equal to 0.50 is called a "neutral" melt because it lacks the Lewis base, bromide, and the Lewis acid, heptabromoaluminate.

In the pure melt systems, a melt made from MEIB and aluminum bromide is called a bromide melt. A melt made from aluminum chloride and MEIC is called a chloride melt. In the mixed melt systems, all of the fractions will be referenced to the amount of the chloride melt present.

Synthesis of the Molten Salts

A melt is made by slowly adding the appropriate amount of the inorganic salt to a known amount of the organic salt. Since the

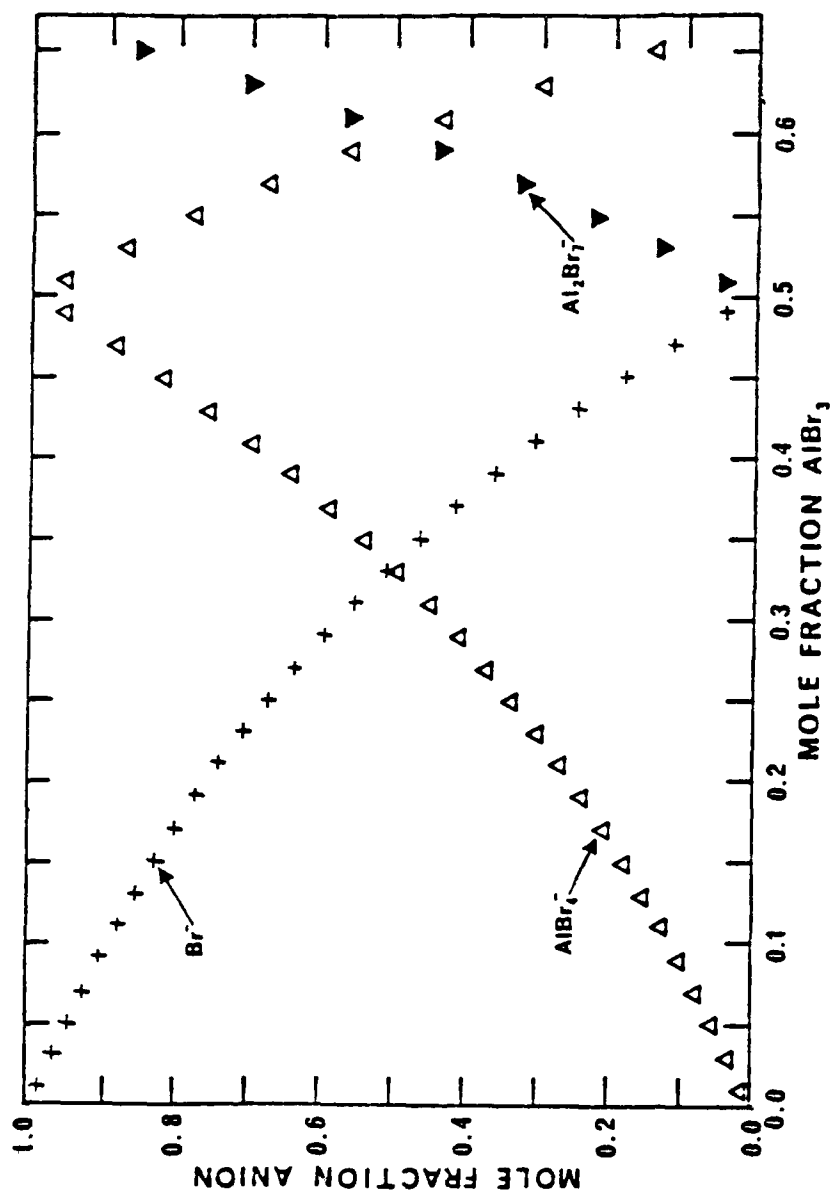


Figure 4. Anionic composition diagram of the bromide melt system.

resulting dissolution reactions are highly exothermic, approximately 0.20 gram increments of the inorganic salt were added, and the mixture was allowed to cool between additions.

It was found that, unlike the chloride system, the dissolution reactions in the bromide melt are appreciably slow. Figure 5A shows the cyclic voltammogram which resulted from a bromide melt which was "titrated" to neutrality in a method analogous to that described by Lipsztajn and Osteryoung.²⁰ The CV was taken approximately thirty minutes after the initial addition of aluminum bromide to the MEIB. Figure 5B shows the CV of the same melt 20 minutes later. The cyclic voltammogram of the melt which resulted from adding enough MEIB to this supposedly neutral bromide melt to theoretically result in a melt with an apparent aluminum bromide mole fraction of 0.490 is shown in Figure 5C. This CV was taken approximately 25 minutes after the initial CV was taken. The melt was allowed to stand for twenty hours and another CV was taken. This CV is shown in Figure 5D. The melt was "retitrated" to neutrality and enough MEIB was again added to the melt to obtain an $N = 0.490$ melt. The CV of this resulting melt is shown in Figure 5E.

The reduction wave, which appears in Figure 5B, continued to grow until it became the cathodic limit of the melt. The decrease in the electrochemical voltage window, and the decrease in the magnitude of the oxidation waves as time progressed indicate a slow acquisition of equilibrium conditions. This indicates either the reaction:



or the reaction:



must be appreciably slow. No attempt was made to quantify the time required to reach equilibrium, other than to insure equilibrium was reached by allowing the melt to stand for twenty hours.

Bromide melts were also observed to degrade over time. Several hours after a bromide melt was made, it started to turn a distinctive brown color, commonly associated with bromine or tribromide species. The color became darker as time progressed, and after several days, the melt appeared black. No electrochemical consequence of the color was observed, but to insure knowledge of the system, the melts were not used after severe discoloration occurred.

Because of the slow kinetics and the problems with degradation of the melts, a routine was developed for working with the bromide melts. Melts were made as close to $N = 0.50$ as possible without "titration", and allowed to remain at 60 °C overnight. The melts were "titrated" to neutrality, as determined by cyclic voltammetry, and the amount of MEIB or AlBr_3 needed to make the desired melt was added to the neutral melt. The relatively small additions of MEIB and AlBr_3 , needed to make the desired melt composition, did not make a noticeable difference in the CVs over time.

The melts were used for no more than three days before being discarded. The discarded melts were destroyed by hydrolysis. The melts were removed from the dry box and slowly added to an excess amount of ice. Once the melt was completely hydrolyzed, it was washed down the drain.

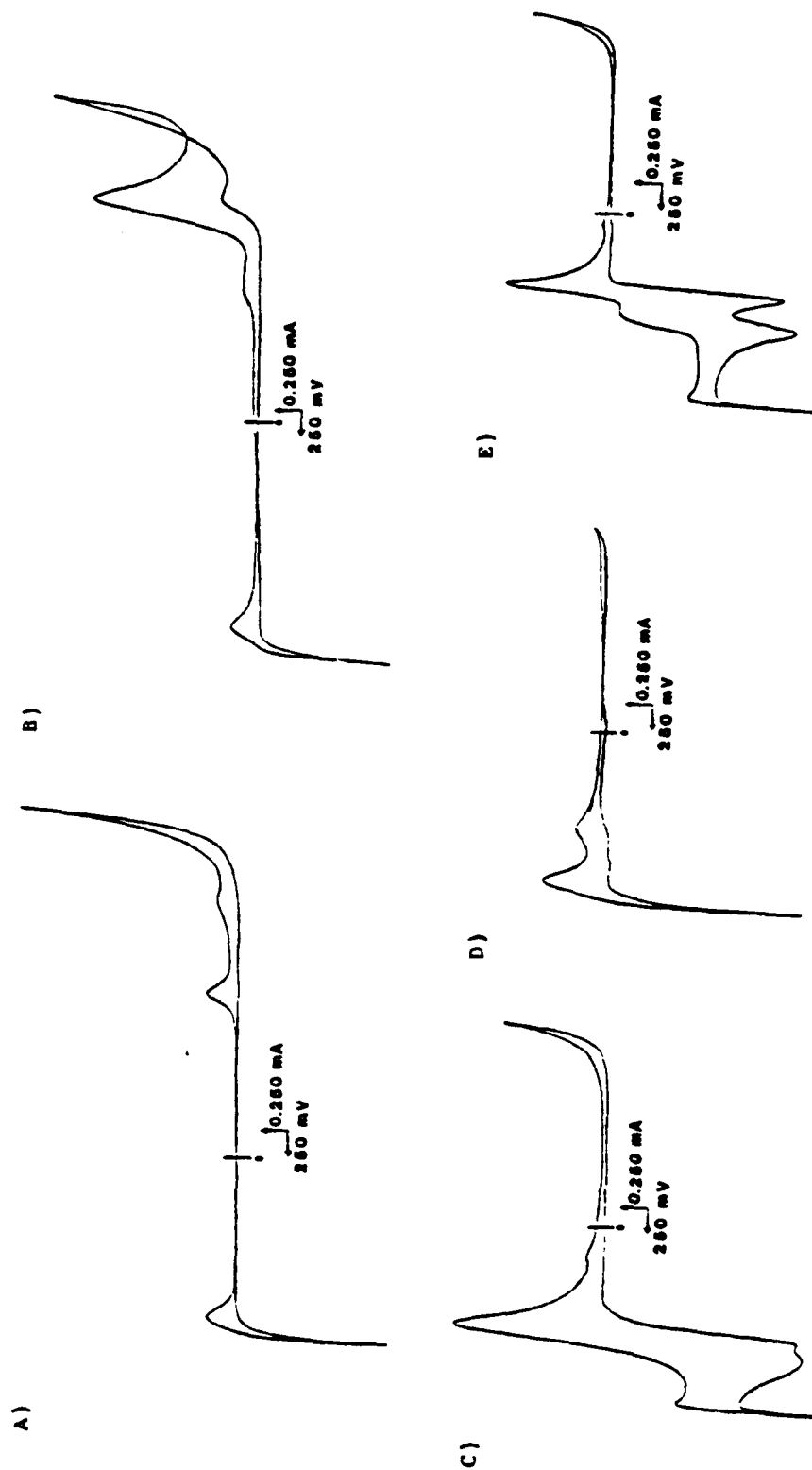


Figure 5. CV of an A) $N = 0.500$ bromide melt at $T = 10$ min., B) at $T = 15$ min., C) $N = 0.480$ bromide melt at $T = 25$ min., D) at $T = 24$ hrs., and E) $N = 0.480$ bromide melt after 24 hrs.

Physical Properties

The electrochemical properties of a species are seriously affected by the physical properties of the material in which it is solvated. The rate at which ions are transported to the electrode double layer affects the observed cell currents and potentials. The rate a species diffuses through a solvent is affected by the viscosity of the solvent. Also, the densities were required to calculate the concentrations of the species.

The physical properties of the chloride molten salt system were determined by Fannin et al.²¹, and Hussey et al. determined the physical properties of the bromide system.^{22, 23} The phase diagrams, densities, and viscosities of the two systems are presented and compared below.

Phase diagrams. The phase diagrams of the chloride and bromide melt systems are shown in Figure 6. Although the bromide system consistently melts 20 - 30 degrees higher than the chloride system, it is still properly called a room temperature molten salt. Both, the bromide and chloride molten salt systems show a distinct dystectic point at $N = 0.500$. Both systems also have several compositions which became glasses instead of freezing. These glassy transitions were reproducible and were never made to freeze.

Densities. The densities of several chloride and bromide melt compositions are shown in Figure 7 as a function of temperature. The densities of the bromide melts were fitted to the equation:

$$\rho = a + bT \quad (1)$$

where T is the temperature in degrees Celsius. The coefficients, a and b , were expanded to the form:

$$a = a_0 + a_1N + a_2N^2 + a_3N^3 \quad (2)$$

and:

$$b = b_0 + b_1N + b_2N^2 + b_3N^3 \quad (3)$$

The values for the coefficients are given in Table 1.

Viscosities. The viscosities of several melt compositions as a function of inverse temperature are shown in Figure 8. Neither the chloride nor the bromide systems exhibited Arrhenius behavior, but the kinematic viscosity of both systems followed the Vogel-Tammann-Fulcher (VTF) relationship. The kinematic viscosities of the bromide system were fitted to the equation:

$$\ln \eta = K/(T-T_0) + 1/2 \ln T + \ln A \quad (4)$$

where T is the absolute temperature. The parameters K , T_0 , and A were fitted by linear regression to the equation:

$$f = c_0 + c_1N + c_2N^2 + c_3N^3 \quad (5)$$

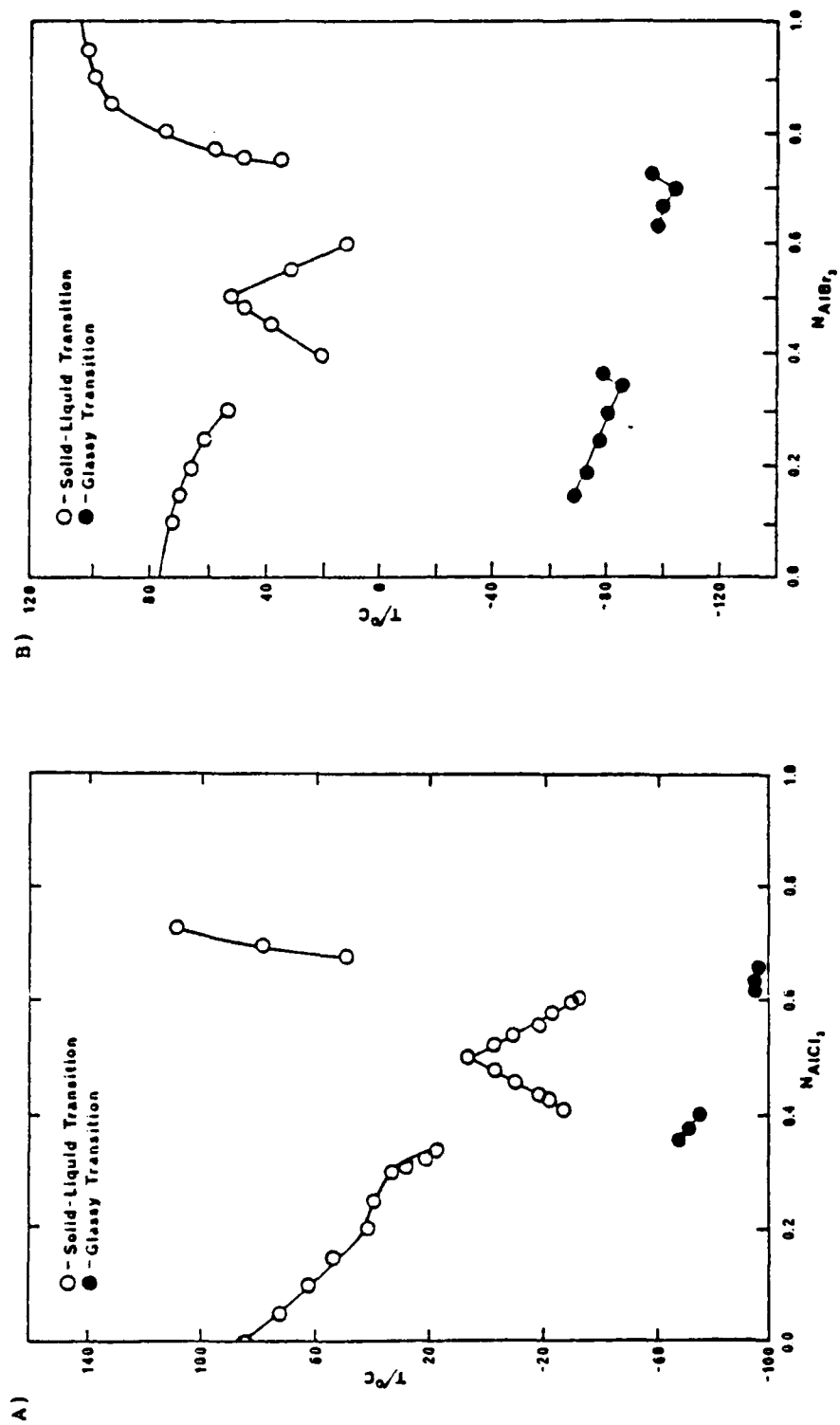


Figure 6. Phase diagrams of A) the chloride melt system, and B) the bromide melt system.

TABLE 1 - Density Coefficients for Equations 1-3.

$$0.30 \leq N \leq 0.50$$

x	a _x	b _x
0	1.0588	1.2907 x 10 ⁻³
1	3.8594	-1.0448 x 10 ⁻²
2	-2.8945	1.1519 x 10 ⁻²
3	0.0000	0.0000

$$0.50 < N \leq 0.75$$

x	a _x	b _x
0	-5.8410	1.7946 x 10 ⁻²
1	3.7009 x 10 ¹	-9.0089 x 10 ⁻²
2	-5.6829 x 10 ¹	1.4121 x 10 ⁻¹
3	3.0474 x 10 ¹	-7.4099 x 10 ⁻²

Table 2- Viscosity Coefficients for Equations 4-6.

$$0.35 \leq N \leq 0.50$$

	c ₀	c ₁	c ₂	c ₃
T ₀	-4.0191 x 10 ¹	1.9867 x 10 ³	-4.5874 x 10 ³	2.4562 x 10 ³
K	3.3582 x 10 ³	-2.0888 x 10 ⁴	4.8630 x 10 ⁴	-3.3051 x 10 ⁴
ln A	-2.8631 x 10 ¹	1.8526 x 10 ²	-4.4919 x 10 ²	3.4788 x 10 ²

$$0.50 < N \leq 0.75$$

	c ₀	c ₁	c ₃
T ₀	-8.8020 x 10 ²	1.3485 x 10 ³	-4.2335 x 10 ²
K	9.3588 x 10 ³	-1.1072 x 10 ⁴	3.4117 x 10 ³
ln A	-3.2068 x 10 ¹	3.5633 x 10 ¹	-1.0983 x 10 ¹

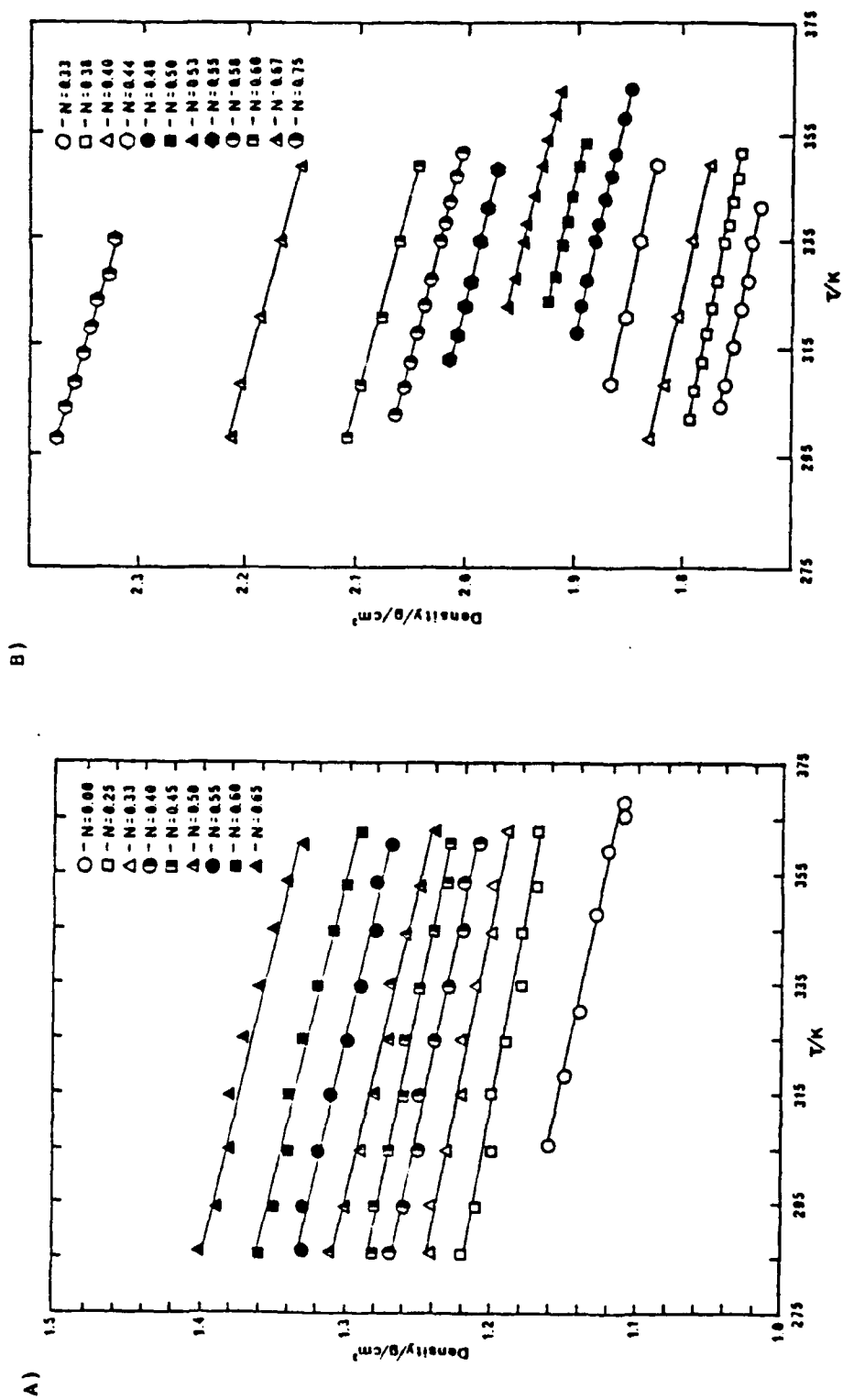


Figure 7. Density diagrams of A) the chloride melt system, and B) the bromide melt system.

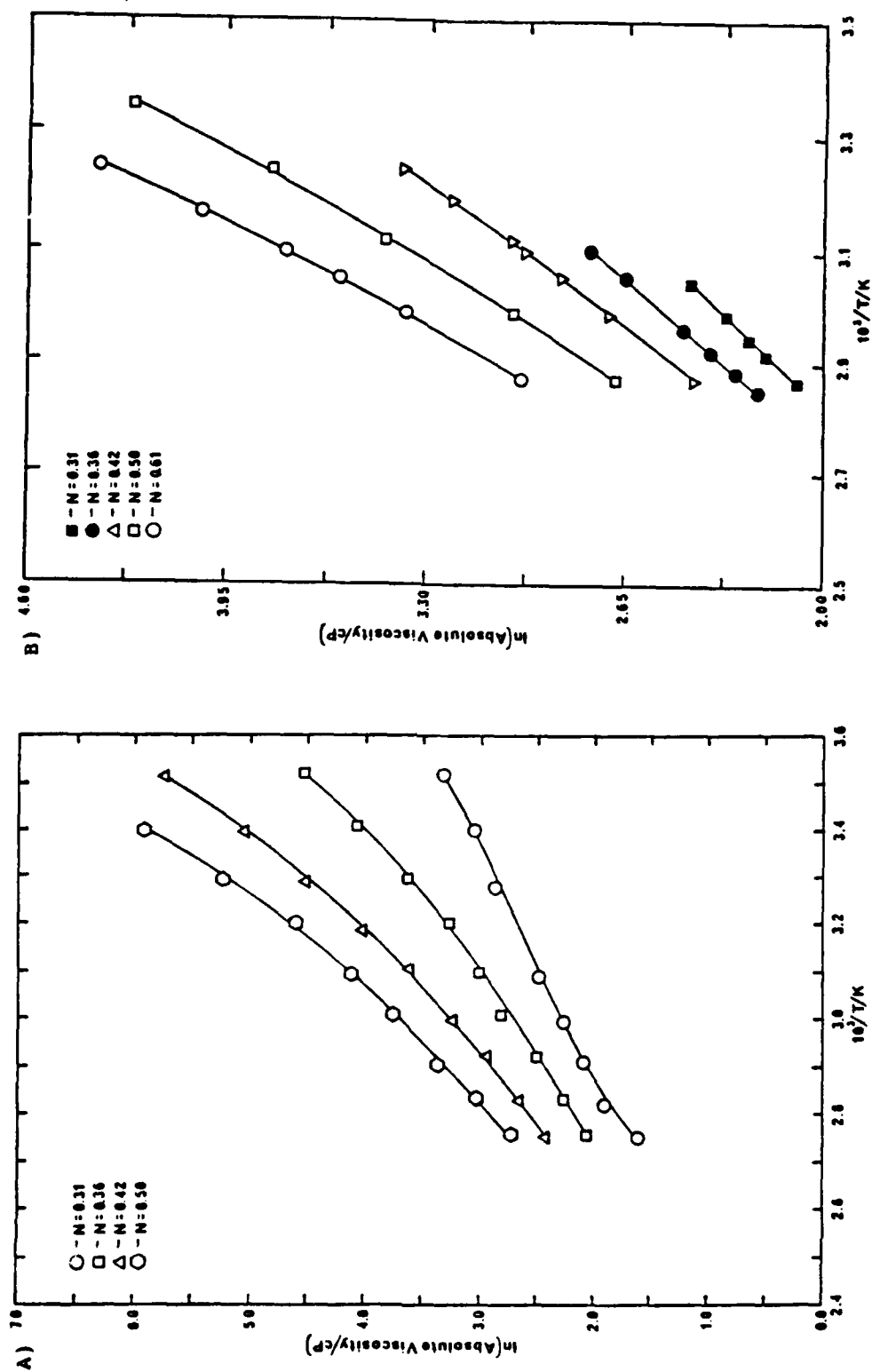


Figure 8. Viscosity diagrams of A) the chloride melt system, and B) the bromide melt system.

for melts with compositions greater than 0.30 and less than or equal to 0.50, and:

$$f = c_0 + c_1/N + c_2/N^2 \quad (6)$$

for melts with compositions between 0.50 and 0.75. The values of the coefficients are given in Table 2.

Summary. In the chloroaluminate molten salt system, the typical working composition range is dictated by where the system forms a homogeneous liquid at room temperature ($0.333 \leq N \leq 0.667$). Since the bromoaluminate system requires only a slightly elevated temperature to become liquid throughout the same range, the same range will be studied.

As mentioned in the discussion of the anionic composition diagram, the working range of the molten salts can be divided into three unique systems. These regions have been termed "basic", "neutral", and "acidic" depending on the composition of the melt.

The non-Arrhenius behavior exhibited by the viscosities is an indication of the nonideality of the molten salt systems. The nonideality affects, and must be taken into account when determining, many of the electrochemical properties of the molten salt system.

Figure 9A shows a plot of the density coefficients as a function of the composition of the melt. Figure 9B shows a plot of the natural log of the absolute viscosity as a function of the melt composition. The phase diagram, as well as the plots shown in Figure 9, shows a distinct break at $N = 0.500$ giving support to the concept of unique physical, and thus electrochemical, behavior in each region. Subsequent analysis of the bromide melts will take advantage of this behavior.

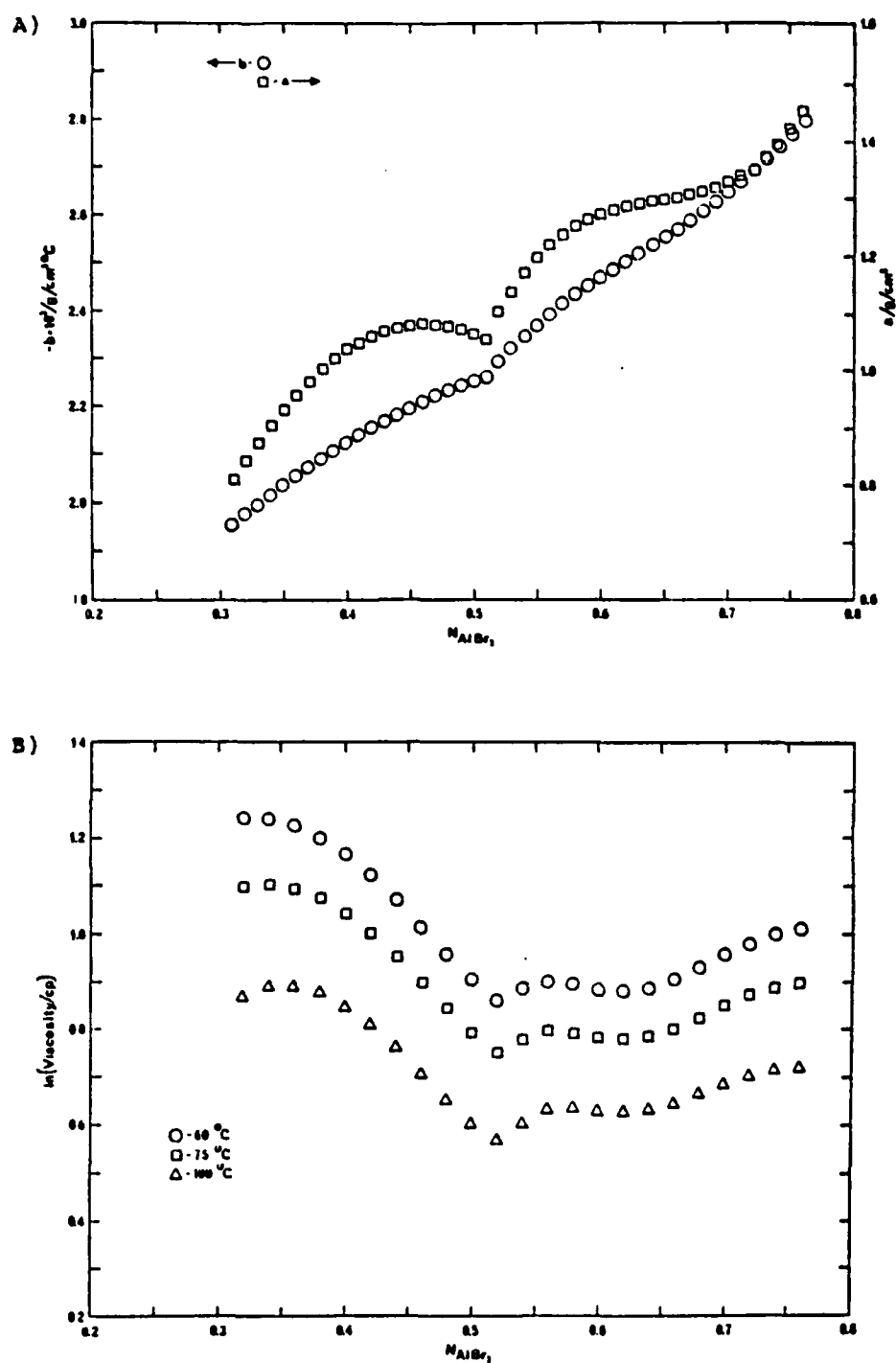


Figure 9. The A) Density coefficients, and B) Viscosity at several temperatures, as a function of the bromide melt composition.

CHAPTER 3

ELECTROCHEMICAL BACKGROUND

Description of Apparatus

All of the electrochemical experiments were performed in a Vacuum Atmospheres dry box filled with an atmosphere of ultra high purity (UHP) grade helium. The atmosphere in the dry box had a combined water, oxygen concentration of no more than 10 ppm. Oxygen and water were continually scavenged by passing the atmosphere through a commercial drying train.

The drying train was filled with molecular sieves to absorb the water, and the oxygen was reduced onto a bed of copper impregnated ceramic beads called "Ridox". The drying train was regenerated by heating and passing a mixture of 90% nitrogen and 10% hydrogen through it. The absorbed water is driven off by the heat, and the reduced oxygen combines with the hydrogen to form water, which is also driven off. The dry box had a set of two dry trains one of which was either being regenerated or was ready for use while the other was being used.

The drying trains are supposed to last indefinitely, but during the course of the experiments it was found the quality of the atmosphere inside the boxes degraded faster than expected. The use of bromine (or bromide, which will auto-oxidize to form bromine) poisons the molecular sieves and the Ridox in the drying train. When this point is reached, the only course of action is to change out the molecular sieves and the Ridox. Once this was discovered, care was taken to minimize the use of free bromine in the boxes. The Vacuum Atmospheres manual suggests placing a condenser in the circulation line in front of the drying trains. This has not been done yet so no comment on the effects of this idea can be made.

A light bulb which had a hole punched in the glass envelope was used to indicate the quality of the atmosphere inside the dry box. Any time the light bulb filament lasted for less than a week, the dry box was switched over to the unused dry train and the old dry train was regenerated. The identity of the contaminant in the dry box could be roughly determined by the color of the residue left on the glass of the bulb when it burned out. A bluish film results from a high water concentration, due to the formation of WO_3 . A white to yellowish film is formed when there is a high concentration of oxygen from the formation of W_2O_5 .

Access was provided to the dry box through a port which was held under a vacuum for fifteen minutes and then refilled with the atmosphere from inside of the box. This procedure was repeated three times. This process continually removes the atmosphere from inside the box, and any chance impurities, and replaces it with the UHP helium from the tank.

All of the electrochemical experiments were performed with a Princeton Applied Research (PAR) model 173 potentiostat/galvanostat equipped with a PAR model 179 coulometer plug-in module. Any potential or current programming was provided by a PAR model 175 programmer. All

of the potentials were monitored on a DANA model 5330 digital voltmeter. The working electrodes were mounted in a Pine MSR electrode rotator. Any scans taken at less than a volt a second were recorded on a Houston Instruments Model 2000 Omnigraphic X-Y recorder. Any scans at a volt a second or greater were fed into a Nicolet model 204A storage oscilloscope and then output to the Omnigraphic recorder. All of the CVs presented in this work were acquired by initially scanning in the anodic direction.

Since not all compositions of the bromide melts are liquid at room temperature, a block heater was used to heat the melts. Temperatures were monitored with a Doric model 412A Trendicator, using a type K (Chromel-Alumel) thermocouple.

All of the N.M.R. spectra were run on a JEOL 90Q FTNMR. All of the molten salts were run neat. All of the proton and carbon spectra were referenced against a sealed glass capillary containing hexamethyldisiloxane (HMDS). The capillary caused a minor degree of line broadening and some small spinning sidebands, but the spectra were all usable. No reference was used in the aluminum spectra.

All of the UV-VIS spectra were run on a Hewlett Packard model 8450A Diode Array Spectrophotometer. Unless otherwise stated all of the samples were solvated in dry acetonitrile. All of the spectra were run in 10 mm quartz cells.

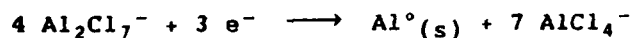
Conventions

Except where otherwise noted, Electrochemical Society conventions have been used throughout these experiments. Figure 10 represents these conventions. Potentials become more negative to the right, and reductive processes become favored. These potentials are termed "cathodic". Currents resulting from a reduction process are shown as positive and above the horizontal axis (typically, quadrant 1). Positive potentials, which are called "anodic" potentials, are to the left, and favor oxidative processes. Oxidative currents are negative and towards the bottom of the graph (typically, quadrant 3).

Reference Electrodes

The purpose of a reference electrode is to provide a stable potential to which the potential of the working electrode is compared. Any reference electrode must have a migration of ions, and thus material, across the interface between the reference electrode material and the analyte solution.

To date, in the chloride molten salt systems, the standard reference electrode used has been an aluminum wire in an $N = 0.600$ chloride melt. The reference couple is thus the reduction of the heptachloroaluminate by the half reaction:



A fine asbestos fiber separated the reference compartment from the sample compartment. Any chloride melt which crossed the interface merely altered the apparent mole fraction of aluminum chloride in the chloride melt being studied. Any chloride melt which would cross the interface to a bromide melt, though, would contaminate the bromide melt, with chloride containing species.

Although a bromide reference would not cause contamination of the bromide melts, the bromide melts suffer from thermal- and

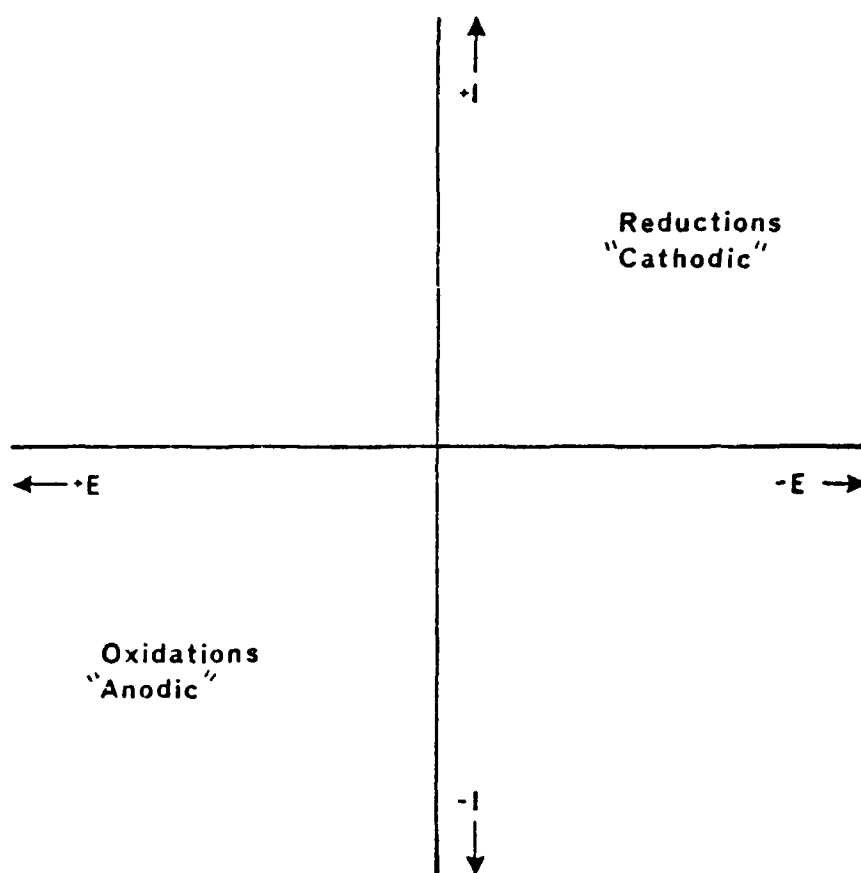


Figure 10. Electrochemical conventions and nomenclature.

photo-decomposition. The change in the composition of the reference electrode caused by the decomposition could result in a drift in the potential of the reference electrode over time.

In an attempt to detect any leakage from the reference electrodes, a background cyclic voltammogram, referenced against a chloride reference electrode, of an acetonitrile solution containing tetraethylammonium perchlorate (TEAP) as a supporting electrolyte was taken. The CV of this electrolyte solution is shown in Figure 11A. Allowing the reference electrodes to remain in this solution for six hours did not noticeably alter the CV. Since the reference electrode was removed from a melt when an experiment was not in progress, during the lifetime of a melt, the reference electrode would not remain in a melt for more than a total of six hours.

To facilitate relating potentials referenced against the chloride and bromide electrodes back to more common reference systems, the potentials for the reduction of ferrocene, in an acetonitrile solution containing TEAP as a supporting electrolyte, against the chloride and bromide reference cells was determined. Figure 11B shows the CV of the ferrocene system against the bromide electrode, and Figure 11C shows the CV of the ferrocene against the chloride system. The bromide reference cell is 0.018 volts cathodic, and the chloride cell is 0.069 volts anodic of the normal hydrogen electrode (NHE).

Both reference electrodes seem to be comparable. Neither noticeably contaminated the acetonitrile/TEAP solutions and the voltages read against these electrodes were comparable. The chloride reference cell was used throughout the rest of the experiments, because it would allow a direct comparison to a wider range of previous work, and would avoid problems with an unsteady reference potential due to the degradation of the bromide melt. In order to minimize any possible contamination problem, care was taken to minimize the flow across the interface by using the smallest asbestos fiber possible and minimizing the pressure head of the melt in the reference cell.

Working Electrodes

Figure 12 shows the CVs of an $N = 0.490$ bromide melt on glassy carbon, tungsten, and platinum working electrodes respectively. The glassy carbon and tungsten electrodes show very broad oxidation waves. This indicates the oxidative couples have a higher degree of electrochemical irreversibility on these electrode materials. On the platinum electrode, however, the couples are much more distinct, indicating a relatively minor degree of irreversibility. Platinum also tends to show the reduction of any protonic impurities which may be present. Because protonic impurities are the major source of contamination of the molten salt systems, the use of platinum will allow for the continual monitoring of the purity of the melts. For these reasons, it was decided to use platinum through out the rest of the experiments.

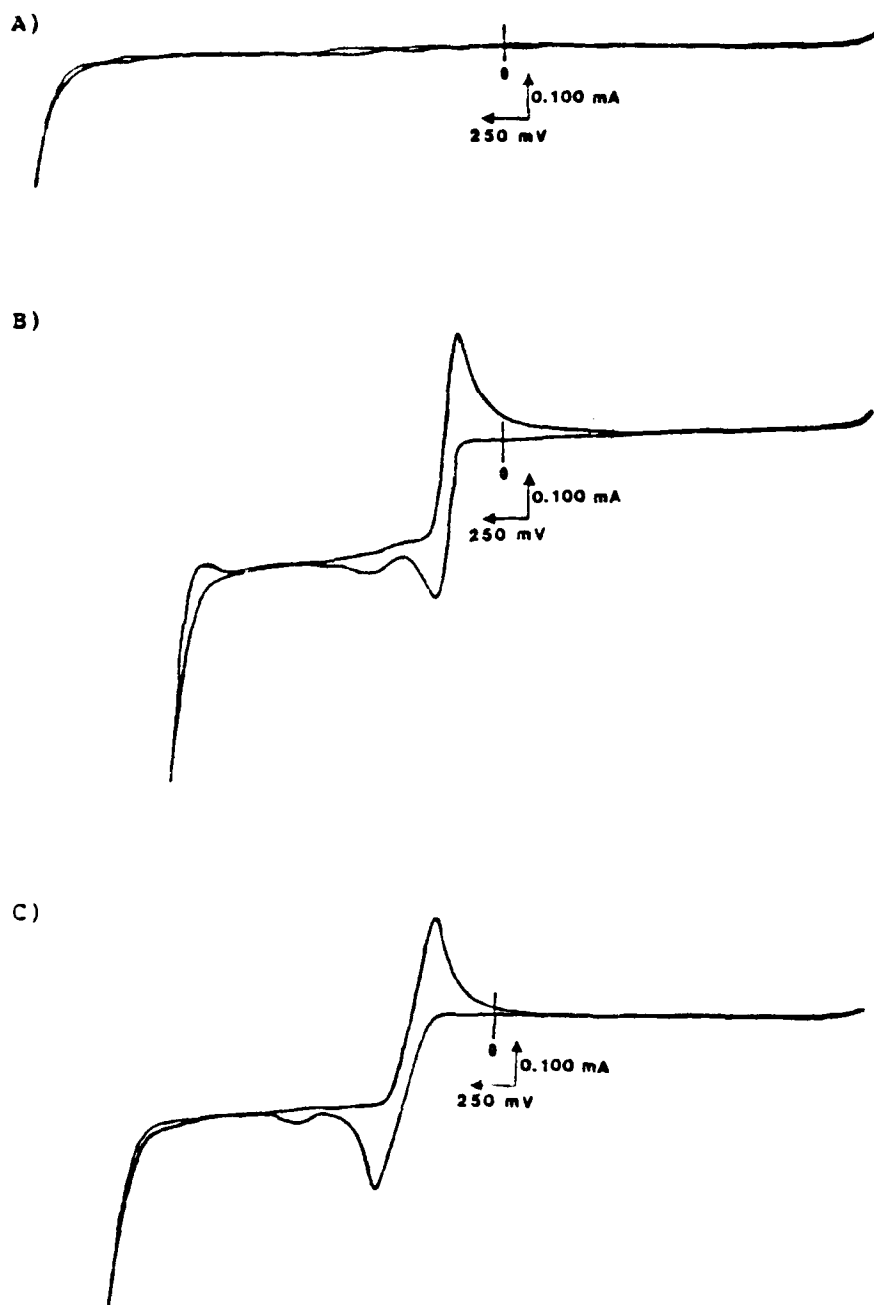


Figure 11. CV of A) acetonitrile with a TEAP as a supporting electrolyte, B) ferrocene in acetonitrile using a chloride reference electrode, and C) ferrocene in actonitrile using a bromide reference electrode.

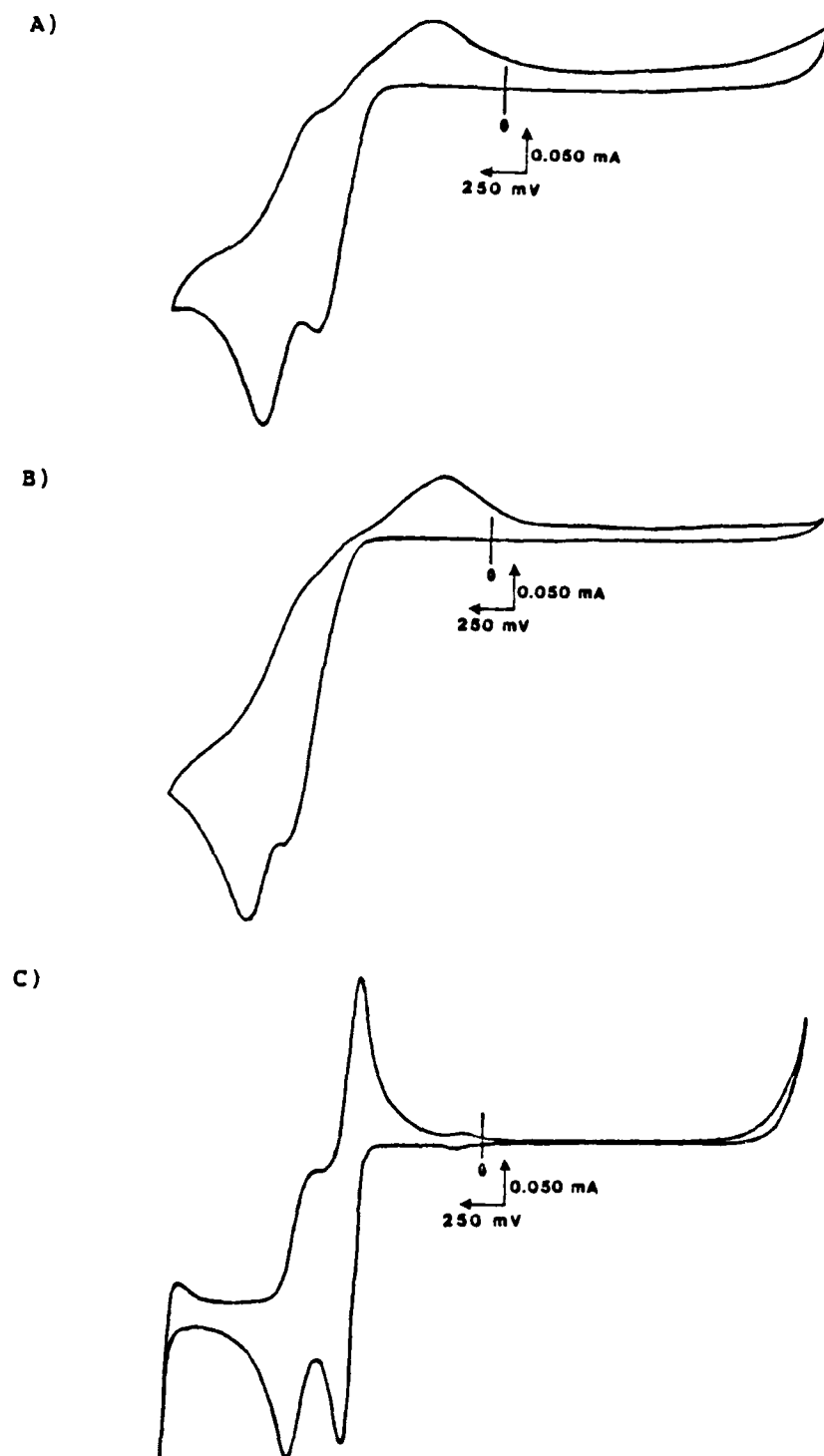


Figure 12. CV of an $N = 0.480$ bromide melt on a A) glassy carbon, B) tungsten, and C) platinum electrode.

CHAPTER 4

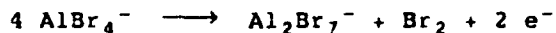
DETERMINATION OF FUNDAMENTAL ELECTROCHEMICAL PARAMETERS

CV of Selected Melt Compositions

An electrochemist's primary method of gaining a preliminary understanding of an electrochemical system is by a technique called cyclic voltammetry (CV). With the information obtained with cyclic voltammetry, an electrochemist can develop other experiments to further investigate the system. As noted in the discussion of the composition diagram, there are several compositions of the molten salt systems, that have relatively simple compositions. These compositions were analyzed initially in an attempt to understand the more complex compositions. The CVs of the chloride and bromide molten salts are shown for comparison, but the discussion is limited to the bromide system.

Neutral melts. The only species present in a neutral bromide melt are the tetrabromoaluminate and the imidazolium cation. The CVs of a neutral bromide and a neutral chloride melt are shown in Figure 13. As can be seen there are no oxidative or reductive processes, of import, occurring other than at the electrochemical limits of the melts. As the concentration of the tetrabromoaluminate is decreased, by adding more aluminum bromide, the anodic limit shifts cathodic, and the cathodic limit remains stable. The anodic limit of the bromide melt occurs at +1.725 V and the cathodic limit occurs at -0.885 V when referenced against the chloride reference electrode.

The dependence of the anodic limit on the concentration of the tetrabromoaluminate indicates the anodic limit is due to the oxidation of some form of the tetrabromoaluminate. The half reaction ascribed to this process is:



This proposal is supported by high scan rate CV experiments. Figure 14 shows the CV of a neutral melt with the potential scanned at both high and moderate rates. At the moderate scan rate, no waves are observed other than the melt limits. As the scan rate is increased, a reduction wave, and the associated reoxidation waves, are observed. The longer the potential is held at a value greater than the anodic limit, the larger the reduction wave occurring at +0.175 V, and the reoxidation waves occurring at +0.425 and +1.075 volts, versus the chloride reference electrode, become. The reduction wave shows the same characteristics attributed to the reduction of the heptabromoaluminate discussed in the section on slightly acidic melts below.

As the potential enters the anodic melt limit, the oxidation dictated by the above half reaction occurs. At moderate scan rates, the heptabromoaluminate completely diffuses away from the electrode surface

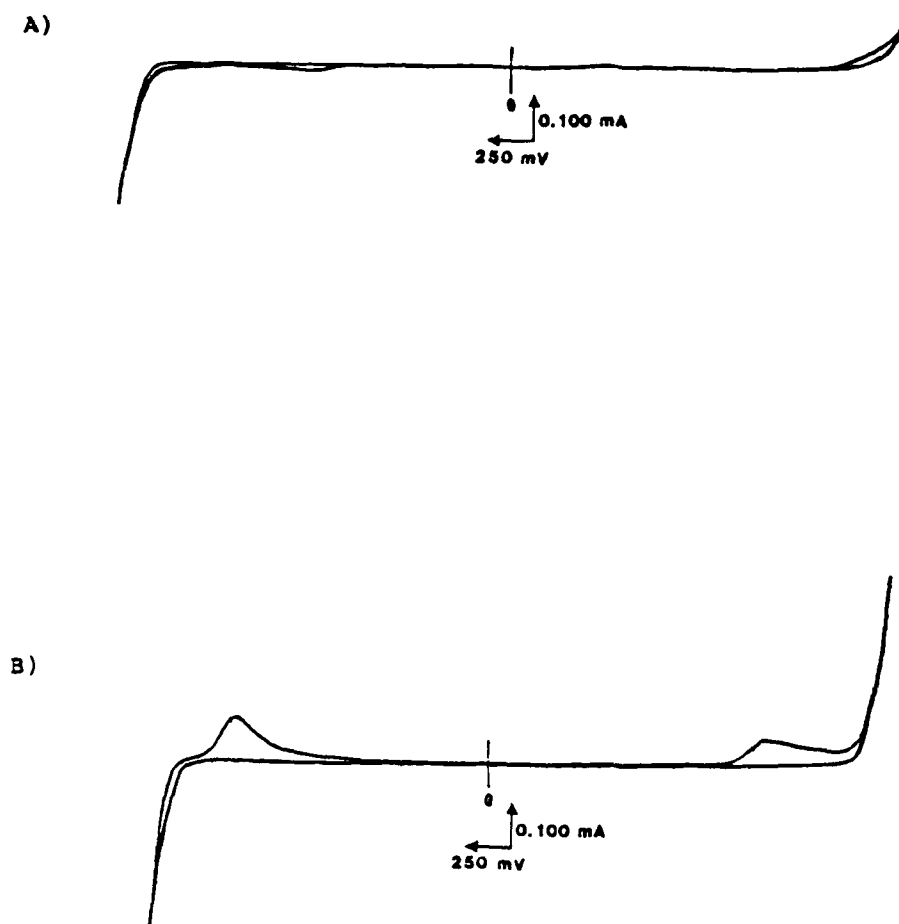
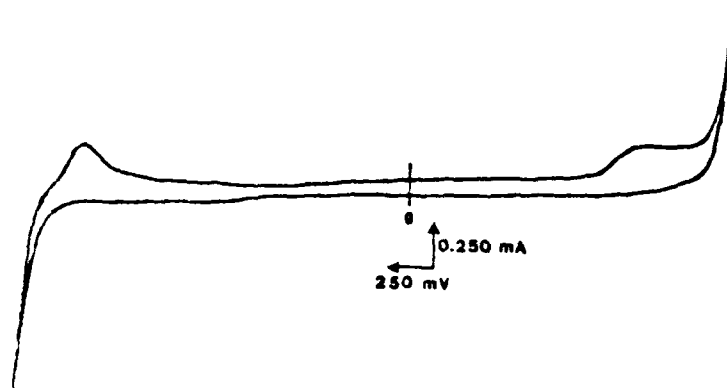


Figure 13. CV of an N = 0.500 A) chloride, and B) bromide melt.

A)



B)

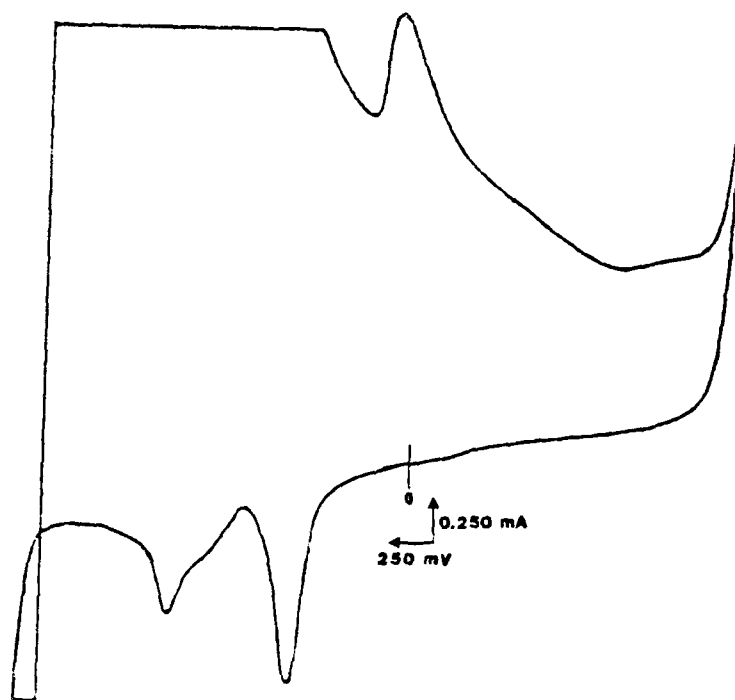


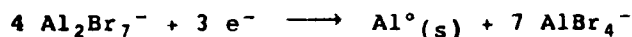
Figure 14. The CV of a neutral bromide melt at A) 50 mv/sec, and B) 500 mv/sec.

before a potential sufficiently cathodic enough to reduce the heptabromoaluminate is reached. At higher scan rates, the heptabromoaluminate does not completely diffuse away from the electrode surface. Since the heptabromoaluminate is still in the vicinity of the electrode, it will be reduced when a sufficiently cathodic potential is reached. The aluminum is plated out onto the electrode and subsequently reoxidized, as discussed below.

The cathodic limit is independent of the concentration of the tetrabromoaluminate. Since the only other species present is the imidazolium cation, the cathodic limit must be due to the reduction of the organic cation. No reoxidation of the products formed in the reduction of the imidazolium cation is seen. This indicates an electrochemically irreversible reaction as is usually seen in the destruction of an organic substrate.

Slightly acidic melts. As aluminum bromide is added to a melt, the melt becomes more acidic. In a neutral or an acidic melt, such an addition will cause the concentration of tetrabromoaluminate to decrease and the concentration of heptabromoaluminate to increase. The species present in an $N = 0.510$ bromide melt are the same as those present in the neutral melt plus a relatively minor concentration of the heptabromoaluminate. The CVs of an $N = 0.510$ bromide and $N = 0.510$ chloride melt are shown in Figure 15. The CV appears the same as that for a neutral melt, but with the addition of a reductive process occurring at +0.235 volts, and the reoxidations occurring at +0.350 and +0.670 volts vs. the chloride reference electrode. The limits occur at the same potentials and are ascribed to the same processes as for the neutral melt.

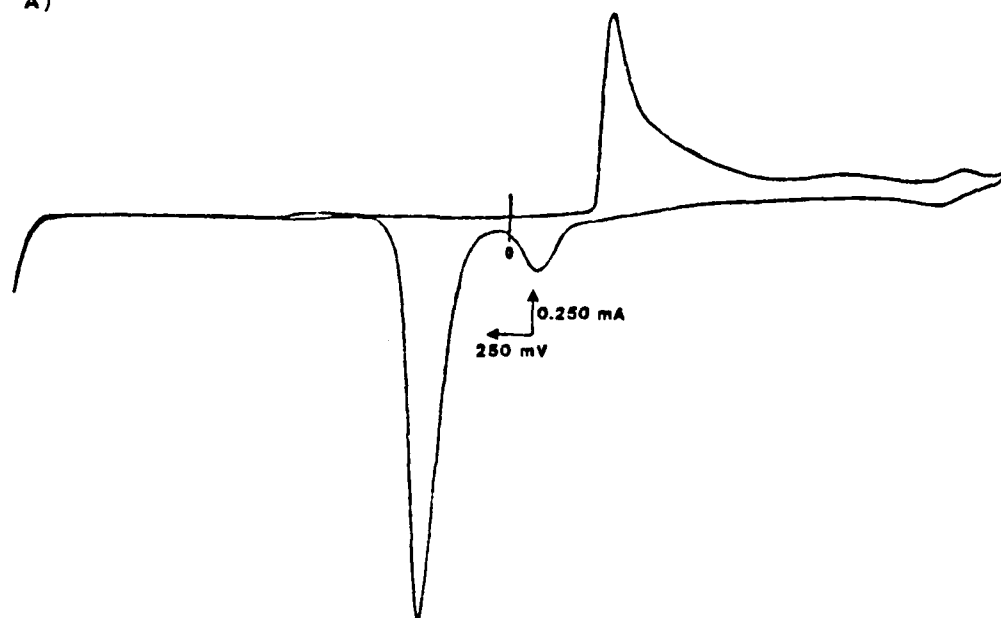
The peak current of the redox couple increases as the concentration of the heptabromoaluminate increases, indicating the couple is due to some form of the heptabromoaluminate. The reduction wave has a characteristic sharp break at the base line which is commonly associated with a nucleation process occurring prior to the deposition of a metal. The reoxidation wave does not follow a typical square root of time decay relationship. The sharp decay indicates a process which is either passivating the electrode surface, or is not diffusion controlled. The combination of these two observations argues that as in the chloride system, this redox couple is the result of the half reaction:



Two oxidation waves are observed. Both are due to the reoxidation of the deposited aluminum off of the electrode surface. The initial wave is due to the oxidation of aluminum off of the electrode which is deposited on top of a aluminum monolayer. The second oxidation wave results from the oxidation of the aluminum which is plated (or bound) to the platinum surface of the electrode. It is easier to oxidize aluminum off of aluminum than if is to oxidize aluminum off of platinum.

Fully acidic melts. As the concentration of the heptabromoaluminate is increased, the peak current, due to the reduction of the heptabromoaluminate increases until it becomes the melt limit. This cathodic limit occurs at +0.250 V vs. the chloride reference electrode. An $N = 0.667$ chloride melt and an $N = 0.667$ bromide melt are shown in

A)



B)

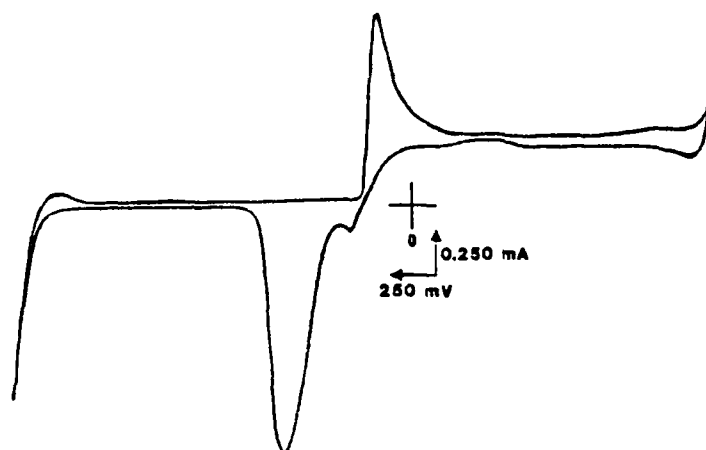
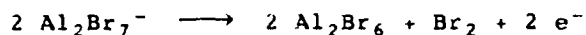


Figure 15. CV of an $N = 0.510$ A) chloride, and B) bromide melt.

Figure 16. Since there is no longer any tetrabromoaluminate present in the melt, the anodic limit becomes the oxidation of the heptabromoaluminate. The anodic limit occurs at approximately +1.930 V vs. the chloride reference electrode. The half reaction of this oxidation process is:



Slightly basic melts. As the concentration of bromide is increased, by adding MEIB to a neutral melt, two redox couples begin to appear. Figure 17 shows the CVs of an $N = 0.490$ chloride melt and an $N = 0.490$ bromide melt. Figure 18 shows peak potentials and currents as a function of the bromide concentration in the melt. The peak potentials shift anodic as the concentration of bromide increases.

The peak currents increase linearly with respect to the bromide concentration indicating the oxidative processes are due to some form of the bromide ion. The fact the currents do not pass through the origin, in Figure 18, is probably due to the presence of a small amount of protonic impurity which will react with the tetrabromoaluminate and the bromide, thereby decreasing the effective aluminum bromide concentration.

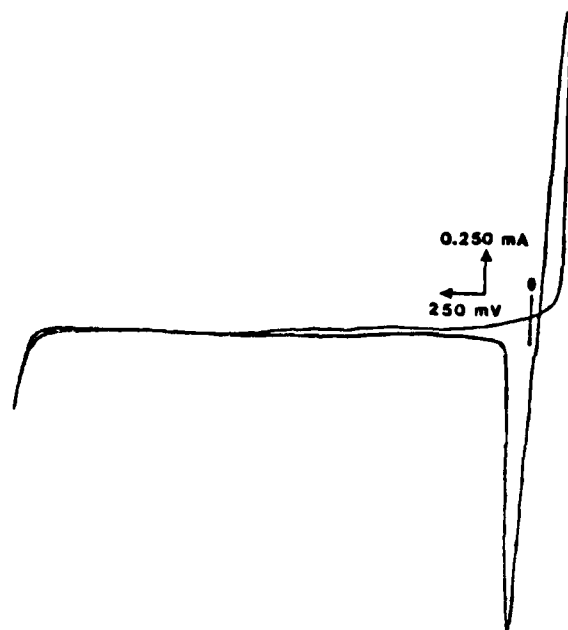
The only species present in a bromide melt are the heptabromoaluminate, tetrabromoaluminate, and bromide anions, and the imidazolium cation. If the oxidation waves were due to some form of the heptabromoaluminate, these waves would also be present in the CV of an acidic melt. If the waves were due to oxidation of the tetrabromoaluminate, they would also be seen in the neutral and acidic melts. If the waves were due to the oxidation of the imidazolium cation, they would be present at all times, because the imidazolium cation is present in all melt compositions. For these reasons it was decided the two oxidation waves must be due to some form of the bromide ion.

Fully basic melts. As the concentration of the bromide is increased further, the point is finally reached where the first oxidation wave becomes the anodic limit. Figure 19 shows the CVs of an $N = 0.333$ chloride and an $N = 0.333$ bromide melt. The cathodic limit, as in a neutral melt, is the irreversible reduction of the imidazolium cation. The anodic limit of the fully basic bromide melt occurs at +0.41 V and the cathodic limit occurs at -1.70 V vs. the chloride reference electrode.

Melt summary. The neutral and acidic bromide melts have been shown to behave electrochemically in a manner completely analogous to the chloride system. The basic bromide system, though, has two oxidative processes, other than the anodic limit, occurring. All of the evidence, both positive and negative, indicates the oxidation waves present in the basic bromide melt system are due to some form of the bromide anion.

While Popov and Geske⁷ have attributed the first of these waves to the oxidation of the bromide to tribromide and the second to the oxidation of the resulting tribromide to bromine, molten salt systems are different enough from typical solvent systems to necessitate the verification of these assignments. The rest of this portion of this project is aimed at, first, verifying these assignments in the molten salt system, and second, determining the electrochemical properties of the bromide species in the basic melts.

A)



B)

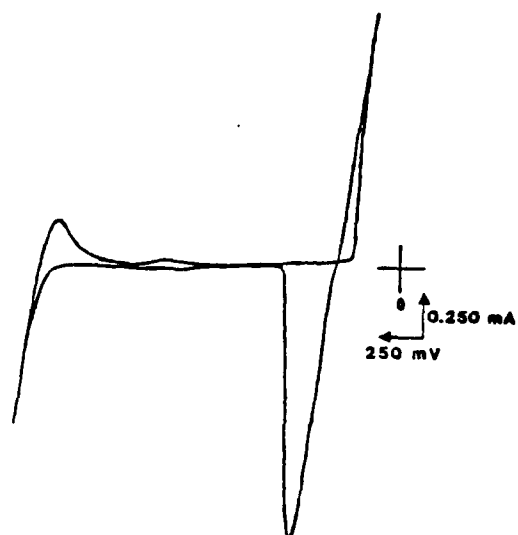


Figure 16. CV of an $N = 0.667$ A) chloride, and B) bromide melt.

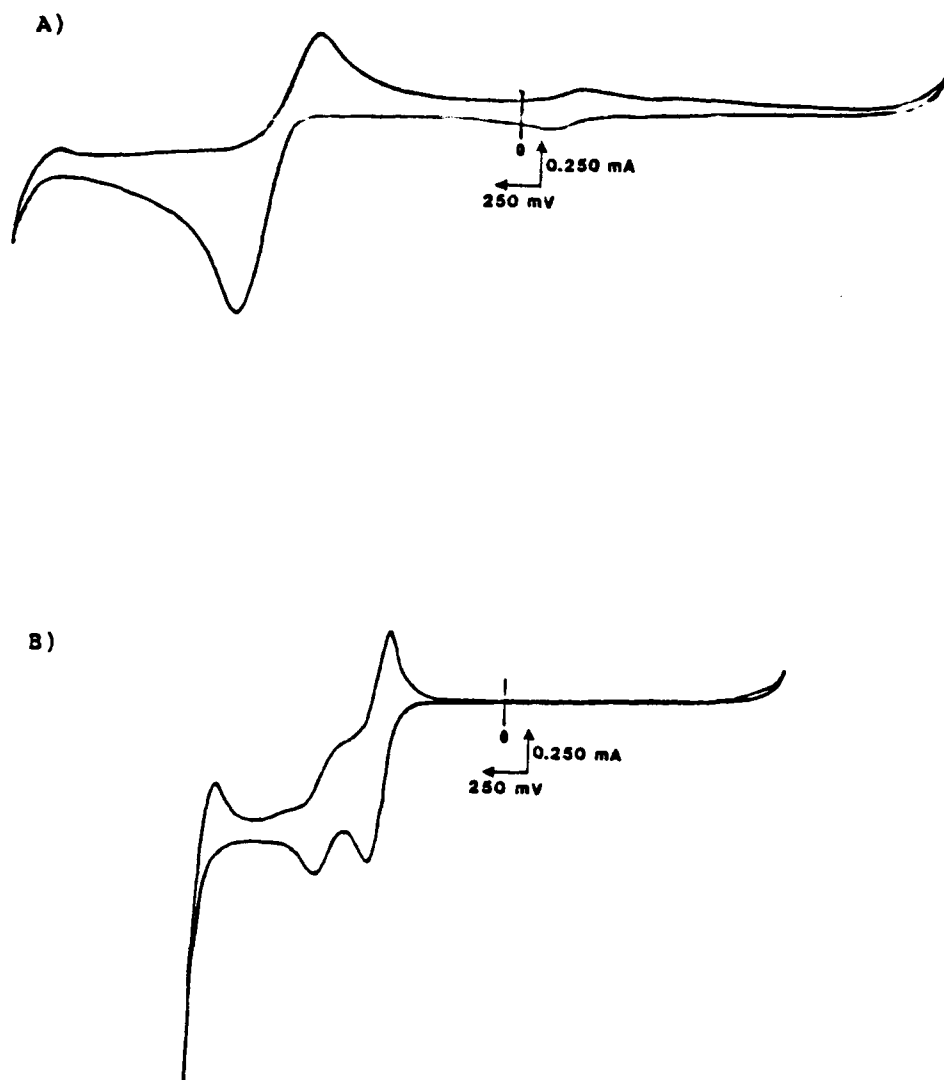


Figure 17. CV of an $N \approx 0.490$ A) chloride, and B) bromide melt.

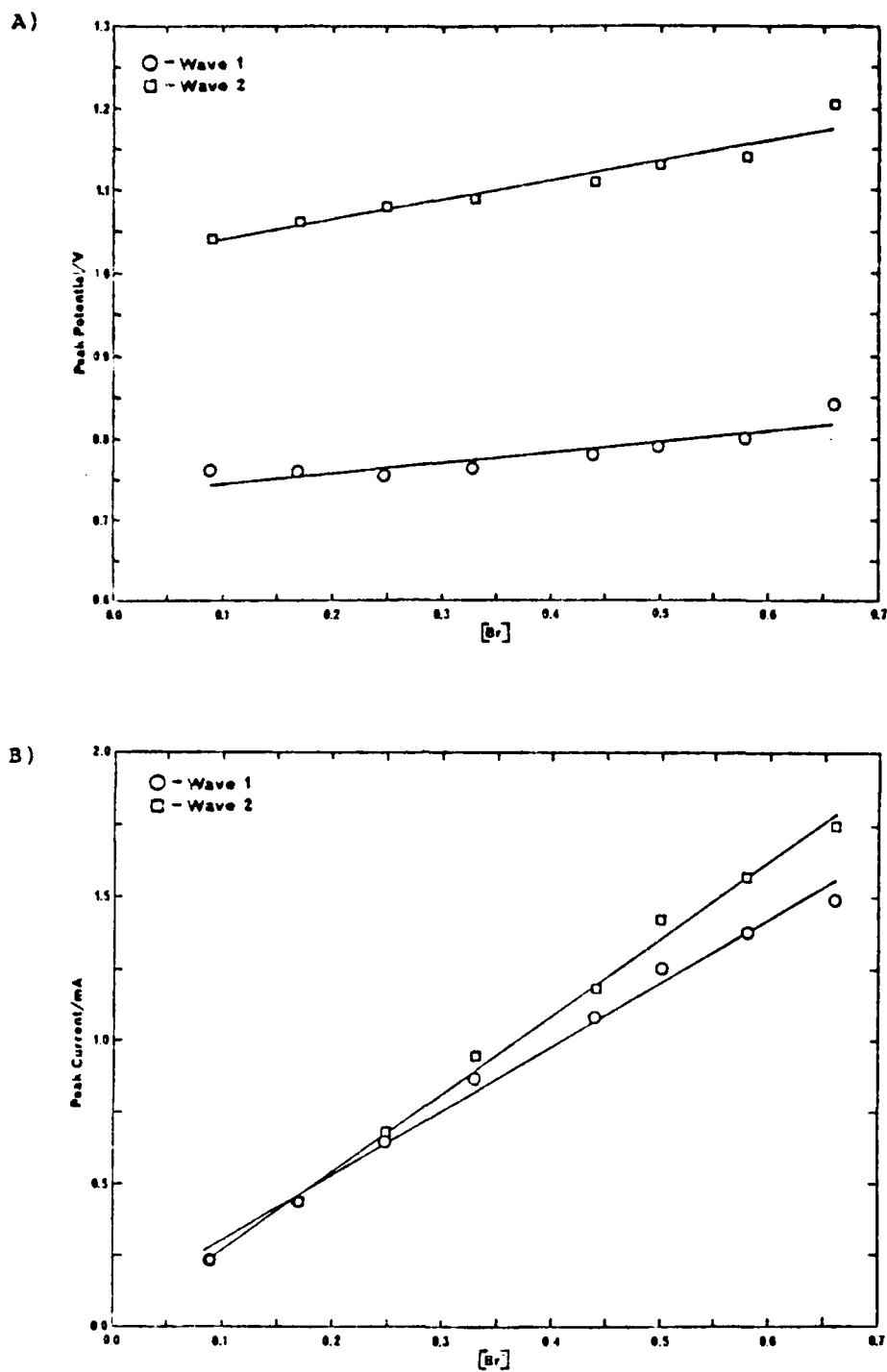


Figure 18. A) peak potential, and B) peak current of the oxidation waves as a function of the bromide concentration.

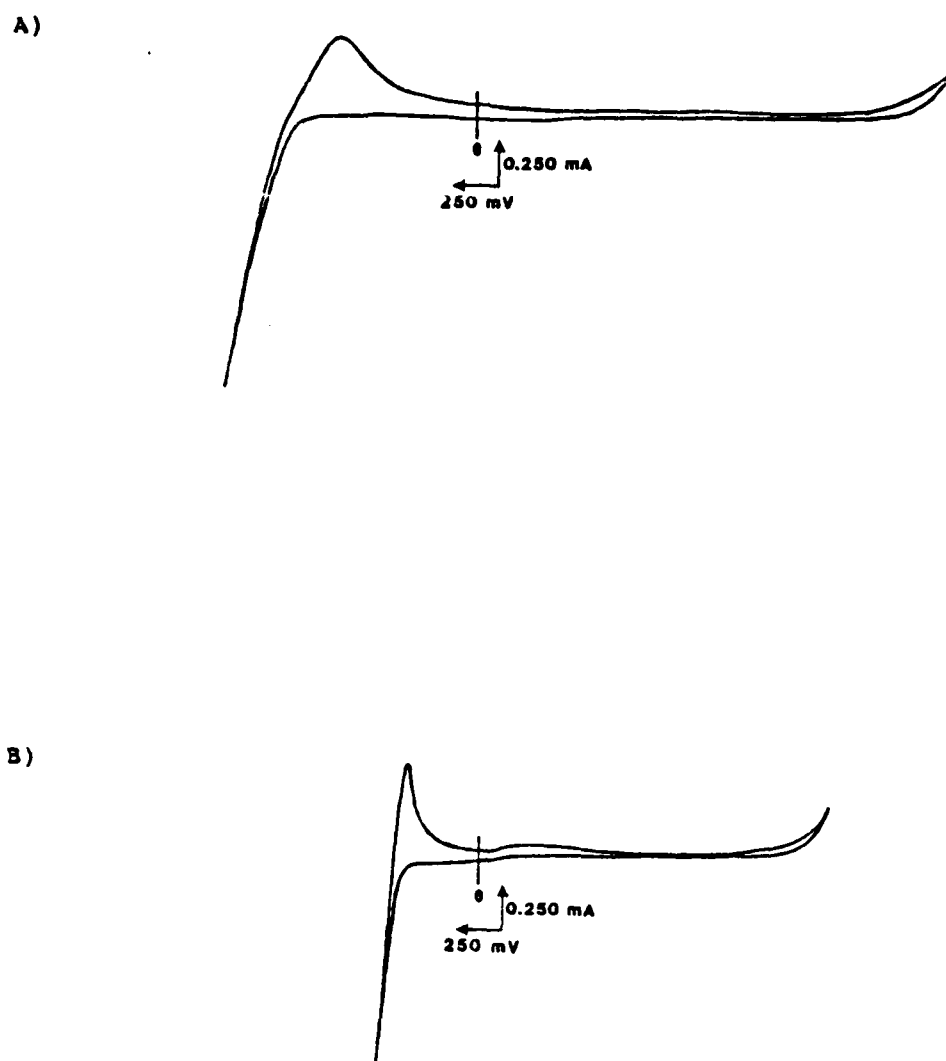


Figure 19. CV of an $N = 0.333$ A) chloride, and B) bromide melt.

Formal Electrode Potentials

The potential, halfway between the cathodic and anodic peak potentials of a process, is called the conditional or formal electrode potential ($E^{\circ'}$) of the process. The formal electrode potential is defined in a manner unique from the standard electrode potential in order to account for any possible solvent interactions. The standard electrode potentials which are found in most tables are usually derived using thermodynamic considerations. Experimentally, it is usually not possible to obtain conditions such as activity coefficients of unity. This non ideality of the experimental conditions can drastically affect the electrochemical properties of a species.

The potentials, halfway between the anodic and cathodic peak potentials, for both of the processes are shown as a function of the square root of the sweep rate in Figure 20. The potential for the first wave is not dependent on the sweep rate. The formal electrode potential for the first oxidative process is 0.684 volts versus the chloride reference cell.

For the second wave, the potential halfway between the cathodic and anodic peak potential is dependent on the sweep rate. This occurs because of an unequal dependence of the anodic and cathodic peak potentials, of the second wave, on the sweep rate. In order to account for this dependence on the sweep rate, the potential was extrapolated back to a sweep rate of 0. This resulted in a value of +1.01 volts for the formal electrode potential for the second wave.

Number of Electrons Transferred

Knowledge of the species involved in an electrochemical process combined with a knowledge of the number of electrons transferred, per mol of the species, often enables the identification of the process. Cyclic voltammetry indicated the two oxidation waves in a basic bromide melt are due to some form of the bromide ion. The processes occurring in the basic bromide melts can be identified if the number of electrons transferred in each process can be determined.

When the heterogeneous rate constant (the rate at which electrons are transferred from the electrode surface to the analyte solution) is not facile, the system is said to be electrochemically irreversible. The degree of electrochemical reversibility can range from completely reversible to completely irreversible, with an intermediate degree being called an electrochemically quasi-reversible system.

The waves of an electrochemically irreversible process appear very broad and spread out, and are apparent by visual inspection. While harder to detect than the irreversible case, an electrochemically quasi-reversible system can be distinguished from an electrochemically reversible one by observing the oxidation and reduction potentials of a couple as a function of the rate at which the potential is varied. Unlike a reversible system, the peak potentials of a wave, in a quasi-reversible system, will shift as a function of the sweep rate.

Figure 21 shows the cyclic voltammogram of an $N = 0.490$ bromide melt at various sweep rates. The potentials of the peaks are also shown as a function of sweep rate in Figure 21. Since both of the oxidation waves shift anodic as a function of the sweep rate, it is apparent the oxidative processes occurring in a basic bromide melt system are electrochemically quasi-reversible. This indicates the rate of electron

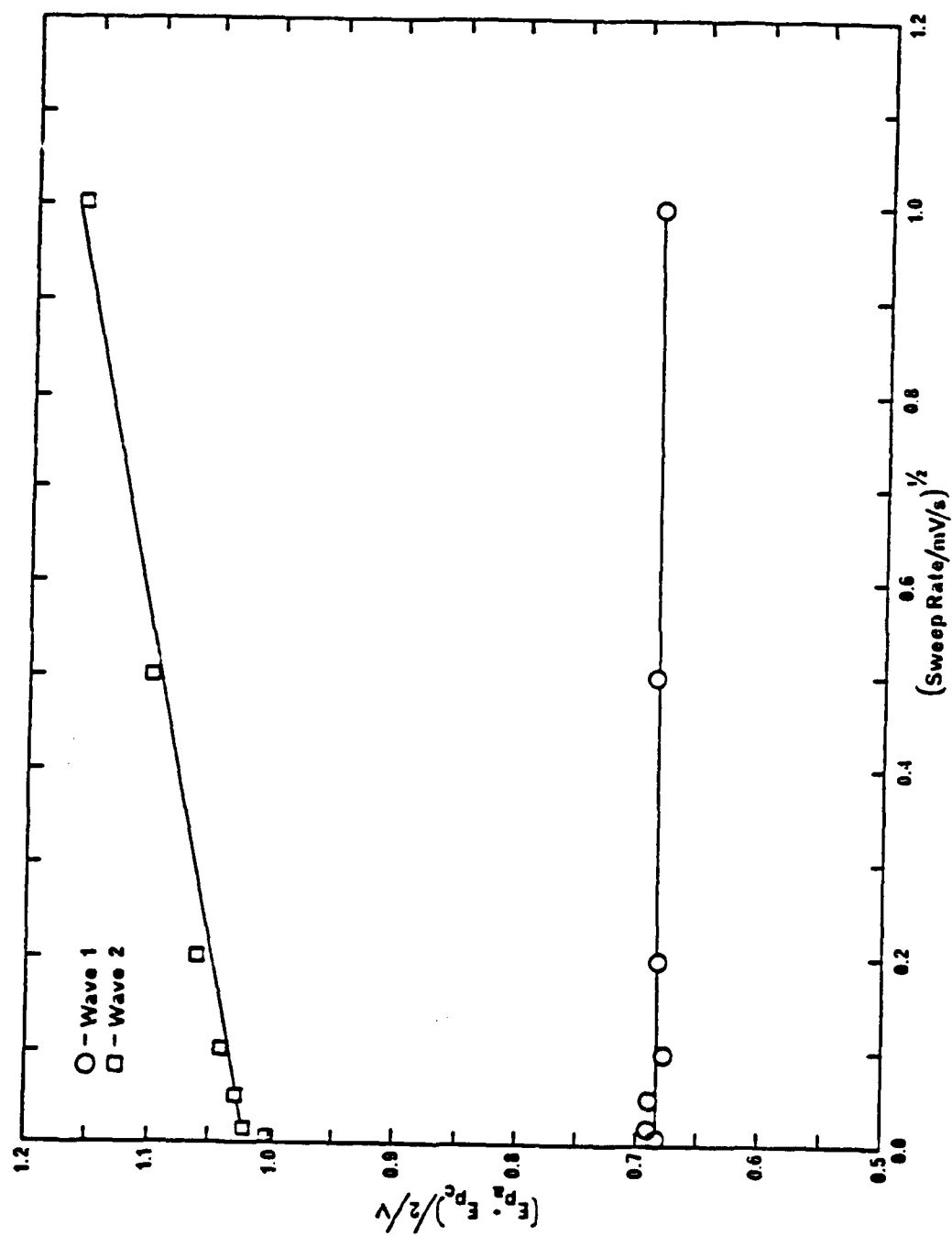


Figure 20. Formal potential as a function of the sweep rate.

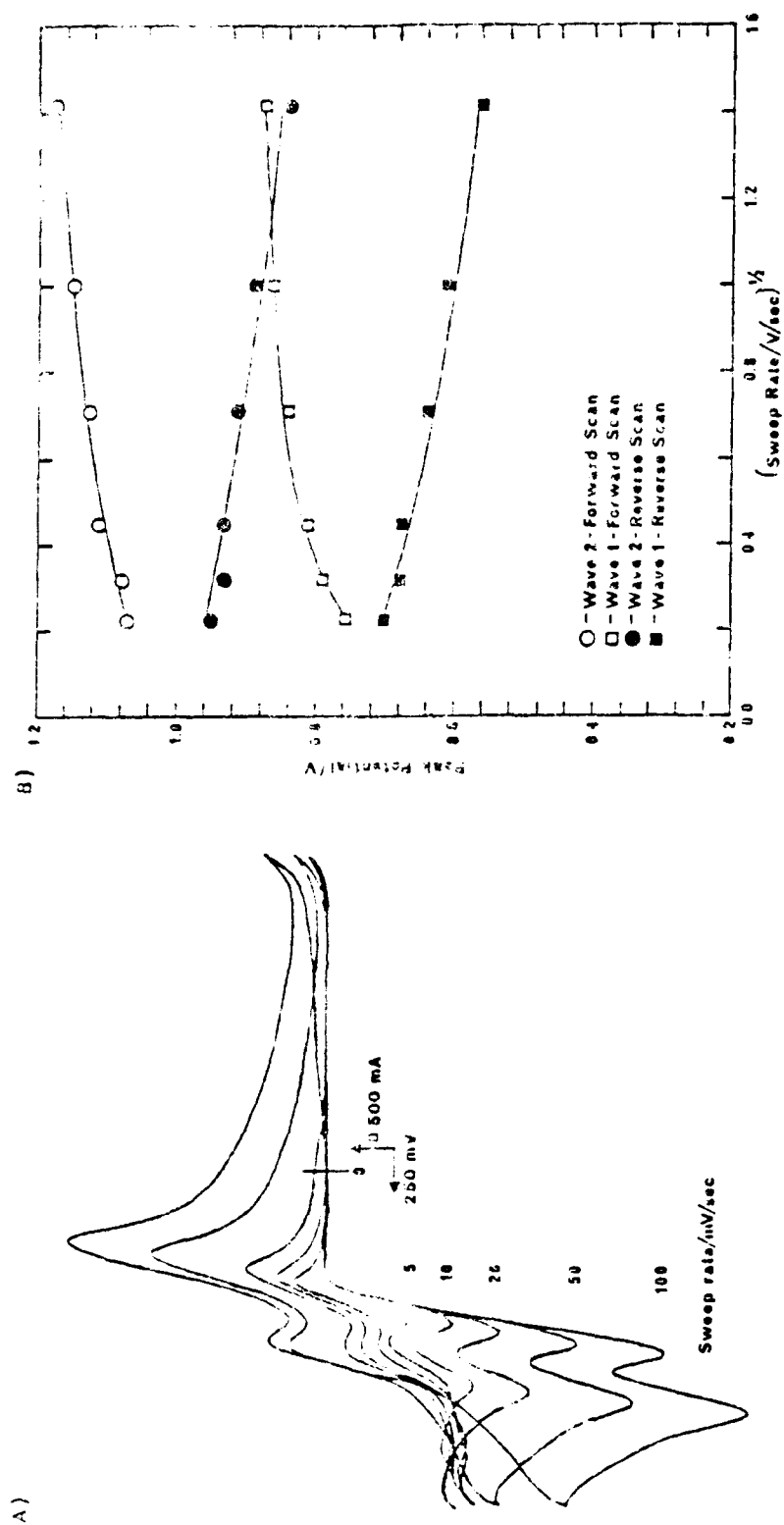


Figure 21. A) The CV of an $N = 0.4800$ bromide melt at different scan rates, and B) the peak potentials as a function of the scan rate.

transfer, from the electrode surface to the electroactive species, must be taken into account.

To account for the slow rate of electron transfer, an indication of the degree of irreversibility must be introduced to the equations describing electrochemical behavior. This is accomplished by adding a term, called the transfer coefficient (α), to the equations. The transfer coefficient is a unitless parameter which modifies the number of electrons transferred (n), per mol of electroactive species consumed, in the rate determining step.

Experimentally, there are several methods of determining the number of electrons transferred in, and of accounting for the transfer coefficient of, an electrochemical process. Several techniques, such as rotating disk linear sweep voltammetry, linear sweep voltammetry, and constant current amperometry, can be used to determine the product of the transfer coefficient and the number of electrons transferred. Other techniques, typically various forms of coulometry, have been devised which can be used to determine the number of electrons transferred, independent of the transfer coefficient.

There are two methods of separating each term of the product of the transfer coefficient and the number of electrons passed from the other. If the number of electrons transferred has been determined independently, the transfer coefficient is easily obtained from the product. If it is not possible to determine the number of electrons transferred independent of the transfer coefficient, both terms must be estimated. Since severe restrictions are placed on the value each term may have, it is usually a fairly simple matter to assign a value to each.

Rotating disk linear sweep voltammetry (RDLSV). As a potential is applied to an electrode surface, any species in the region of the electrode, which is electroactive at that potential, will be converted by an electrochemical process. As the species is consumed, diffusion to the electrode surface will begin to occur. In a voltammetric experiment with no convective means of mass transport, such as in cyclic voltammetry and linear sweep voltammetry, the current passing through the cell will reach a maximum and then decay back towards zero current as the electroactive species is depleted from the region surrounding the working electrode.

If the electrode is rotated, forced convection to the electrode surface will occur. The induced convection moves the electroactive species from the bulk of the solution to the vicinity of the electrode surface, where it will be reduced or oxidized. At some minimum rotation rate, the rate the electroactive species is brought to the electrode surface, through a combination of convection and diffusion, will be greater than the rate it is removed from the solution by the electrochemical process.

In rotating disk linear sweep voltammetry, the cell currents reach a limiting value, called the limiting current, as distinguished from the peak currents observed in experiments with no convective means of mass transport. When the species is brought to the electrode surface, by both the convective and diffusive processes, the measured current is proportional to the rate at which the electroactive species is transported by each process. Since, in rotating disk linear sweep voltammetry, the rate of the convective process is altered in a known manner, the observed current becomes proportional to the rate at which the material is brought to the surface by the diffusive process.

If the potential is swept from a non-Faradaic region (a potential where none of the species present in the analyte solution are electroactive) to a Faradaic region (a potential where a current begins to flow through the cell due to the oxidation or reduction of at least one electroactive species) a current will begin to flow. For an oxidative process, the relationship of the limiting current (i_L) to the current (i) observed at any point on the decreasing portion of the I-E curve as a function of the potential is given by the equation²⁴:

$$i = i_L \frac{1 - \alpha}{1 - \alpha + \exp\left(\frac{nF}{RT}(E - E^0)\right)} \quad (7)$$

A plot of the potential as a function of $\ln(i_L - i)/i$ should be linear with a slope of $RT/(1 - \alpha)n$. Figure 22 shows this relationship for both of the oxidative processes in an $M = 0.480$ bromide melt for several different rotation rates. Table 3 gives the values of $(1 - \alpha)n$ for both of the processes at the various electrode rotation rates.

The observed current-potential curve is actually the sum of two curves resulting from separate anodic processes. The two waves are not resolved enough to determine the product of the number of electrons and the transfer coefficient for the first wave independent of the product for the second wave. Since current observed for the oxidative process is the sum of the currents of the two oxidative processes, the current due to the first process is the difference between the currents observed for the first and second waves. Experimentally, this is accounted for by taking the difference between the slopes of the lines obtained when the potential is plotted as a function of $\ln[(i_L - i)/i]$ for each wave.

It is usually difficult to distinguish a transfer coefficient less than 0.3 from a completely irreversible case and greater than 0.7 from an electrochemically reversible system. If the degree of irreversibility is observable, 0.5 is a reasonable initial estimate of the transfer coefficient, as experimental values of the transfer coefficient typically fall in the 0.3 to 0.7 range. Since a discrete number of electrons must

TABLE 3 - The Product of the Transfer Coefficient and the Number of Electrons Transferred as a Function of the Rotation Rate (ω).

ω (rpm)	$(1 - \alpha)n$	
	Wave 1	Wave 2
300	1.020	0.623
500	0.960	0.573
700	0.918	0.493
900	0.890	0.480
	0.947	0.542

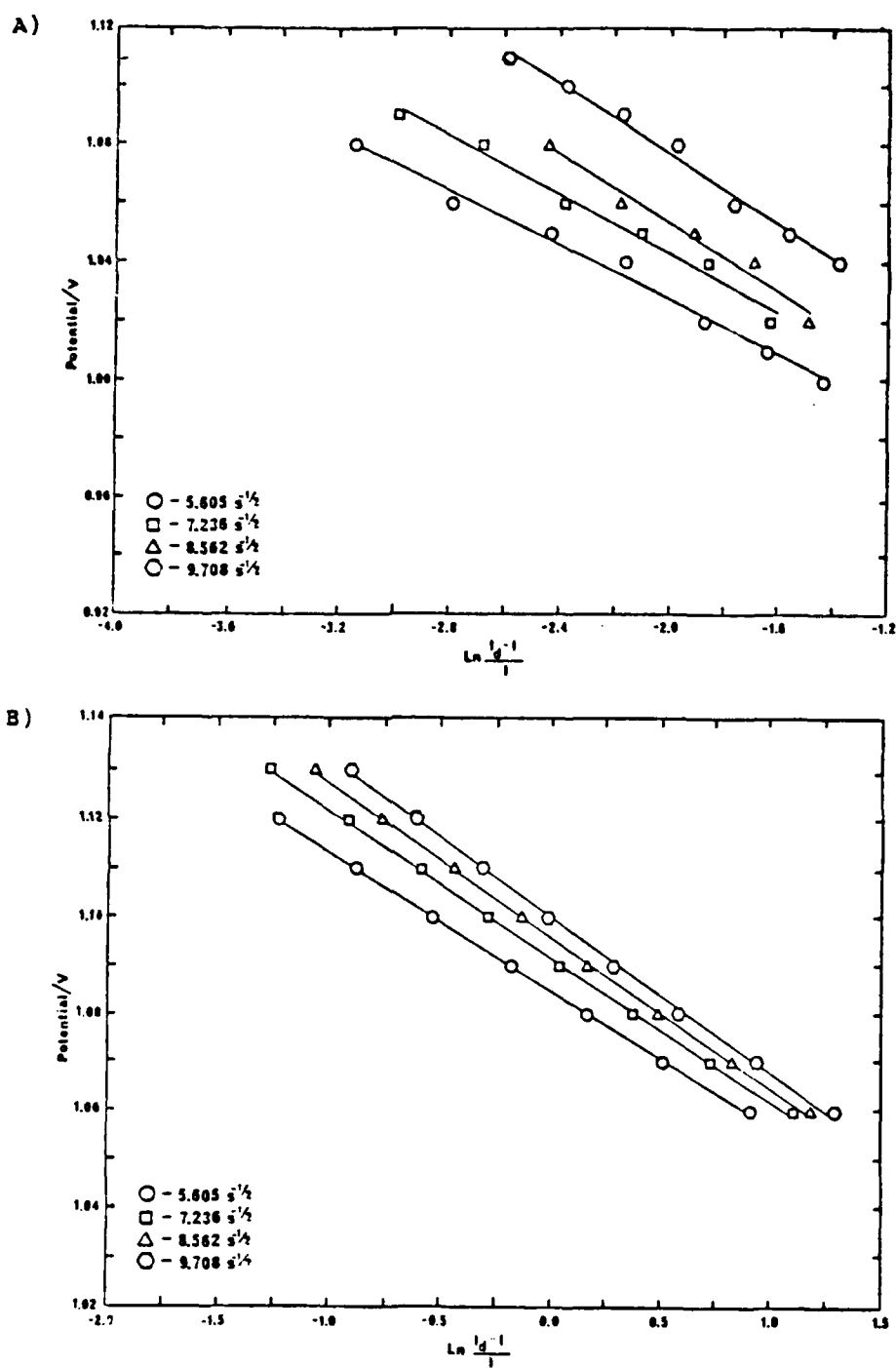


Figure 22. The potential as a function of $\ln [I_d - I/I]$ for A) the first, and B) the second oxidation waves for several different melt compositions.

be transferred in any elementary electrochemical process, the number of electrons transferred, per mol of reactive species, is restricted to having one of only a few values.

Even though a discrete number of electrons must be transferred in an elementary electrochemical process, the number of electrons transferred, per mol of electroactive species, need not be an integer (i.e. if two electrons are passed in a process which consumes three molecules of the electroactive species, n equals $2/3$). After rounding n to a value corresponding to an integer number of electrons transferred, the transfer coefficient can be redetermined. Using this process, it was determined one electron was transferred in each of the electrochemical processes. With the number of electrons transferred, the transfer coefficient was found, from the product of the transfer coefficient and the number of electrons transferred, to be 0.59 for the first oxidation wave and 0.46 for the second.

Linear sweep voltammetry (LSV). Chryssoulakis et al. have demonstrated how the term $(1-\alpha)n$ can be estimated from the slope of the leading edge of a voltammetric wave.²⁵ The greater the electrochemical irreversibility, the broader the wave and thus the smaller the slope. Figure 23 shows the difference between the potential of the peak current (E_p) and the potential corresponding to the current at half the peak height ($E_{p/2}$) for the first oxidation wave as a function of the square root of the sweep rate. By extrapolating the values for $E_p - E_{p/2}$ back to a sweep rate of 0, the working values were obtained. The average of the working values for $E_p - E_{p/2}$ was +0.082 V.

If the process were electrochemically reversible, the peak separation would be given by the equation²⁶:

$$E_p - E_{p/2} = \frac{2.2 RT}{nF} \quad (8)$$

If the process were electrochemically irreversible, the peak separation would be given by the equation²⁷:

$$E_p - E_{p/2} = \frac{1.857 RT}{(1-\alpha)nF} \quad (9)$$

Equation 8 indicates 0.77 electrons would be transferred per mol of electroactive species, if the system were electrochemically reversible. Equation 9 shows the product of the transfer coefficient and the number of electrons transferred would equal 0.65, if the system were electrochemically irreversible. If it is assumed α has a value of 0.5, n would have a value of 1.3 for an electrochemically irreversible case.

There are two methods of evaluating the quasi-reversible system. First, assuming the oxidative process is actually half way between the reversible and irreversible cases (quasi-reversible with a transfer coefficient of 0.5), the number of electrons transferred can be estimated by the average of the values for the two cases. This method results in a value of 1.04 electrons transferred for every mol of electroactive species consumed.

In the second method, a more rigorous approach to the quasi-reversible system is given by the equation:²⁸

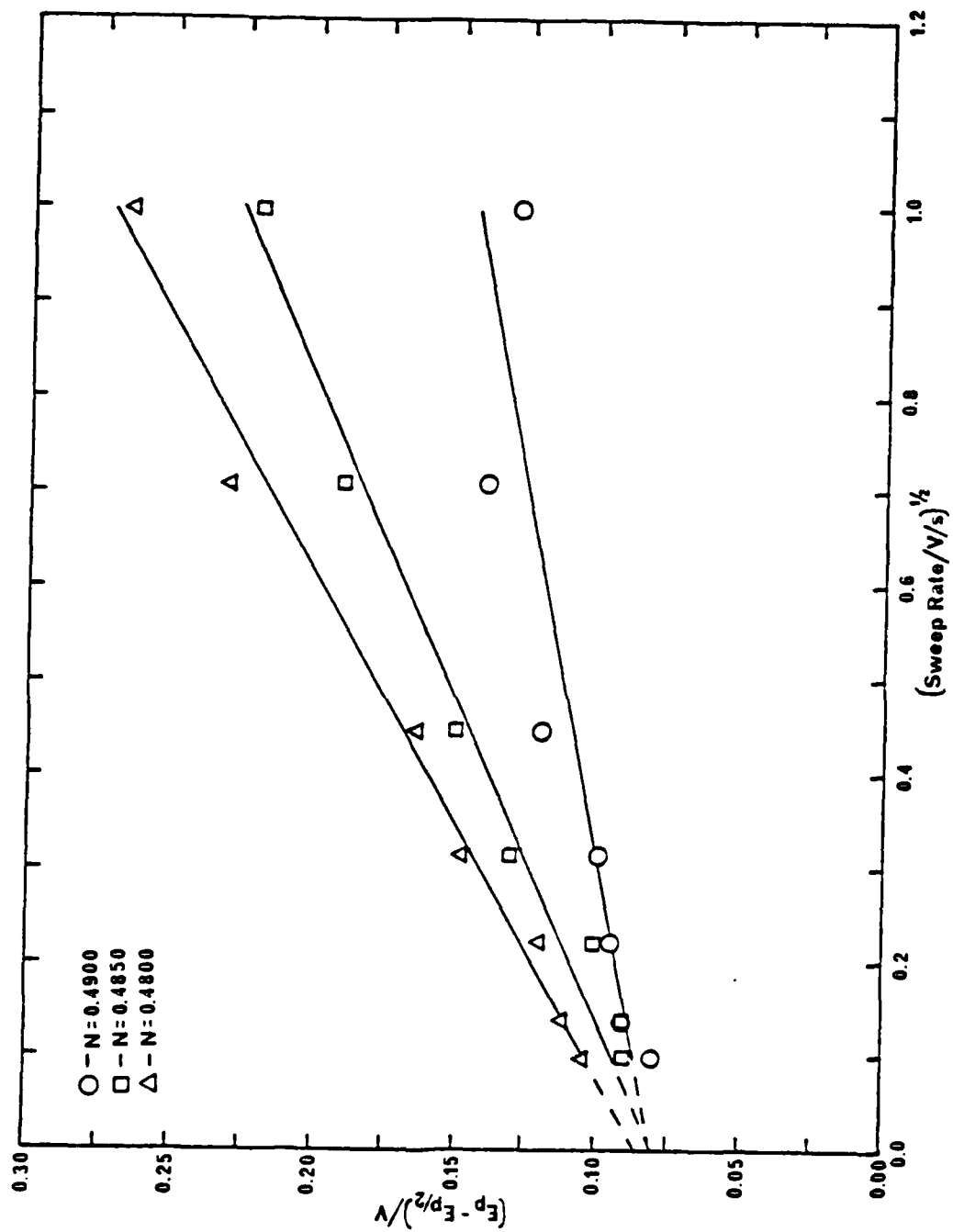


Figure 23. $E_p - E_{p/2}$ as a function of the sweep rate for the first oxidation wave.

$$E_p - E_{p/2} = \frac{\Delta RT}{nF} \quad (10)$$

The term Δ is a complex term describing the kinetics of the electron transfer and the concentration of the electroactive species in the region of the electrode. Δ has a value of 2.2 in the reversible system and 3.7 in the irreversible system. Assuming a mid-range value of 3.0 for Δ gives a value of 1.05 for the number of electrons transferred.

In both of these techniques, the actual number of electrons transferred must be between 0.77 and 1.30 corresponding to the electrochemically reversible and irreversible cases respectively. Table 4 lists a series of possible number of electrons transferred (X) and moles of electroactive species involved (R), along with the resulting value for n . To obtain a value of n within the specified range, it can be seen that at least 4 electrons must be transferred for every 5 molecules of electroactive species converted, but no more than five electrons can be transferred for every 4 molecules of electroactive species converted.

As mentioned previously, the degree of electrochemical reversibility appears to be approximately halfway between the irreversible and reversible cases. The number of electrons and molecules of the electroactive species required to give a reasonable value of n would be quite large, requiring a complex mechanism to explain the transfer. The simplest explanation, fitting all of the observations, is the transfer of one electron for each molecule of the electroactive species consumed, resulting in a value of 1 for n .

Amperometry. If a current is forced to flow, under steady state conditions, through a cell, a potential great enough to oxidize and reduce enough electroactive species to carry the current will be induced. The difference between the induced potential and the "rest" potential observed when no current is flowing is called the overpotential (η), and is measured in volts.

The relationship between the induced current and the overpotential required to carry the current is described by the Tafel equation²⁹:

$$\eta = a + b \ln i \quad (11)$$

where a and b are terms which depend on the conditions under which the experiment is performed. If the experiment involves a completely

TABLE 4 - n for Several Different Moles of Electroactive Species and Number of Electrons Transferred.

X	R	n
1	1	1.00
4	5	0.80
5	6	0.83
5	4	1.25
6	5	1.20

irreversible process and high overpotentials, the Tafel equation takes on the form:³⁰

$$\eta = \frac{\alpha n F}{RT} \ln i_0 - \frac{\alpha n F}{RT} \ln i \quad (12)$$

If the electrochemical process under study is irreversible, equation 12 indicates, a plot of the natural log of the applied current as a function of the observed overpotential will have a linear portion with a slope of $\alpha n F / RT$ for the cathodic, and $(1-\alpha) n F / RT$ for the anodic branch. The extrapolation of the linear portions to a 0 overpotential gives an intercept equal to the natural log of the exchange current (i_0) of the system.

Bard and Faulkner³¹ describe a method, originally put forth by Allen and Hickling, for analyzing systems which are electrochemically quasi-reversible. If the Butler-Volmer equation is rewritten to the form:

$$\ln \frac{i}{1 - e^{nf\eta}} = \ln i_0 - \alpha n f \eta \quad (13)$$

where:

$$f = \frac{F}{RT}$$

a plot of $\ln[i/(1 - e^{nf\eta})]$ as a function of the overpotential, a straight line should result. The slope of the line will equal $-\alpha n F / RT$ for cathodic overpotentials and $(1-\alpha) n F / RT$ for anodic overpotentials, and the intercept is equal to the natural log of the exchange current.

An $N = 0.4883$ and an $N = 0.4688$ bromide melt were made. Each melt was put in an electrochemical cell in which the platinum working electrode was rotated at a rate of 750 rpm, and the potential was observed for a series of imposed oxidative currents.

Figures 24A and 25A show the graphs of the natural log of the current as a function of the overpotential (called a "Tafel Plot"), for the first oxidation wave of each melt composition. As can be seen there are not obvious linear portions of the curves. This non-linear dependence reinforces the belief that the oxidation waves in the basic bromide melt system are due to electrochemically quasi-reversible processes.

Figures 24B and 25B show the plot of $\ln[i/(1 - e^{nf\eta})]$ as a function of the overpotential (called an "Allen-Hickling Plot"), for the first oxidative process. In both of these graphs there is a portion which is linear. The slopes result in a value for $(1-\alpha)n$ of 0.43 and 0.47, for the $N = 0.4883$ and the $N = 0.4688$ bromide melts respectively. Using the method of determining the transfer coefficient and the number of electrons transferred from the product, as discussed in the section on linear sweep voltammetry, it was found that one electron was transferred for the first oxidative wave. The transfer coefficient was found to be 0.57 for the $N = 0.4883$ melt and 0.53 for the $N = 0.4688$ melt.

Even ideal Tafel and Allen-Hickling plots have a limited range (usually from 100 to 200 mV of overpotential) of linearity. Below approximately $\eta = 50$ mV, the reverse electrochemical reaction becomes noticeable, and shifts the current more negative. Above approximately $\eta = 200$ mV, the observed current is limited by mass transfer effects,

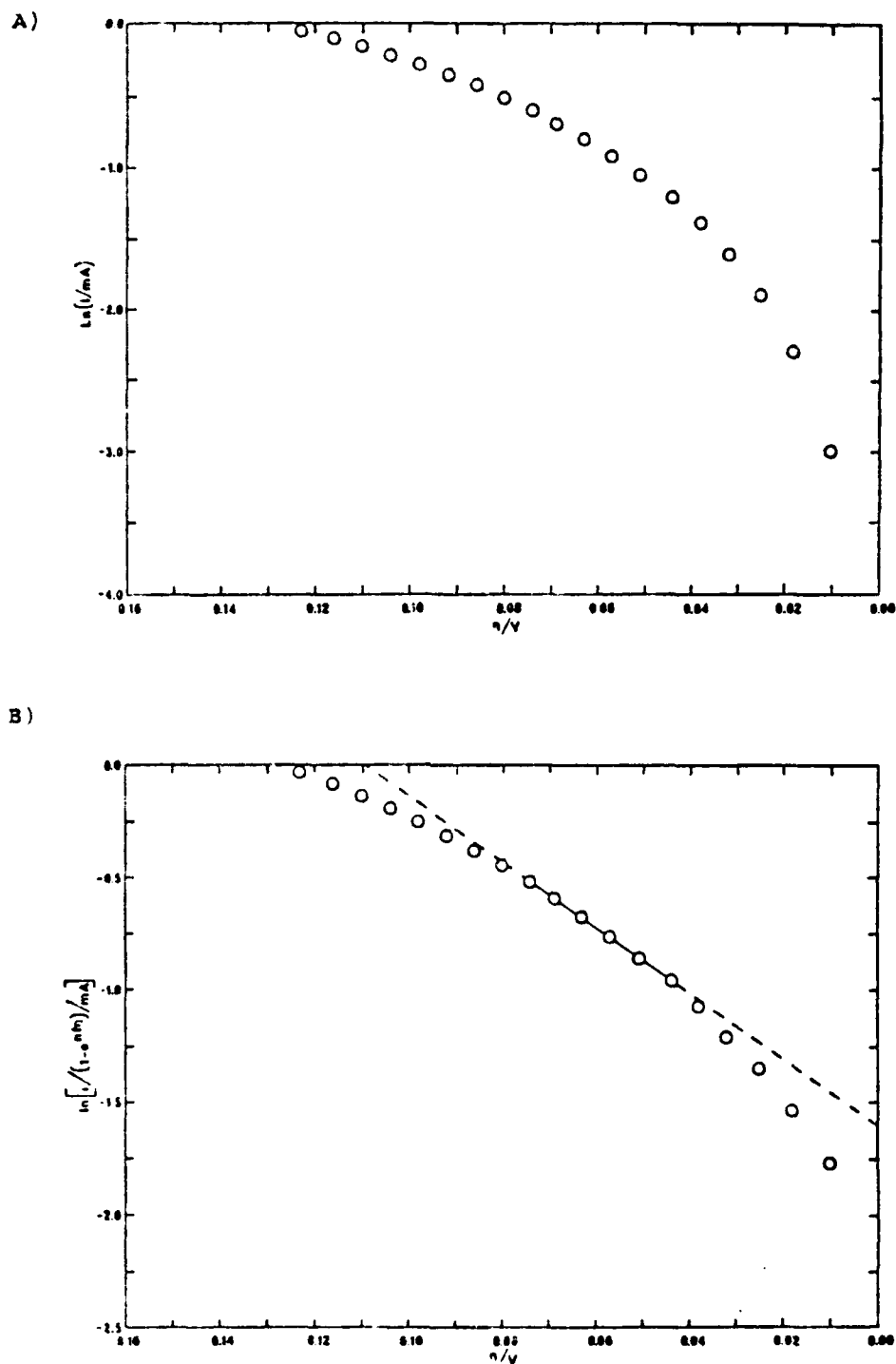


Figure 24. The A) Tafel plot and B) Allen-Hickling plot for the first oxidation wave of an $N = 0.4883$ bromide melt.

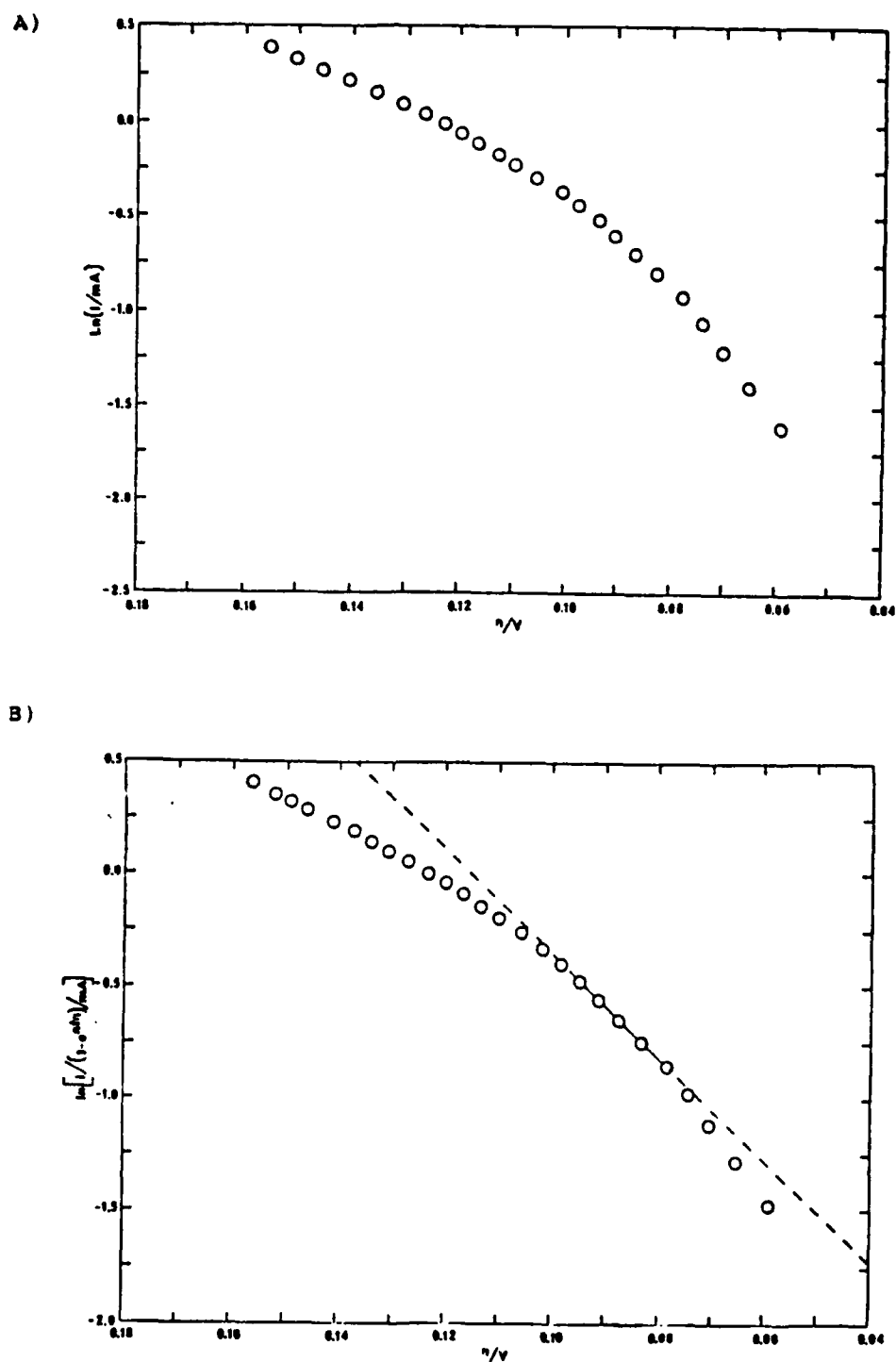


Figure 25. The A) Tafel plot and B) Allen-Hickling plot for the first oxidation wave of an $N = 0.4688$ bromide melt.

causing the observed current to be less than would be expected by the Tafel relationships. The oxidation of the bromide to bromine shows a Allen-Hickling curve whose linear region is limited, not only by the usual processes described above, but also by the overlap of the second wave.

Because of the factors limiting the linear portion of the curve, the position of the line drawn to the Allen-Hickling plot is suspect. Irrespective of the position of the line, the linearity of the Allen-Hickling plots confirms the electrochemical quasi-reversibility of the bromide oxidation. Although the placement of the line, to the curve, should affect the calculation of the number of electrons transferred, per mol of electroactive species, in practice, the constraints put on the values n may have, allows for a reasonable deviation in the positioning of the line without affecting n . These considerations indicate that all of the error, in placing the line to the Allen-Hickling plot will manifest itself in the transfer coefficient. Because of this, the values of α , determined by this method, must be considered suspect.

When there is no net current flowing through the cell, there is still an equilibrium forward and reverse current flowing at each electrode. At the working electrode, this current is called the exchange current. When the exchange current is normalized for the area of the working electrode, it is called the exchange current density (j_0). The exchange current was found to be 0.20 mA for the $N = 0.4983$ melt and 0.19 mA for the $N = 0.4688$ melt. This corresponds to an exchange current density of 0.71 mA/cm², and 0.66 mA/cm² for the $N = 0.4853$ and $N = 0.4688$ melts respectively.

Coulometry. A method of determining the number of electrons transferred in an electrochemical step, independent of the degree of irreversibility, is constant potential coulometry. In this technique, a potential great enough to induce the electrochemical process under investigation, is maintained across a cell containing a known amount of analyte, and the amount of charge required to convert the analyte is observed.

The amount of charge required to consume a given amount of the analyte is determined by one of two means. In the first method, called exhaustive coulometry, a potential is applied long enough to consume all of the analyte. Once all of the analyte is consumed, the current will cease to flow. In the second method, either the formation of the product, or the consumption of the analyte is followed by an independent analytical technique.

In either technique, the charge passed (Q) is related to the amount of analyte (N) present in the sample by the equation:

$$Q = nNF \quad (14)$$

For the first method, once the amount of charge required to convert a known amount of analyte is found, it is a simple matter to determine the number of electrons transferred per mol of analyte. In the second method, if the amount of charge passed is plotted as a function of the amount of analyte converted, a straight line with a slope of nF should result.

Since the products, of the oxidative processes, have been tentatively identified as tribromide and bromine, UV-VIS spectroscopy can be used to

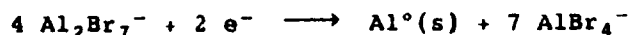
monitor the progress of the coulometry. Calibration curves of bromine and tetramethylammonium tribromide were made, and are shown in Figure 26. Dry acetonitrile was used as the solvent, and 10 mm matched quartz cells were employed. The bromine was found to have a maximum absorbance at 398 nm, and a molar absorptivity of 179. The tribromide ion was found to have a maximum absorbance at 269 nm, and a molar absorptivity of 5110. The linear range of both was found to be acceptable and the degree of linearity was excellent. The maximum concentration of bromine in the linear portion of the calibration curve was found to be 15 mM, and the maximum linear concentration of the tribromide was found to be 0.30 mM.

An $N = 0.4979$ bromide melt was made and a cell was constructed as shown in Figure 27. The working electrode was a platinum mesh and the counter electrode was an aluminum wire in an $N = 0.6061$ bromide melt. Care was taken to have the melt level in the counter cell equal to that in the working cell in order to minimize the hydrostatic pressure and the resultant convective mixing. A potential of +1.250 V, referenced against the usual chloride reference electrode, was applied between the working and the counter electrodes. This potential is sufficiently anodic enough to cause both of the oxidative processes.

Aliquots of the melt were taken at different times during the course of the experiment. The aliquots were dissolved in acetonitrile and the UV-VIS spectra of the resulting solutions were taken. Figure 28 shows the UV-VIS spectra of an aliquot of melt after approximately 30 coulombs were passed through the cell. The absorbance at 269 nm is due to the tribromide anion, indicating the product of one of the electrochemical steps must be tribromide.

Figure 28 also shows the spectra of the same solution approximately 15 minutes after the dilution. Obviously, the concentration of the tribromide observed in the diluted aliquot decreased over time. Since the standard solutions (tetramethylammonium tribromide in acetonitrile) were shown to be stable over time, some component of the melt must allow for the reaction of the tribromide in solution. For this reason it was not possible to determine the concentration of the tribromide in the aliquot and thus a Q vs. N plot could not be constructed.

When the potential is applied to the cell, an oxidative process is forced to occur in the working compartment of the cell, and a reductive process takes place in the counter cell. The bromide in the working compartment of the cell will be oxidized by a process which will be determined at the conclusion of the experiment. The most likely cathodic process, occurring in the counter cell, is the reduction of the heptabromoaluminate by the reaction:



As the potential is maintained across the cell, a positive charge will build up in the working compartment of the cell, due to the consumption of bromide, and a negative charge will build in the counter cell, due to the formation of tetrabromoaluminate. In order to maintain charge balance in each of the compartments, ions must migrate between the two compartments. Since a positive charge is built up in the working compartment, and a negative charge is built up in the counter cell, the charge will be balanced by cations migrating from the working compartment to the counter cell, and anions migrating from the counter to the working compartment of the cell.

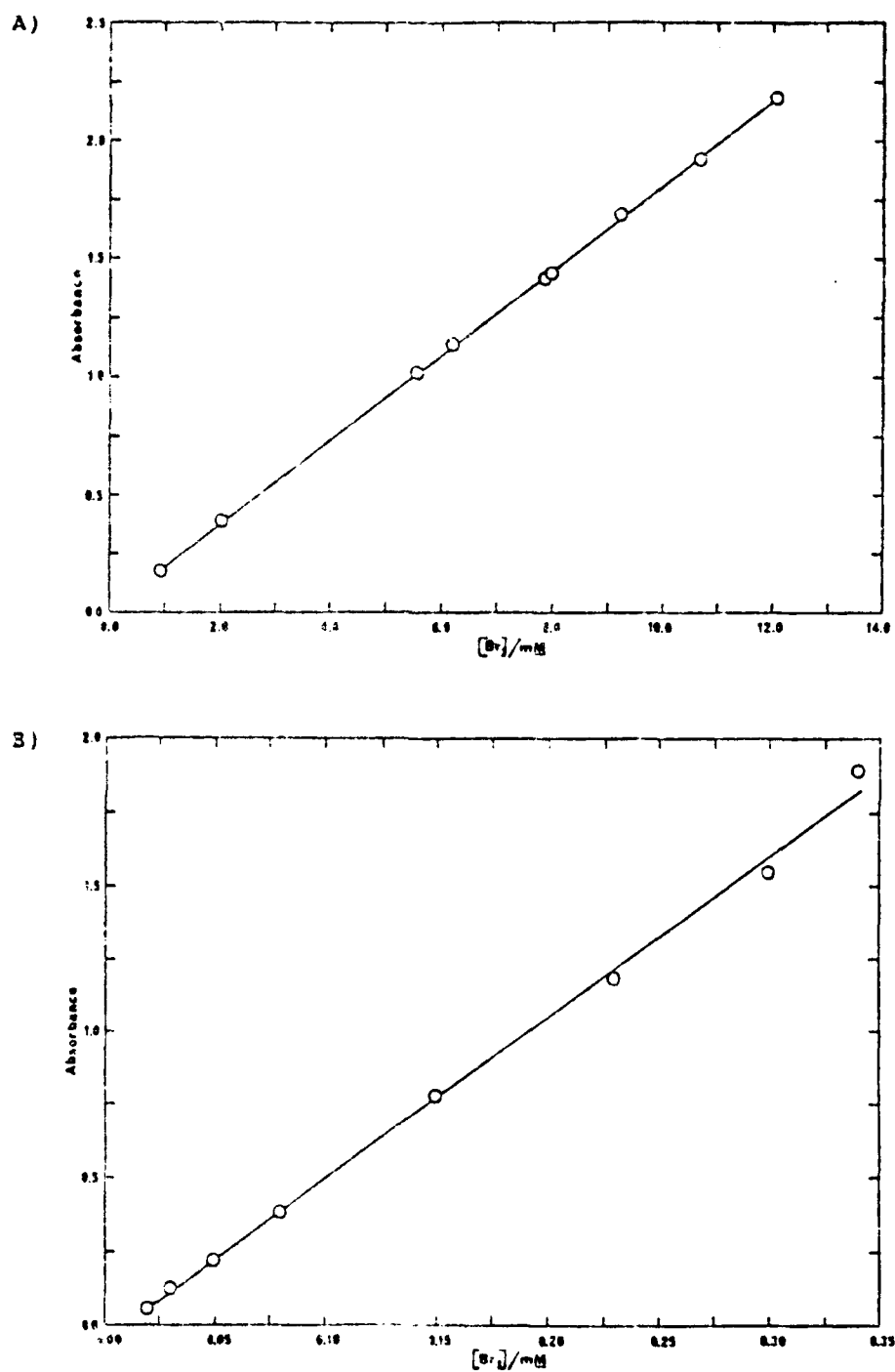


Figure 27. The UV-VIS calibration curves for A) tribromide, and B) bromine.

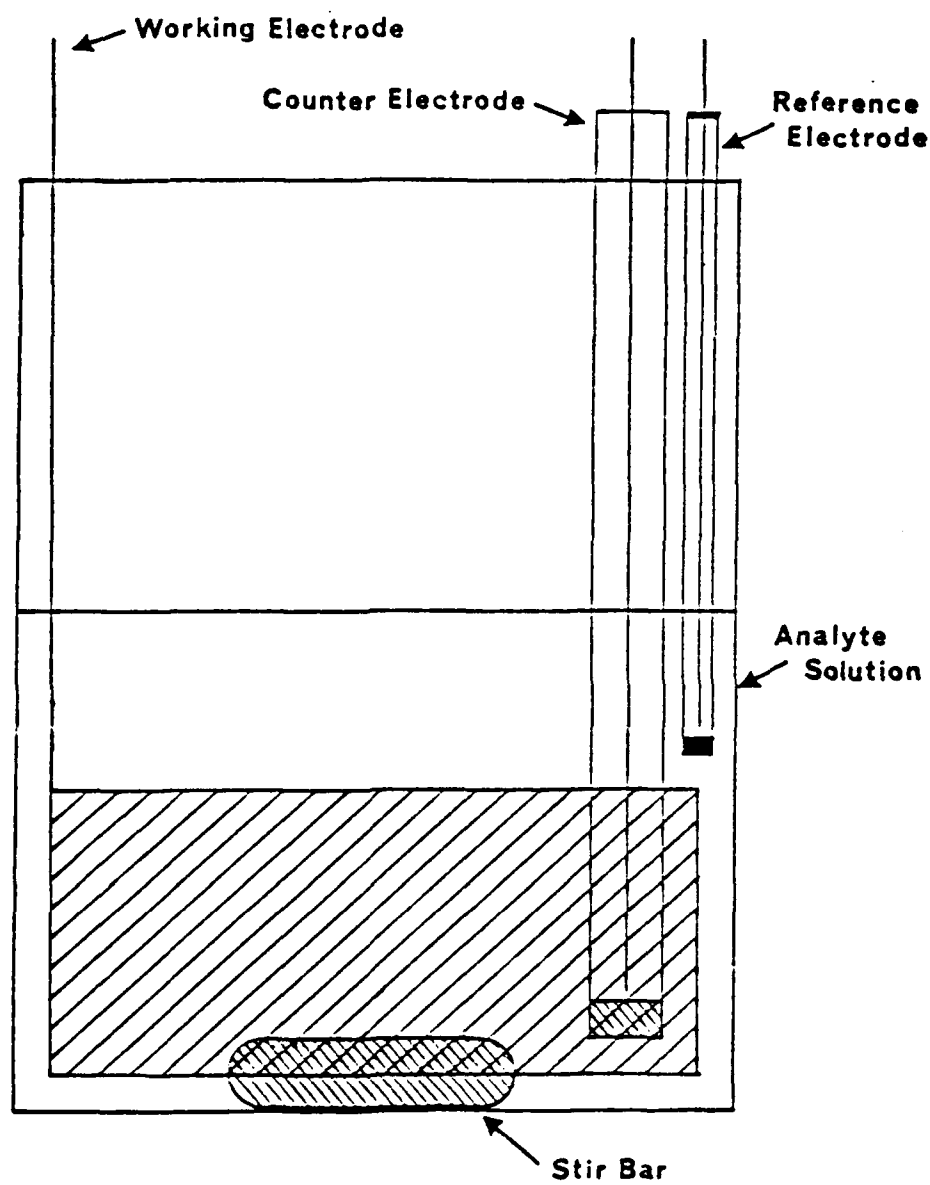


Figure 27. Coulometric Cell.

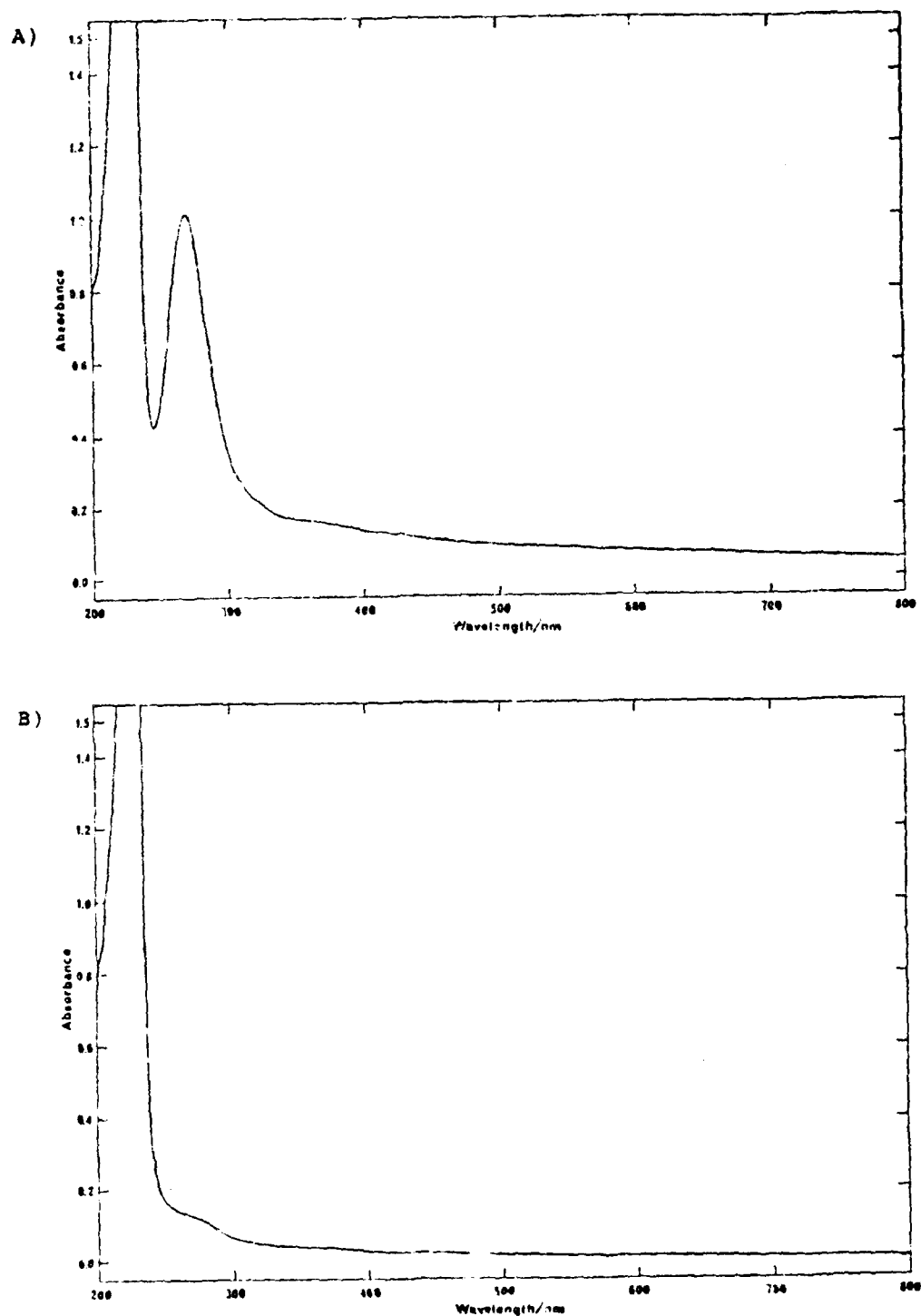


Figure 23. UV-VIS of an aliquot A) immediatly, and B) 10 minutes after being removed from the coulometric cell.

The only cations present, in the molten salt system, are the imidazolium cations, thus all of the positive charge will be transferred by the imidazolium ions. A couple of different types of anions, though, are present in the counter cell compartment. The negative charge will be transferred by both the hepta- and the tetrabromoaluminate. Although the tetrabromoaluminate is stable in the working compartment, any heptabromoaluminate reaching the working compartment will react with the bromide ion, by the reaction:



effectively decreasing the bromide ion concentration.

The fraction of the charge carried by the different ionic species present in the bromide melt, called the transference number (t) of the species, was determined by Hussey et al.²³ It was found that 76% of the charged is carried by the imidazolium cation, irrespective of the composition of the melt. The transference numbers of the anionic species, though, are dependent on the composition of the melt. This dependence is shown in Figure 29. Since the melt in the counter cell had a composition of approximately $N = 0.61$, graphically it was found that 10% of the total charge transferred was carried by heptabromoaluminate anions, and 14% of the charge was carried by the tetrabromoaluminate.

Correcting for the volumes of the aliquots removed, 46.49 coulombs of charge were passed to exhaustively oxidize the bromide. Since, at the beginning of the experiment, there were 29.401 gms of an $N = 0.4979$ bromide melt in the working compartment of the cell, there were initially 5.3987×10^{-4} mols of bromide present. Adding 10% to the charge passed, to account for the migration and subsequent reaction of the heptabromoaluminate anions with the bromide anions, 51.14 coulombs of charge were effectively consumed by the oxidative process. Substituting these values into equation 14 results in a value of 0.98 for n . This can be rounded to the transfer of one electron for each molecule of bromide oxidized.

Summary. All of the techniques gave results consistent with the processes first proposed by Popov and Geske⁸ for bromide dissolved in acetonitrile. The rotating disk linear sweep voltammetry showed one electron was transferred in each of the oxidative processes. While amperometry and linear sweep voltammetry were not able to indicate the number of electrons transferred in the second process, the techniques did support the idea that one electron was passed in the first oxidative process.

The coulometry indicates not only that one electron is transferred for the combination of the first and second anodic processes in the basic bromide melt, but also that the product of one of the oxidative processes is tribromide ion. Since the other techniques indicate one electron is transferred for each of the individual processes, the two processes must be linked through a chemical reaction. The coulometry indicates the overall (sum of the two individual processes) process is:



which can also be written as:

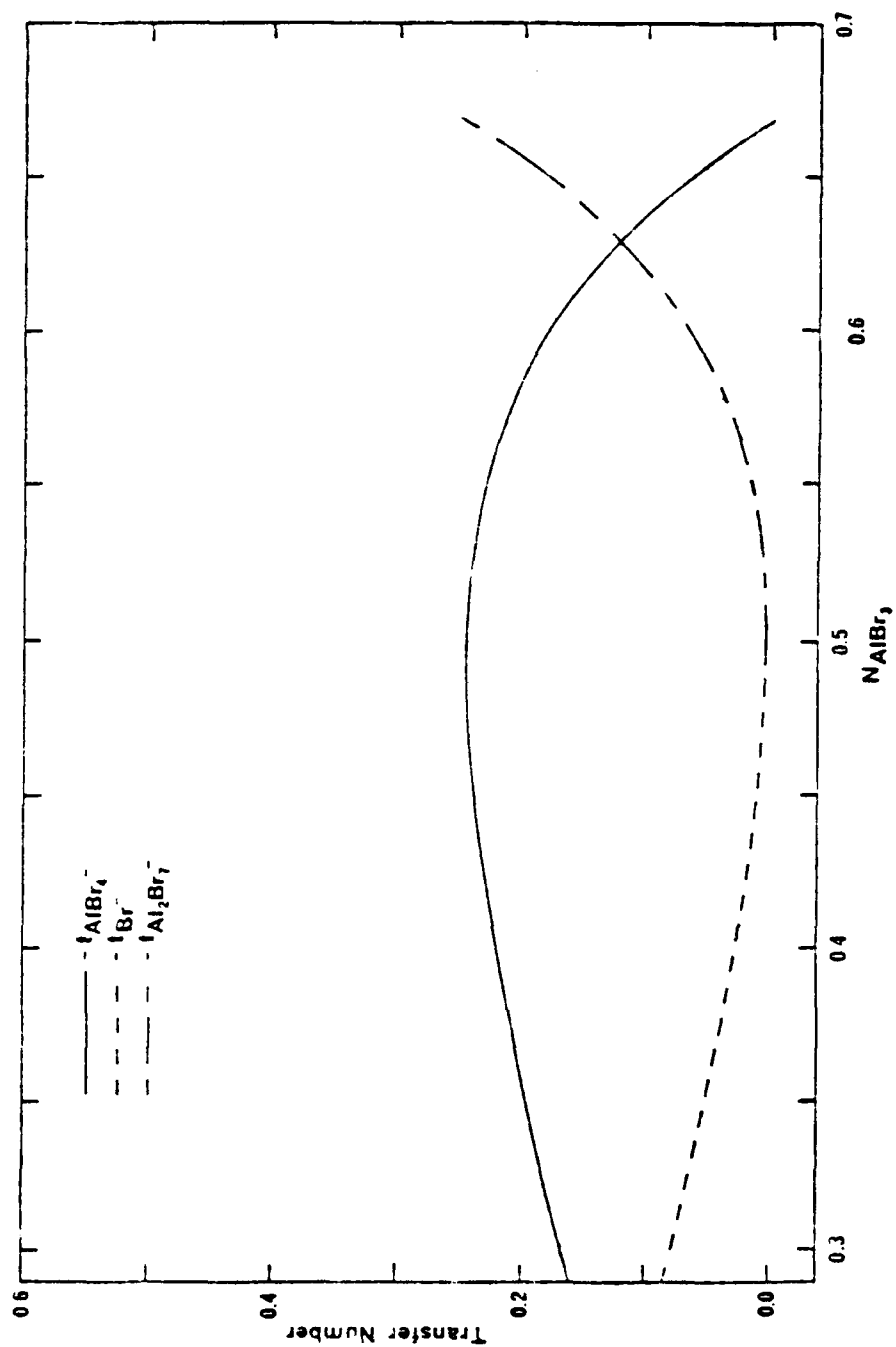
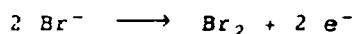
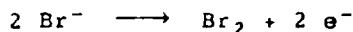


Figure 29. The transference numbers of the anionic species as a function of the melt composition.



This evidence indicates the couple responsible for the first wave is:



The chemical reaction:



occurs to remove the bromine produced in the first oxidative step from the melt. The second oxidative process is described by the reaction:



The number of electrons transferred and the transfer coefficients are summarized in Table 5 for the different techniques. Iwasita and Giordano³² studied the electrochemistry of lithium bromide and bromine in an acetonitrile solvent system. Using a platinum working electrode and a silver-silver bromide reference electrode, they determined one electron was transferred in each of the oxidative processes. They also found the transfer coefficient ranged from 0.44 to 0.52 for the first wave and 0.49 to 0.63 for the second. The values for the number of electrons transferred and the transfer coefficients found in this work agree well with those determined by Iwasita and Giordano.

Chemical Additions

Since the current observed in a voltammetric process is proportional to the concentration of the electroactive species, increasing the concentration of the species will increase the observed current. To take advantage of this, tetramethylammonium tribromide was prepared and added to the melt. If, as proposed above, the second oxidation wave of the basic bromide melt system is due to the oxidation of the tribromide anion to bromine, the current of the second wave should increase, upon the addition of tribromide.

TABLE 5 - Summary of the Transfer Coefficient and the Number of Electrons Transferred for the Various Techniques

Technique	Wave 1		Wave 2	
	α	n	α	n
RDLSV	0.407	1.0	0.542	1.0
LSV	N.A.	1.0	N.A.	N.A.
Amperometry	0.549	1.0	N.A.	N.A.
Coulometry		n = 1.0*		

*number of electrons transferred for the first and second processes combined.

The CV of an $N = 0.490$ bromide melt is shown in Figure 30. Upon addition of the tribromide anion to the melt, the rest potential (the potential observed when no current is flowing, defined by the types and concentrations of the species present in the system) shifted from -0.053 V to -0.281 V vs. the chloride reference electrode. The CV of the resulting solution is also shown in Figure 30. Since the current of the second oxidation wave increased markedly, this wave is probably due to the oxidation of the tribromide anion.

Electrochemistry is a notoriously bad technique for the resolution of electrochemical processes with similar oxidative or reductive potentials. Since the typical reversible voltammetric wave is on the order of 50 mV wide at half of the peak height, any other electroactive species with a formal electrode potential within approximately 50 mV of the actual species will be indistinguishable from the analyte species. For this reason, chemical additions can not be used as absolute proof of the species involved in an electrochemical process, but it is another piece of evidence to support the assignments made in the previous section.

Diffusion Coefficients

An important property in the electrochemistry of a system is the diffusion coefficient of the electroactive species in the solvent being used. The rate a species is transported to a point in space, by the diffusive process, is called the flux of the species. The flux (J) of a species, at any point in space, is described by Fick's first law:

$$J = -D \frac{\partial C}{\partial x} \quad (15)$$

where D is the diffusion coefficient of the species and $\partial C/\partial x$ is the concentration gradient at that point in space.

Since the diffusion coefficient of a species is a constant, for any defined solvent system, the flux of the species, and thus the current observed for the process, is proportional to the concentration gradient of the species at the electrode surface. By altering the concentration gradient in a known manner, the diffusion coefficient is readily obtained.

The area around the electrode, where the only means of mass transport is through the diffusive process, is called the diffusion layer. Since, at the outer edge of the diffusion layer, the concentration of the electroactive species is equal to the concentration in the bulk of the solution, and the concentration of the species at the electrode surface can be controlled to equal zero, it is apparent that altering the thickness of the diffusion layer will alter the concentration gradient.

Two techniques are typically used to alter the thickness of the diffusion layer in a well defined manner. In the first technique, called rotating disk linear sweep voltammetry, the thickness of the diffusion layer is altered by forcing hydrodynamic transport of the species towards the electrode surface. In the second technique, called chronoamperometry, the thickness of the diffusion layer varies as the region around the electrode is depleted of the electroactive species.

Rotating disk linear sweep voltammetry. As an electrode is rotated in the analyte solution, hydrodynamic convection towards the region of the electrode occurs. Although the electrode is rotated, the region immediately next to the electrode surface remains stationary relative to

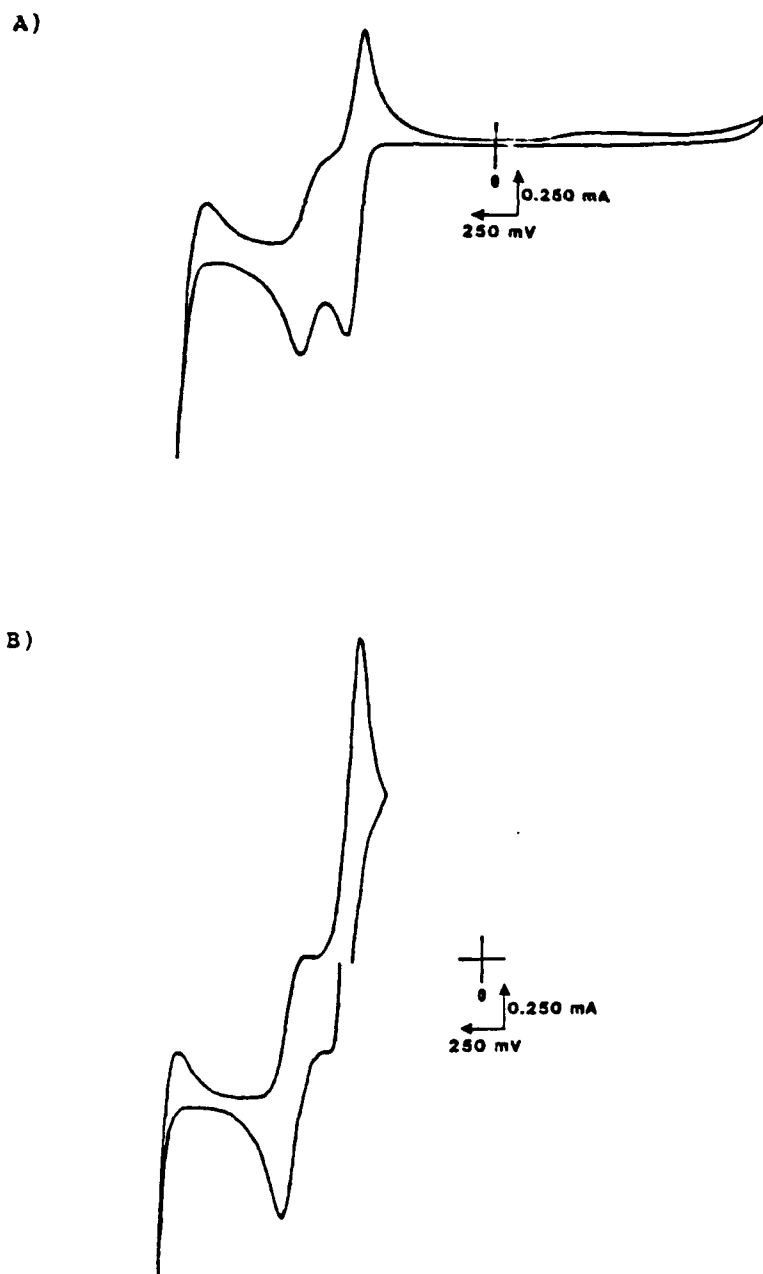


Figure 30. The CVs of an $N = 0.4900$ bromide melt A) before, and B) after adding tetramethylanmonium tribromide.

the electrode surface. The angular velocity of the analyte solution, with respect to the electrode surface, increases as the distance from the electrode increases. The faster the electrode is rotated, the thinner the diffusion layer becomes.

At slow rotation rates, the diffusion layer is relatively thick, and thus the concentration gradient is small. As the rotation rate is increased, the thickness of the diffusion layer decreases, and the concentration gradient increases. As the rotation rate is increased, the current observed for the electrochemical process will also increase, due to the increased concentration gradient.

The current-rotation rate relationship is described by the Levich equation³³:

$$i_{lim} = 0.620nFAD^{2/3}\omega^{1/2}\nu^{-1/6}C_r^* \quad (16)$$

where i_{lim} is the limiting current at any given rotation rate, ω , in rad/s. D is the diffusion coefficient, and C_r^* is the concentration, of the analyte in the bulk of the solution. The kinematic viscosity of the analyte solution is given by ν . If the limiting current is plotted as a function of the square root of the rotation rate, a straight line, with a slope of:

$$m = 0.620nFAD^{2/3}\nu^{-1/6}C_r^* \quad (17)$$

should result. Any deviations of the plot of the current as a function of the rotation rate from linearity indicates the electroactive species is being brought to, or away from, the electrode surface by a process other than the hydrodynamic convection induced by the rotating electrode.

Figure 31 shows the limiting current of several bromide melt compositions as a function of the square root of the rotation rate. Since the waves are a combination of two processes, the limiting current of each process is determined by extrapolating the linear portions of both, the rising portion of the voltammogram and the observed plateau. The intersection of the two extrapolations corresponds to the limiting current of the process. The diffusion coefficients for each species are listed in Table 6. The plots for each rotation rate show good linearity, indicating the system is under diffusion control.

Chronoamperometry (ChAmp). When a potential is placed across a solution containing a species which is electroactive at that potential, the species is consumed by either a reductive or oxidative process. When the species is consumed, diffusion towards the electrode surface, at a rate dictated by the diffusion coefficient of the species, begins to occur. As the electroactive species diffuses towards the electrode surface, the region around the electrode becomes depleted of the electroactive species.

As the diffusion proceeds, the distance from the electrode, at which the concentration of the electroactive species is equal to the concentration in the bulk of the solution (the diffusion layer) increases. As the diffusion layer becomes thicker, the concentration gradient, and therefore the current, decreases.

The decrease in the concentration of the species, in the region of the electrode, over time, manifests itself as a decrease in the current

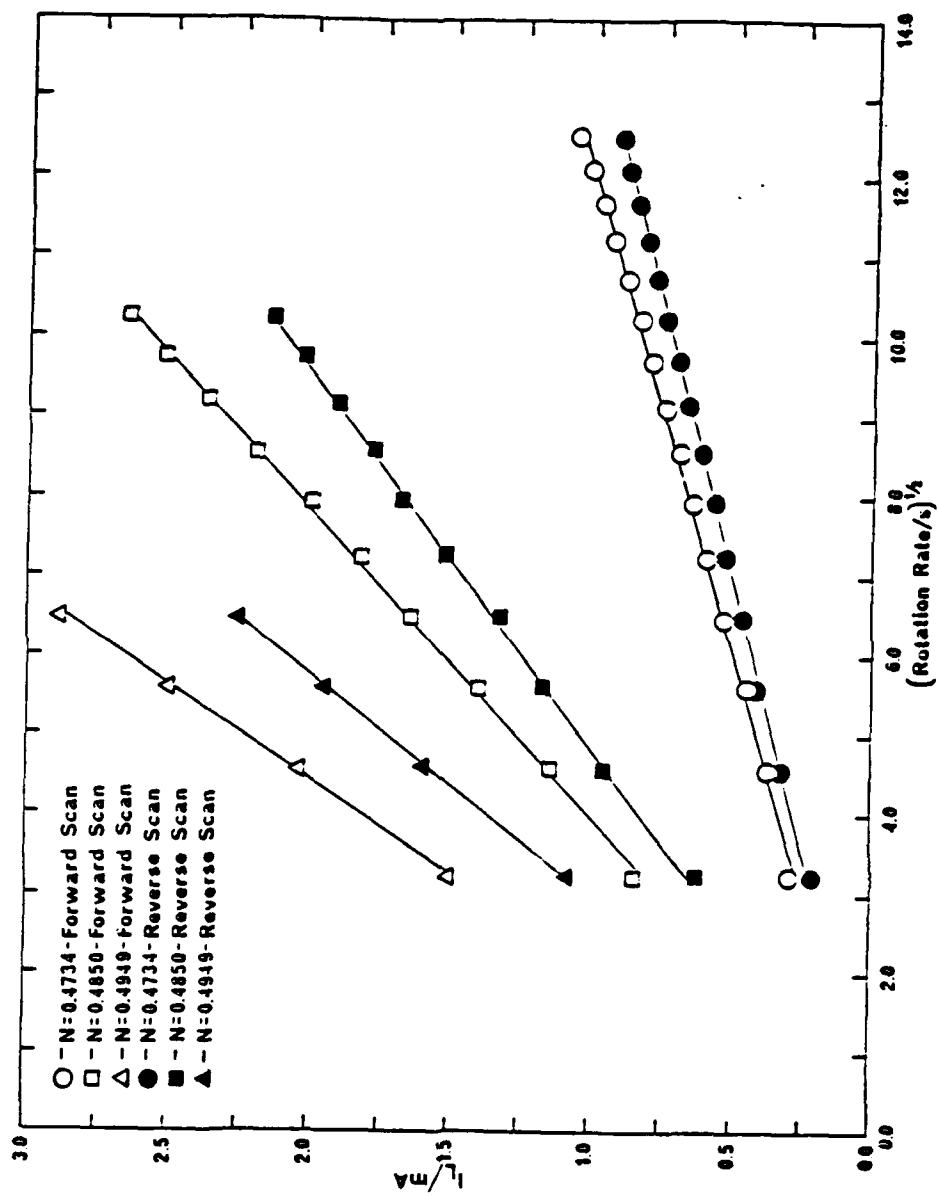


Figure 31. The limiting current as a function of the square root of the rotation rate for several melt compositions.

TABLE 6 - Diffusion Coefficient as a Function of Anionic Composition by RDLSV.

Wave 1		
N	[Br ⁻]/M	D/cm ² /s
0.4949	8.51 x 10 ⁻²	7.05 x 10 ⁻⁷
0.4850	2.49 x 10 ⁻¹	7.69 x 10 ⁻⁷
0.4734	4.40 x 10 ⁻¹	7.40 x 10 ⁻⁷
		7.38 x 10 ⁻⁷
Wave 2		
N	[Br ₃ ⁻]/M	D/cm ² /s
0.4949	2.83 x 10 ⁻²	9.41 x 10 ⁻⁶
0.4850	8.31 x 10 ⁻²	9.78 x 10 ⁻⁶
0.4734	1.46 x 10 ⁻¹	9.04 x 10 ⁻⁶
		9.41 x 10 ⁻⁶

flowing through the cell. This current time (t) relationship is described by the Cottrell equation³⁴:

$$i = \frac{nFAD^{1/2}C_r^*}{\pi^{1/2}t^{1/2}} \quad (18)$$

The Cottrell equation indicates that, barring any non-diffusive loss of the analyte, the current will decay as the inverse square root of time, in a manner proportional to the diffusion coefficient.

If the current observed in a Chronoamperometry experiment is plotted as a function of the inverse of the square root of time, a straight line with an intercept of zero and a slope of:

$$m = \frac{nFAD^{1/2}C_r^*}{\pi^{1/2}} \quad (19)$$

will result. Figure 32 shows this current time relationship, and Table 7 gives the diffusion coefficients for a series of melt compositions.

The plots of the current as a function of the inverse square root of time show a noticeable degree of non linearity at short times. This is due to some process occurring at the surface of the electrode which decreases the amount of current which may flow through the cell. As will be shown later, at very high scan rates, bromine can be seen to adsorb on the electrode surface.

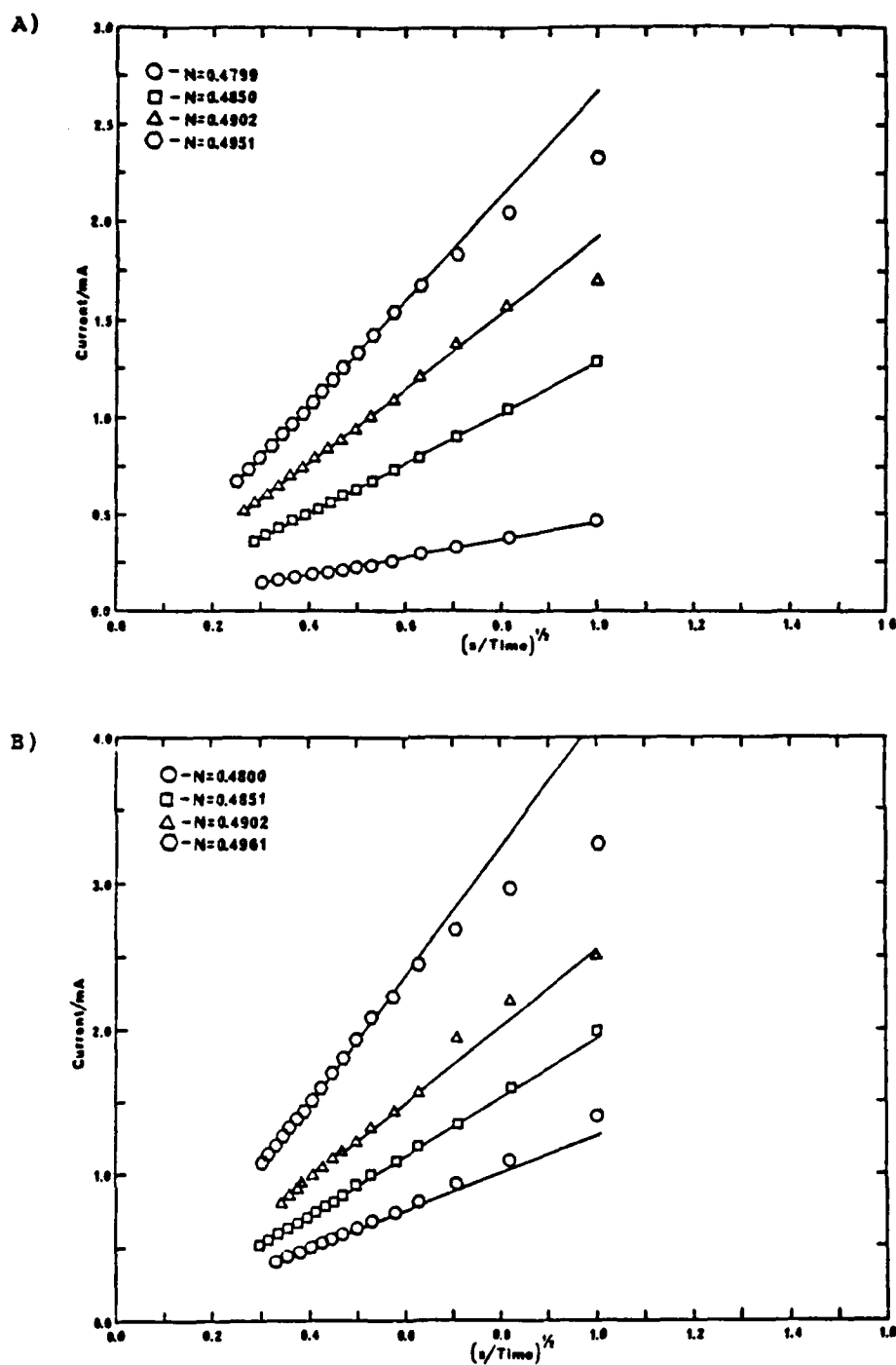


Figure 32. Current as a function of the inverse square root of time for several melt compositions.

TABLE 7 - Diffusion Coefficient of the Bromide as a Function of the Melt Composition by ChAmp

N	[Br ⁻]/M	D/cm ² /s
0.4961	6.51 x 10 ⁻²	2.14 x 10 ⁻⁷
0.4951	8.12 x 10 ⁻²	1.44 x 10 ⁻⁷
0.4902	1.62 x 10 ⁻¹	2.83 x 10 ⁻⁷
0.4902	1.16 x 10 ⁻¹	5.54 x 10 ⁻⁷
0.4851	2.48 x 10 ⁻¹	2.84 x 10 ⁻⁷
0.4850	2.47 x 10 ⁻¹	2.64 x 10 ⁻⁷
0.4800	3.32 x 10 ⁻¹	2.58 x 10 ⁻⁷
0.4799	3.31 x 10 ⁻¹	2.79 x 10 ⁻⁷
0.4750	4.41 x 10 ⁻¹	4.35 x 10 ⁻⁷
		3.02 x 10 ⁻⁷

At very short times there is a large concentration of bromine formed, which takes a finite amount of time to be removed from the region of the electrode, by the subsequent reaction. During this time the bromine is adsorbed to the electrode surface, effectively decreasing the area of the electrode, and thus inhibiting the current. As the experiment proceeds, the adsorbed bromine is removed from the electrode by the subsequent chemical reaction, and the current approaches its expected values.

Summary. The diffusion coefficient for the bromide was found to be 7.39×10^{-7} cm²/s or 3.02×10^{-7} cm²/s depending on the method used. This difference (59%) is typically attributed to differences in the techniques used. The diffusion coefficient for the tribromide was estimated to be 9.4×10^{-6} cm²/s. It was not possible to determine the diffusion coefficient for the bromine by either technique.

Mastragostino, Valcher, and Lazzari³⁵ determined the diffusion coefficients of the bromide system in an acetonitrile solvent system. They found the diffusion coefficients of the bromide and the tribromide to be equal to 7.3×10^{-5} cm²/s and the diffusion coefficient of the bromine to be 15.8×10^{-5} cm²/s. The ratio of the diffusion coefficients of the bromide solvated in acetonitrile to that when it is solvated in a melt is 21.

Lipsztajn and Osteryoung³⁶ determined the diffusion coefficient of the chloride ion, in an almost neutral chloride melt, to be 9.55×10^{-7} cm²/s. This compares to the values they reported that Macagno and Giordano determined of 2.4×10^{-5} cm²/s in an acetonitrile solvent. The ratio of the diffusion coefficients of the chloride solvated in acetonitrile to that when it is solvated in a melt is 25.

As can be seen, the diffusion coefficient of a species, in a melt, is much less than that for the same species in an acetonitrile solution. This is due to the size and shape of the ionization sphere around the species in an ionic melt. Since the bromide is negatively charged, it will draw positively charged species around it. When a species diffuses, not only the species under study, but also the electrostatically associated species, must diffuse. Mastragostino et al.³⁵ used a low concentration of TEAP as a supporting electrolyte. The size of the ion sphere is relatively small and sphere-sphere interactions are minimal.

In the chloroaluminate molten salts, however, considerable evidence suggests the anionic species of a melt exist in a fairly rigid and ordered system. The structure proposed by Dieter et al.³⁷ is shown in Figure 33. The chloride, and the tetrachloroaluminate, are alternately sandwiched between two fairly large imidazolium cations, in a structure not unlike a polymeric chain. Not only are these solvation spheres large, but, a considerable amount of sphere-sphere interactions also exists. Since the chloride must break this structural order to be able to diffuse, the species diffuses at a much slower rate. The similarity of the differences between melt and acetonitrile solutions for the chloride and bromide systems (as shown by the ratios of the diffusion coefficients) argues that the bromoaluminate molten salt system has a structural rigidity similar to that of the chloride system.

The tribromide is seen to diffuse quicker than the bromide, even though it is much larger in size. This difference can be explained in two ways. First, the structure of the solvation sphere may be disrupted by the differences in the size of the ions. Second, the charge to size ratio is less for the tribromide than for the bromide, allowing the bromide to form a tighter solvation sphere than the tribromide. The actual explanation is probably a combination of the two mechanisms, but either mechanism results in the bromide having a tighter solvation sphere than the tribromide. Since the tribromide is held less rigidly, it will tend to diffuse by itself, without the associated solvation sphere. Because of this, although the tribromide ion is, in itself larger than the bromide ion, the species which actually diffuses is smaller for the tribromide than it is for the bromide ion.

Heterogeneous Rate Constant

The rate at which electrons are transferred from the electrode surface to the electroactive species is called the heterogeneous rate constant (k°). Since the electrode takes part in the reaction (transfer) of the electrons with the electroactive species, the composition of the electrode affects the rate constant. The only electrode for which the heterogeneous rate constant was determined was platinum.

The heterogeneous rate constant was determined by two means. The two methods can be distinguished from one another by the assumptions used in each. The first technique uses the separation of the peak potentials, as a function of the rate the potential is scanned, to determine the rate constant. This method assumes no information about the rate constant is given by the rest of the I-E curve. In the second method, called "semiintegral electroanalysis", all of the information found in the forward scan of a CV is employed, by integrating the area under the I-T curve. Unlike a method later proposed by Bond, Henderson and Oldham³⁸, the semiintegral technique uses only one point of the reverse scan to determine the rate constant.

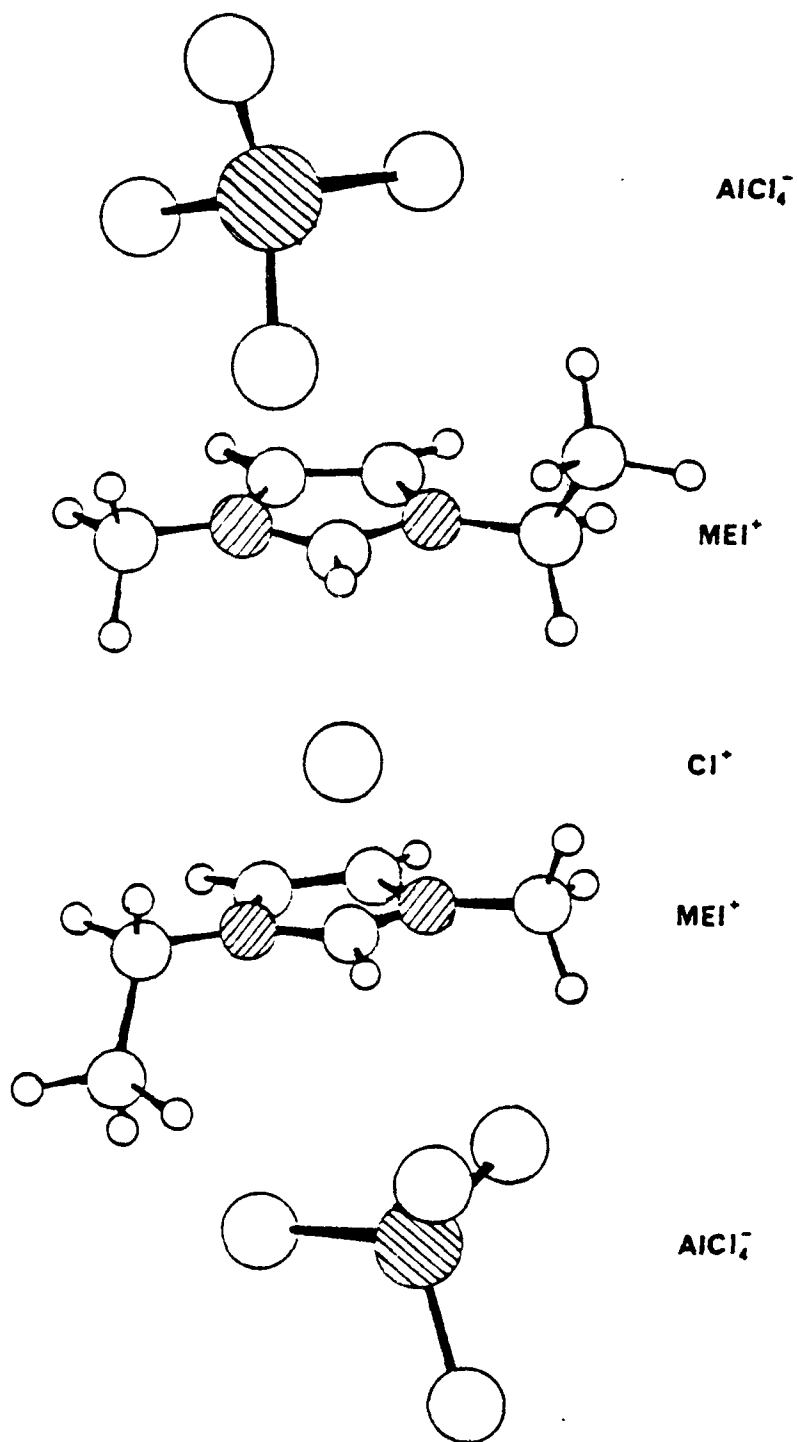


Figure 33. Proposed structure of a chloroaluminate molten salt.

Peak separation. In 1965 Nicholson described a simple method of quickly determining the heterogeneous rate constant from the separation of the anodic and the cathodic peak potentials of an electrochemical process.³⁹ The shape, and position, of the oxidation and reduction waves of an electrochemical process are dependent on the kinetics of the electron transfer of the process. As the rate of electron transfer becomes slower, the degree of electrochemical irreversibility becomes greater and the oxidation and reduction peaks become more separated. Because of the effect of the rate of electron transfer on the peak separation, the peak separation as a function of the sweep rate can be used to estimate the heterogeneous rate constant.

In the basic bromide melt system, not only is the peak separation dependent on the sweep rate, but also on the concentration of the bromide in the melt. As the concentration of the bromide increases, the peaks become more separated. Figure 34 shows the peak separation as a function of the bromide concentration. A working value of the separation was determined by extrapolating the peak separation back to a value corresponding to a value of 0 bromide concentration.

In his paper, Nicholson defined a term, ψ , which is an indication of the degree of electrochemical reversibility. As the system approaches an electrochemically reversible system, ψ approaches a limit of 7. If ψ has a value of 0.001, the system acts as if it were electrochemically irreversible. Nicholson also worked out the value of ψ for various values of ΔE_p , using a value of 0.5 for the transfer coefficient. Figure 35 shows a plot of ψ as a function of ΔE_p , using the values determined by Nicholson.

Once the value of ψ is graphically determined from the peak separation, the heterogeneous rate constant is determined from the equation:

$$\psi = \frac{\left[\frac{D_o}{D_r} \right]^{\alpha/2} k^\circ}{\left[\frac{\pi n F \nu D_o}{RT} \right]^{1/2}} \quad (20)$$

where D_o is the diffusion coefficient of the oxidized form, and D_r is the diffusion coefficient of the reduced form of the analyte. The rate at which the potential is varied is given by the term ν . If, as Nicholson suggested, it is assumed the value of the diffusion coefficients of the oxidized and reduced forms of the species are equal, equation 15 simplifies to:

$$\psi = \frac{k^\circ}{\left[\frac{\pi n F \nu D_o}{RT} \right]^{1/2}} \quad (21)$$

Since it was not possible to determine the diffusion coefficient of the bromine, the values of the heterogeneous rate constants were determined by equation 16 for the oxidation of bromide to bromine, and for the oxidation of tribromide to bromine. The values of the rate constants are listed in Table 8.

Semiintegral electroanalysis. Keith B. Oldham⁴⁰ first coined the term "semiintegral analysis" in 1972, when he introduced semiintegral and

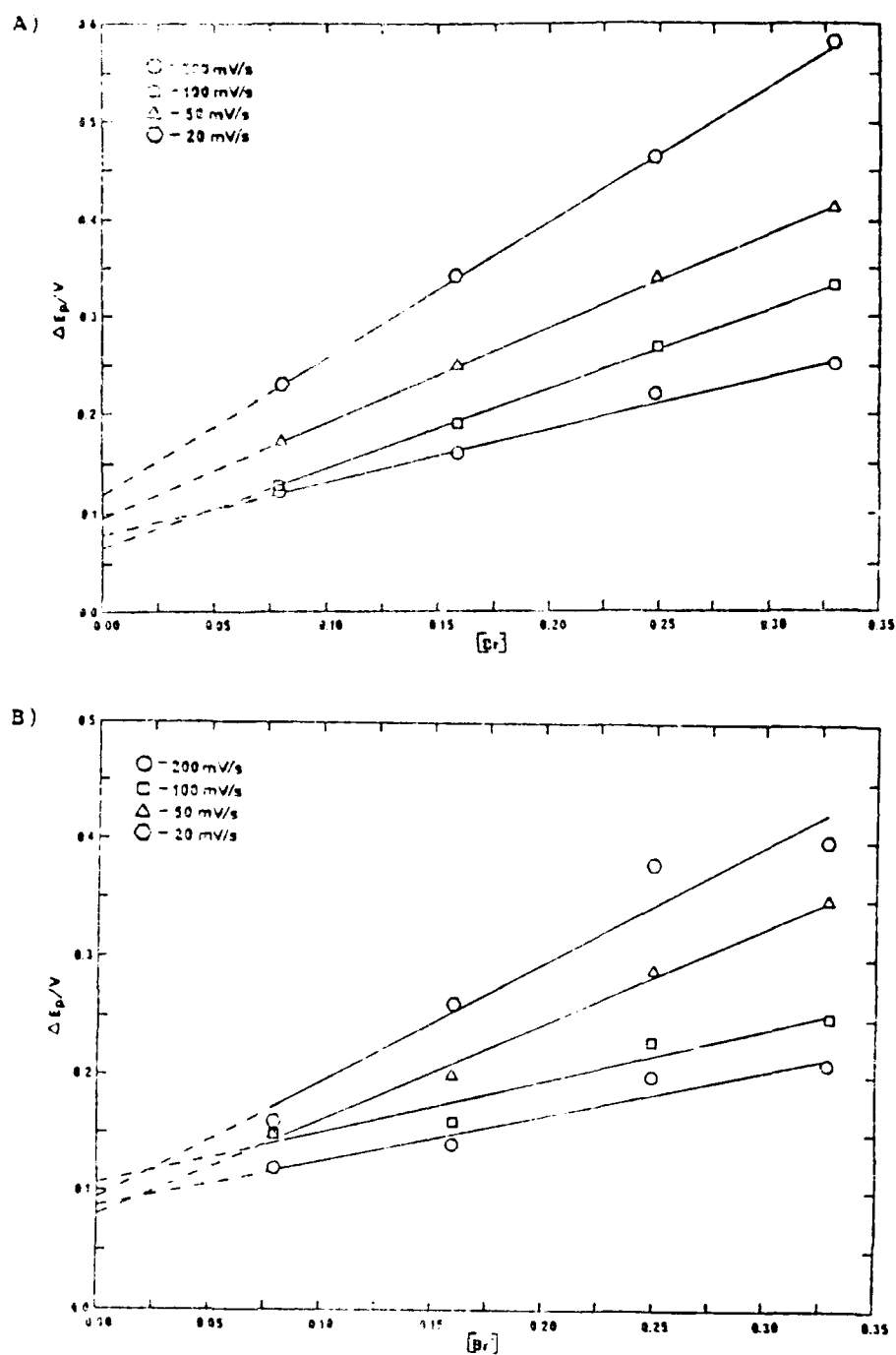


Figure 3a. The peak separation as a function of the bromide concentration for the A)first, and B)second oxidation wave.

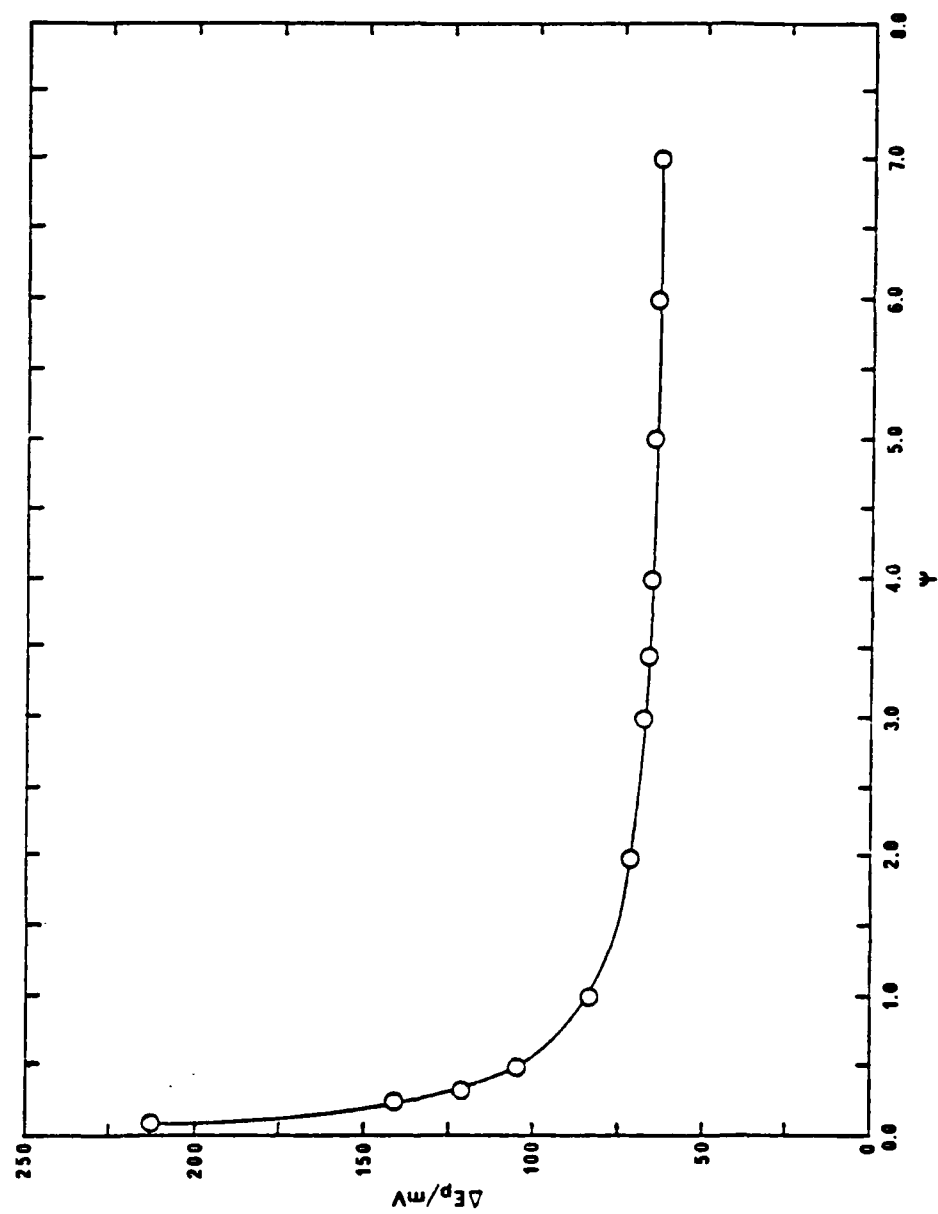


Figure 35. The peak separation as a function of ψ .

TABLE 8 - Heterogeneous Rate Constant as a Function of the Sweep Rate

Wave 1			
$v/\text{mV/s}$	$\Delta E_p/\text{mV}$	ψ	$k^0/\text{cm/s}$
50	77	1.31	8.37×10^{-3}
100	81	1.07	9.67×10^{-3}
200	96	0.62	7.92×10^{-3}
500	117	0.38	7.68×10^{-3}
			8.41×10^{-3}

Wave 2			
$v/\text{mV/s}$	$\Delta E_p/\text{mV}$	ψ	$k^0/\text{cm/s}$
50	86	0.90	3.68×10^{-3}
100	107	0.47	2.71×10^{-3}
200	79	1.20	9.80×10^{-3}
500	94	0.69	8.91×10^{-3}
			6.28×10^{-3}

semidifferential operations and proposed their usefulness in electrochemical analysis. In 1972, Grenness and Oldham⁴¹ introduced a method called "semiintegral electroanalysis", which is a much more rigorous approach to the determination of electrode kinetics, than the peak separation method of Nicholson. In this paper, Grenness and Oldham carefully derived the theory for the semiintegral analysis of current functions. The proposed semiintegral (m) has the general form:

$$m(t) = \frac{d^{1/2} i}{dt^{1/2}}(t) \quad (22)$$

where i is the current at any time t . It was shown the semiintegral technique is valid for any current function where the mass transport is limited to semiinfinite linear diffusion.

Two methods have been proposed for performing the integration. First, Oldham⁴² described a method of using a resistor ladder to obtain a real time analog representation of the semiintegral during the course of the experiment. Second, Bond, Henderson, and Oldham³⁸ described a digital technique using a method called the RLO integral approximation, to determine the value of the semiintegral at any point in time.

The RLO approximation uses the equation:

$$m = \frac{4\Delta}{3\pi} i_J + \sum_{j=1}^{J-1} i_j \left[(J-j+1)^{3/2} - 2(J-j)^{3/2} + (J-j-1)^{3/2} \right] \quad (23)$$

to determine the semiintegral (m) for the J^{th} data point. Δ is the time interval between the data points, and i is the current at the specified data point. Figure 36 shows the currents of the two oxidation waves, as well as the semiintegral as a function of time. As can be seen, a plot of the semiintegral as a function of time closely approximates a polarogram observed at a dropping mercury electrode, and has been termed a "neopolarogram".

As a process becomes more irreversible, the waves tend to spread out. This spreading of the waves results in a slower increase in the area under the current time curve. The kinetics of the electron transfer can be obtained from these neopolarograms in a manner similar to that for the linear sweep experiments.

Goto and Oldham have shown that the shape of the neopolarogram is described by the equation:

$$E = E_h + \frac{RT}{(1-\alpha)nF} \ln \frac{k_s}{(D^{1-\alpha} D' \alpha)^{1/2}} + \frac{RT}{(1-\alpha)nF} \ln Q \quad (24)$$

where:

$$Q = \frac{m_{\infty} - m \left[1 + \exp \frac{nF}{RT} (E - E_h) \right]}{i} \quad (25)$$

Equation 24 indicates that a plot of $\ln Q$ as a function of the potential will yield a straight line with a slope of $RT/(1-\alpha)nF$. With the slope, and the value of $\ln Q$, when the potential is equal to E_h , the value of the heterogeneous rate constant can be determined.

E_h is a potential corrected for the non-ideality of the solvent system, much in the same manner as described in the earlier section on the formal electrode potentials. Goto and Oldham use the equation:

$$E_h = E_s + \frac{RT}{2nF} \ln \frac{D'}{D} \quad (26)$$

to find E_h . Since the values of E_h , determined by this method, were one to two orders of magnitude larger than was reasonable, it was felt that the diffusion coefficients for the oxidized and reduced forms of the bromide species varied too greatly for this method to give reasonable values for E_h . Instead, Goto and Oldham also showed that, according to the equation:

$$E = E_h + \frac{RT}{(1-\alpha)nF} \ln \frac{m_{\infty} - m}{m} \quad (27)$$

a plot of the potential as a function of $\ln[(m_{\infty} - m)/m]$ will give a line with a slope of $RT/(1-\alpha)nF$ and an intercept of E_h . Figure 37 shows this relationship for the first and second oxidation waves. The values of E_h were determined to be +0.753 V for the first, and +1.124 for the second oxidative processes.

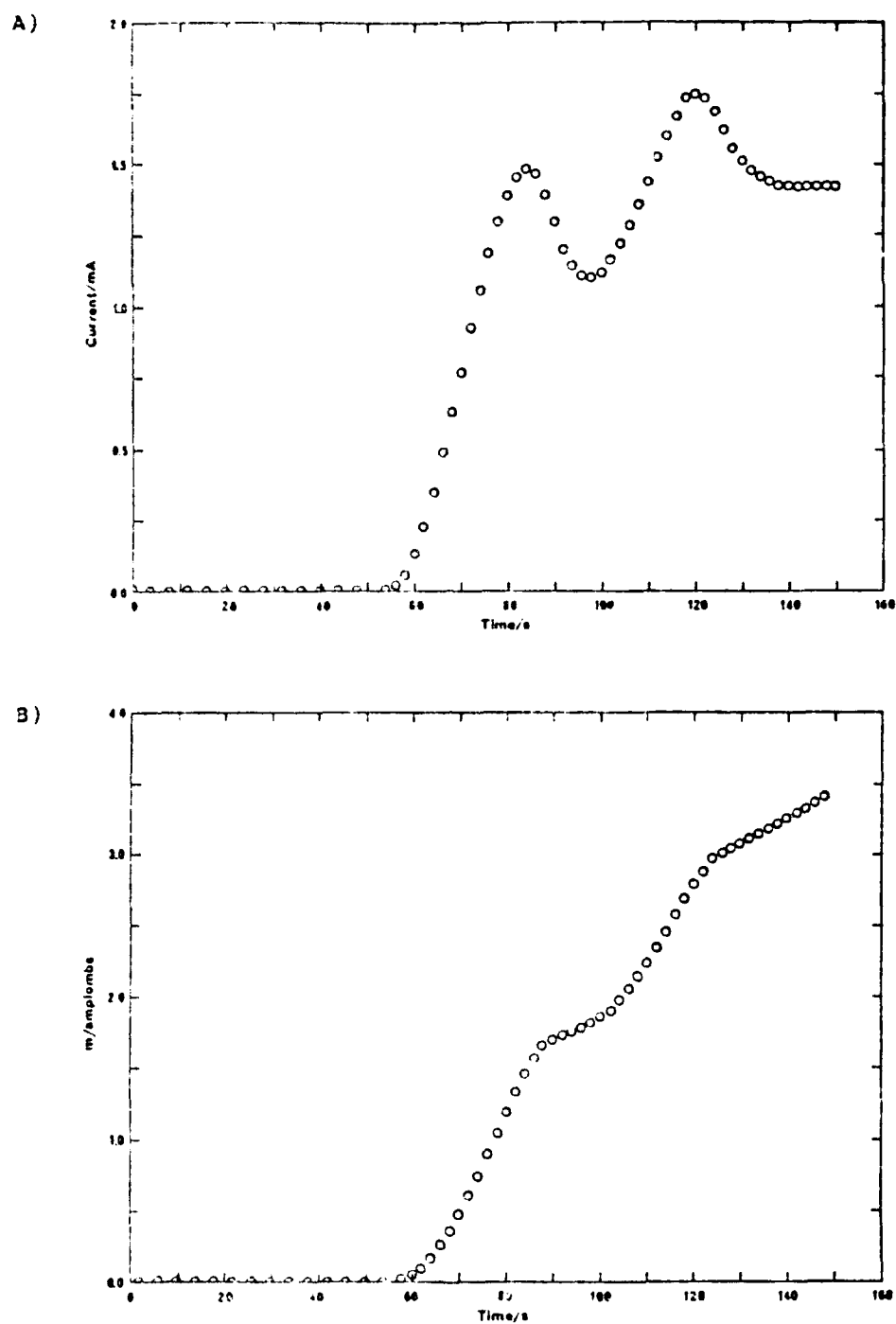


Figure 36. The A)current, and B)semiintegral as a function of time for an $x = 0.4600$ bromide melt.

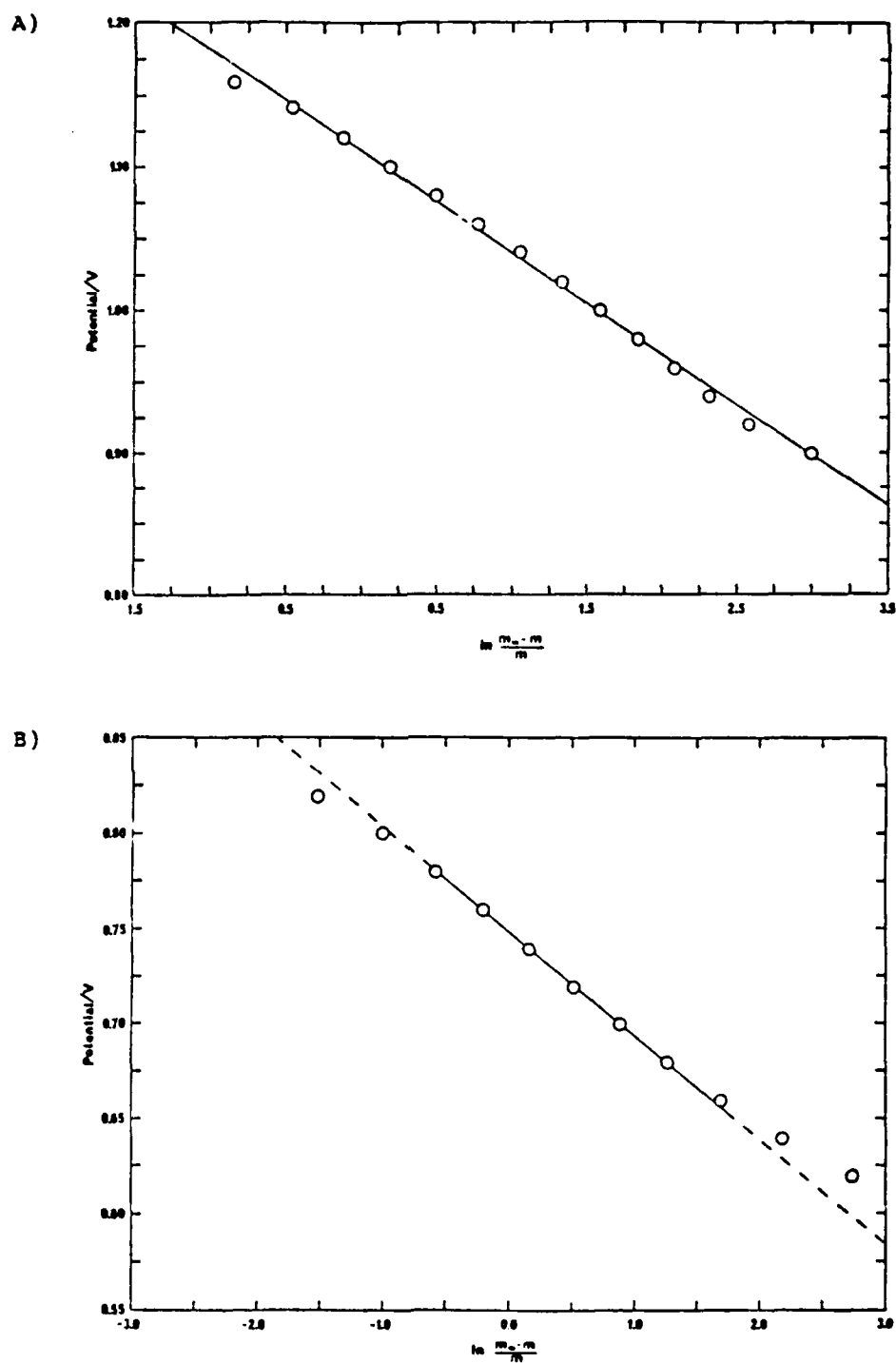


Figure 37. The potential as a function of $\ln [m_\infty - m/m]$ for A) the first, and B) the second oxidation waves.

The graphs of $\ln i$ as a function of the potential are shown in Figure 38 for both of the oxidative processes. Both graphs show regions of linearity. The heterogeneous rate constants were found to be 6.74×10^{-3} cm/s and 4.64×10^{-10} cm/s for the first and second waves, respectively.

Summary. The heterogeneous rate constant, for the oxidation of the bromide to tribromide, was found to be 8.41×10^{-3} cm/s, by the peak separation method, and 6.74×10^{-3} cm/s by the semiintegral method. The difference (24.3%) is usually attributed to differences in the methods used, and the assumptions made in each procedure. Differences of less than an order of magnitude are usually considered acceptable. For the oxidation of the tribromide to bromine, the heterogeneous rate constant was found to be 6.28×10^{-3} cm/s, by the peak separation method, and 4.64×10^{-10} cm/s, by the semiintegral method. This difference is obviously not reasonable. Not only is the value of the rate constant determined by the semiintegral technique less than the smallest rate constant ever determined, but a rate constant of 4.64×10^{-10} cm/s would indicate the oxidation is electrochemically irreversible. The oxidation of the tribromide to bromine has already been shown to electrochemically quasi-reversible, indicating the value of the rate constant determined by the semiintegral technique is in error. This error can be attributed to an overlap of the two oxidation waves, as well as an incomplete understanding of the theory behind the semiintegral technique.

Bard and Faulkner⁴³ indicate the fastest heterogeneous rate constants, determined to date, range from 1 to 10 cm/s, and the slowest are less than 1×10^{-9} cm/s. The rate of the electron transfer, to the electroactive species, is usually determined by the amount of rearrangement the species must undergo to accept the charge. The fastest rate constants are typically for the oxidation or reduction of an aromatic organic molecule, and the slowest is for something which requires a large amount of rearrangement such as the reduction of oxygen to hydrogen peroxide.

The 10^{-2} to 10^{-3} range for the heterogeneous rate constants argues that, although the oxidation of bromide and tribromide is not electrochemically reversible, it is on the high end of quasi-reversibility. The relatively high rate constant indicates the electrode kinetics are reasonably fast and should not be a concern in the study of the bromoaluminate molten salt systems for high energy density storage applications.

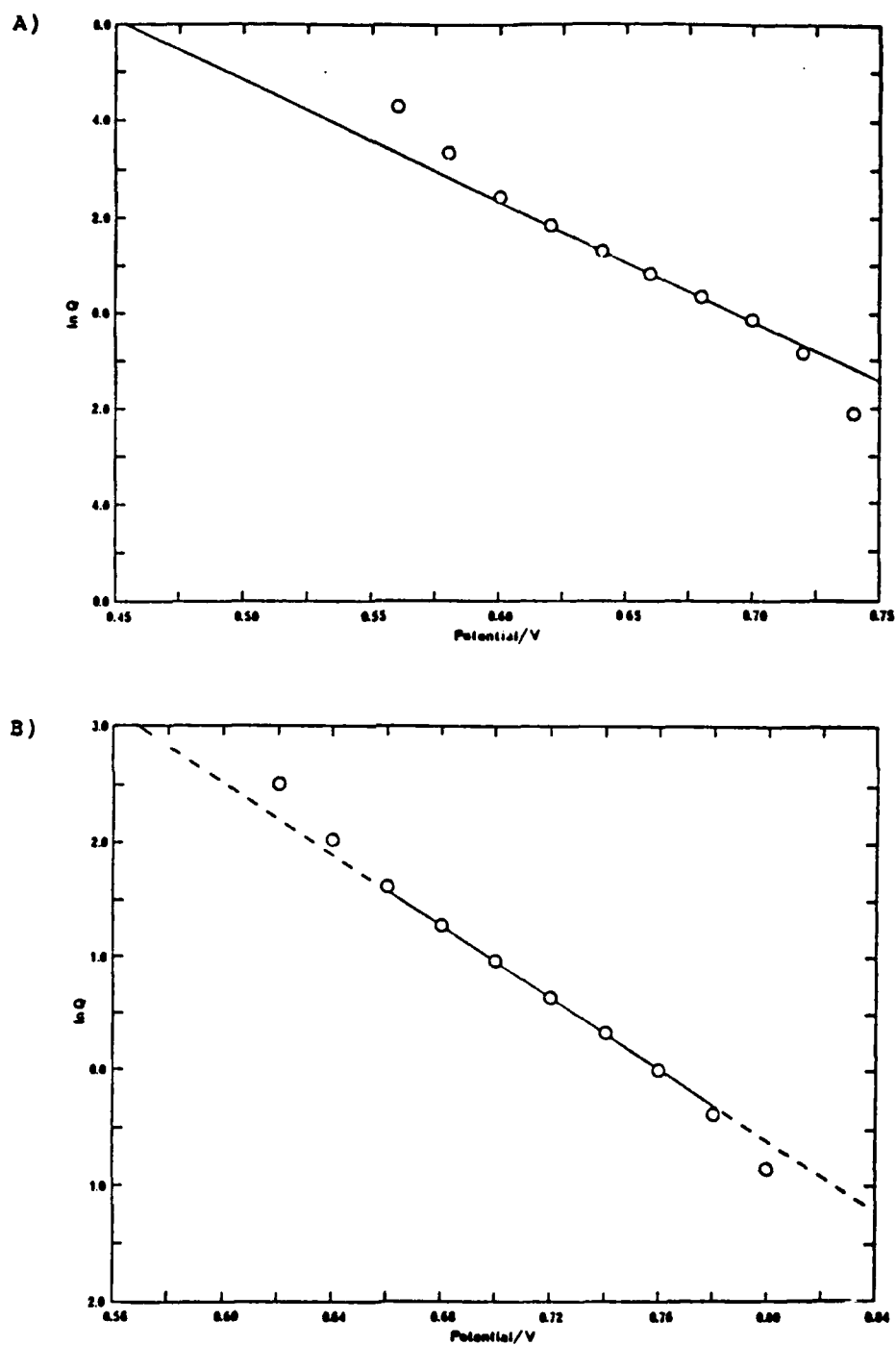


Figure 38. $\ln Q$ as a function of the potential for A) the first, and B) the second oxidation waves.

CHAPTER 5

DISCUSSION OF THE CHEMICAL PARAMETERS

Reaction Rate

As shown in the previous chapter, the first oxidative process, in the basic bromoaluminate molten salt system, is due to the oxidation of bromide to bromine, which then undergoes a chemical reaction with bromide to form tribromide. The oxidation and the following chemical reaction can be generalized by the equations:



and:



Several electrochemical techniques exist, which may be used to monitor the rate of a following chemical reaction. These techniques can be broken down into two types, depending on the species monitored. In the first type, the loss of the product, formed by the electrochemical reaction, is observed electrochemically. In the second type of experiment, the buildup of the product of the following chemical reaction, is monitored.

Typical examples of the first type of experiment are chronopotentiometry with current reversal and double potential step chronoamperometry. In these techniques, the current or the potential is stepped to a value which will force the production of Ox. As Ox is produced, it will be removed from the region of the electrode not only by diffusion, but also by the following chemical reaction. Therefore, when the potential or the current is reversed, less Ox, than predicted by theory, will be in the region of the electrode to undergo the reduction to form R. In the case of double potential step chronoamperometry and chronopotentiometry with current reversal, the decrease in Ox will result in lower observed currents and shorter transition times, respectively.

All of the experiments of the first type rely on the product of the chemical reaction (Ox') not being electroactive at the potential or the current needed to reverse the electrochemical process. For the bromide system, the bromine produced in the first oxidative process reacts to form tribromide. Since one molecule of bromine reacts to form one molecule of tribromide, and both the bromine and the tribromide are reduced at a potential less than the potential of the first wave, the number of electroactive molecules remains constant. Because the number of electroactive molecules remains constant, this type of experiment, which relies on the decrease in the concentration of the electroactive species, would not be helpful in determining the kinetics of the chemical reaction.

An example of the second type of experiment is fast scan linear sweep voltammetry. As the potential is scanned through the wave of the process

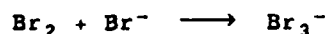
of interest, Ox is produced. As the scan continues, some of the Ox is consumed by the following chemical reaction, forming Ox'. If the product of the chemical reaction is itself electroactive, a wave due to the oxidation of the Ox' will be observed. As the rate at which the potential is scanned is increased, less Ox' will be formed, and the current due to the oxidation of the Ox' will decrease. If the potential is scanned rapidly enough, no current for the oxidation of Ox' will be seen.

Figure 39 shows the CV of an N = 0.49 bromide melt at several different scan rates. At a scan rate of 1 V/s, the two oxidative processes are well defined. As the scan rate is increased, the current due to the second oxidative process decreases, and finally becomes a small shoulder on the trailing edge of the first wave. At a scan rate of 100 V/s, a sharp break becomes apparent on the top of the first oxidation wave, indicating a passivation of the electrode surface. Passivation is usually due to the adsorption of a species onto the surface of the electrode, which interferes with the transfer of electrons from the electrode to the electroactive species in the solution.

Several researchers^{11,32,44} have found that, in acetonitrile, the actual mechanism for the oxidation of the bromide to bromine is for bromide ions to be oxidized, to monatomic bromine, and adsorbed onto the surface of the electrode. Two adsorbed bromine atoms then combine to form a bromine molecule. The bromine molecule then desorbs from the electrode surface, into solution, where it subsequently reacts with the bromide in the solution, forming tribromide. The passivation of the electrode seen in high scan rate experiments, and the lowering of the current seen in the chronoamperometric experiments, indicate the mechanism proposed by other workers for other non-aqueous solvent systems also reasonably explains the behavior of the oxidation of the bromide in the bromoaluminate molten salt system.

Equilibrium Constant

It has been shown that the bromine formed by the initial oxidation of the bromide undergoes the following chemical reaction:



Since the melt system has been shown to affect the electrochemical properties of the bromide, it is reasonable to assume the chemical parameters of the reaction are also altered by the melt system. The preferred electrochemical method of determining the equilibrium constant of a reaction is with a potentiometric titration.

The Nernst Equation:

$$E = E^\circ + \frac{RT}{nF} \ln \frac{[\text{Ox}]}{[\text{R}]} \quad (28)$$

is used to relate the equilibrium potential observed in an electrochemical system to the concentrations of the species in the solutions. Experimentally, a neutral bromide melt was made, and a series of MEIB additions were made to the melt. While the working electrode was rotated, the rest potential was observed after each addition of MEIB.

A similar titration was also performed on a system of bromine dissolved in acetonitrile with a TEAP supporting electrolyte. In order

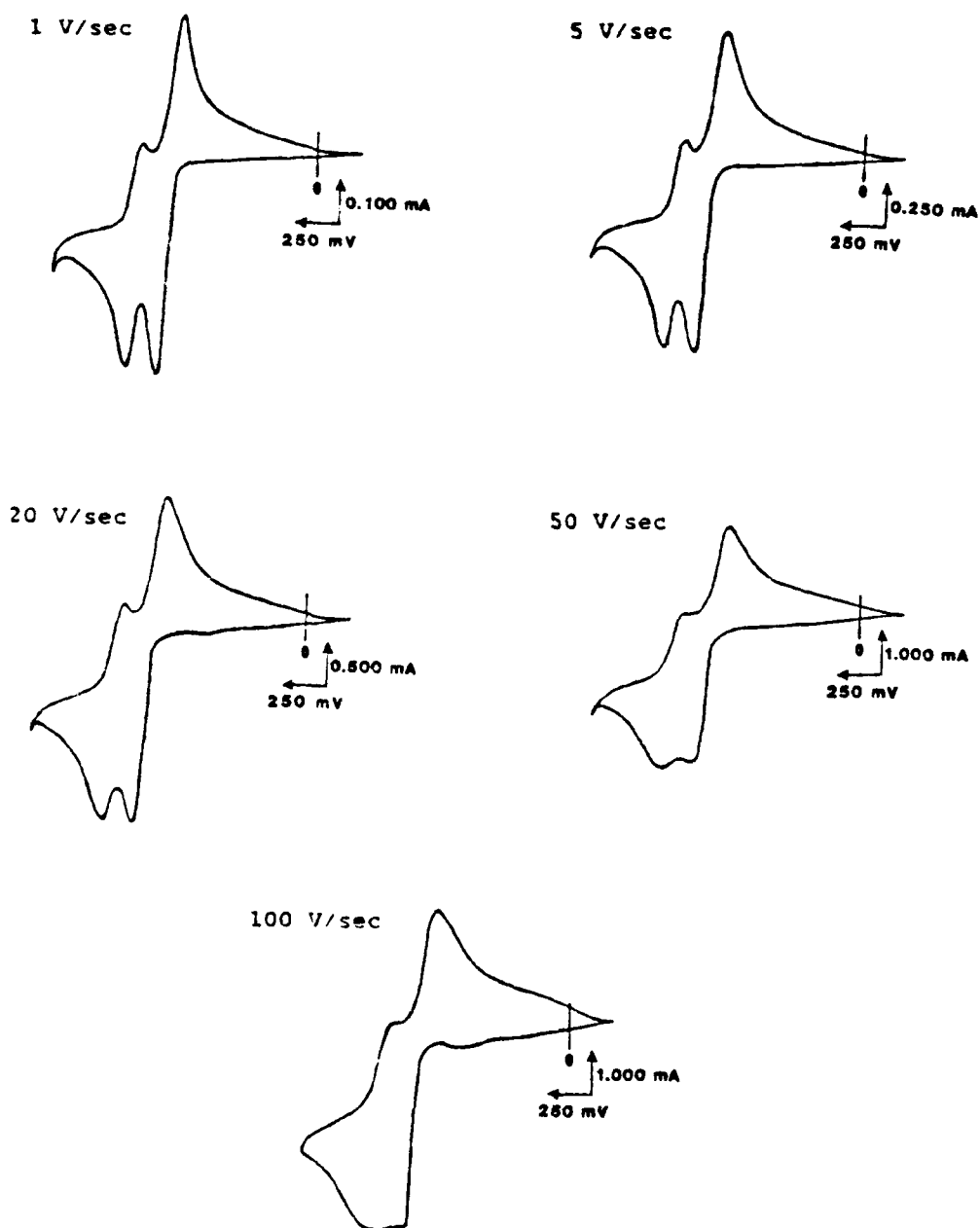
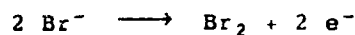


Figure 39. The CVs of an $N = 0.4900$ bromide melt at various scan rates.

to compare the two titrations, which had different initial bromine concentrations, both of the titration curves were normalized to the bromine concentrations. Figure 40 shows the two normalized titration curves.

Assuming an intermediate equilibrium constant, at any point during the titration, Br^- , Br_2 , and Br_3^- will be present in the melt. Because of the presence of these species, three couples will be responsible for the potential observed at any point in the titration. These couples are:



The three Nernst equations corresponding to the above half reactions are:

$$E = E_1^0 + \frac{RT}{nF} \ln \frac{[\text{Br}_2]}{[\text{Br}^-]^2} \quad (29)$$

$$E = E_2^0 + \frac{RT}{nF} \ln \frac{[\text{Br}_3^-]}{[\text{Br}^-]^3} \quad (30)$$

$$E = E_3^0 + \frac{RT}{nF} \ln \frac{[\text{Br}_2]^3}{[\text{Br}_3^-]^2} \quad (31)$$

Where E is the observed potential and E_1^0 , E_2^0 , and E_3^0 are the formal potentials for the corresponding electrochemical half reactions. $[\text{Br}^-]$, $[\text{Br}_3^-]$, and $[\text{Br}_2]$ are the equilibrium concentrations of the three species, and are determined from the initial concentrations of the bromide and bromine, and the equilibrium constant by the equations derived in Appendix 1. Since there are four equations (29, 30, 31, and A3) and four unknowns (E_1^0 , E_2^0 , E_3^0 , and K), a unique solution for each unknown theoretically exists. Solutions to this problem were attempted by Newton's method of linear interpolation, and by the Simplex method. The solutions were not determined, more as a result of a lack in programming ability rather than a lack in the theory.

Although the equilibrium constant was not specifically determined, a couple of comments can be made about the magnitude of the equilibrium constant. First, fitting the data to a model, in which the equilibrium constant is very large, was not successful. This would indicate the equilibrium constant is less than approximately $10^2 - 10^3$. Second, in the CVs of the basic bromide melts, the currents observed when scanning through the bromide and tribromide oxidations, are approximately equal. Assuming comparable diffusion coefficients, the concentrations of bromide and tribromide are approximately equal. This would indicate the equilibrium constant is greater than approximately 10^0 .

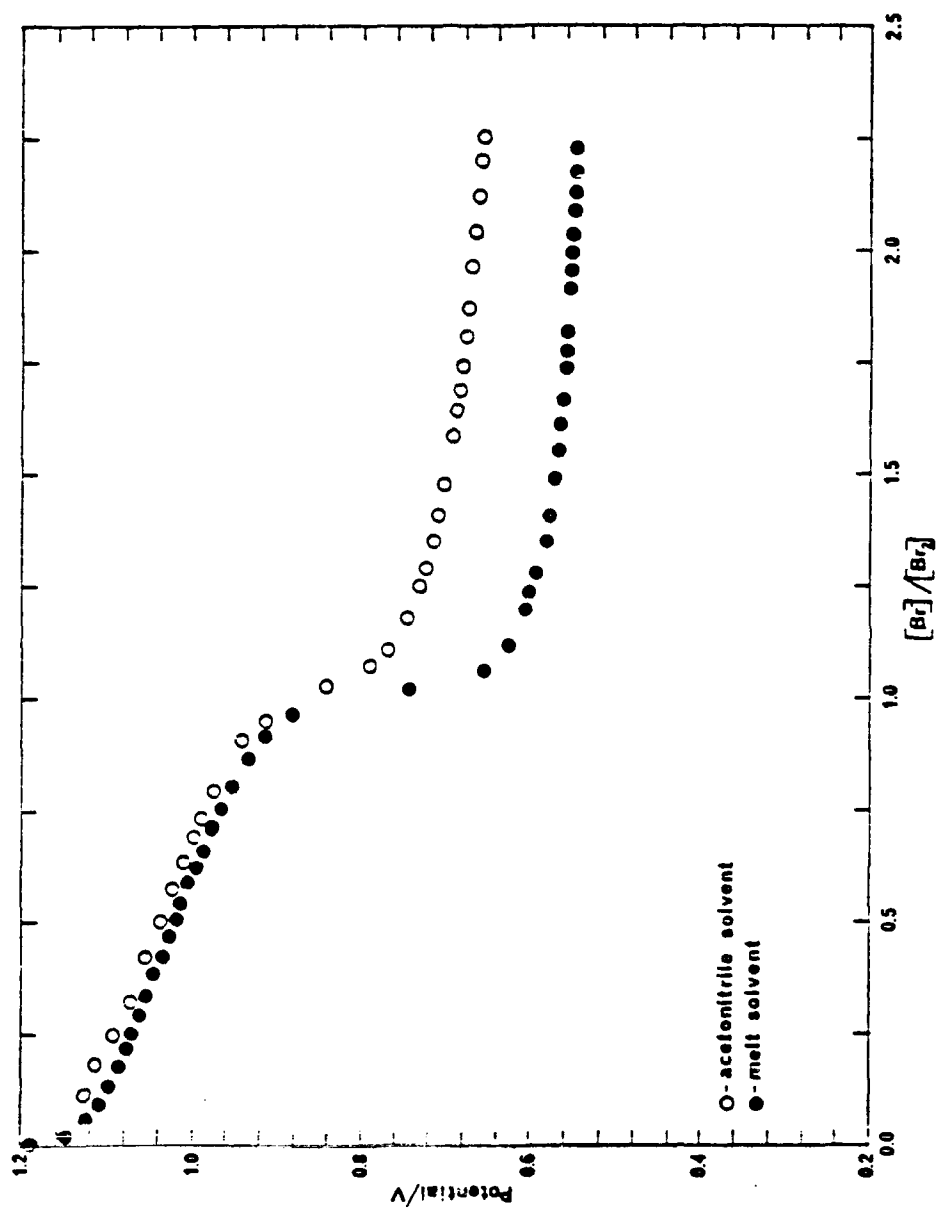


Figure 40. Normalized curves for the titration of bromine with MEIB.

Summary

Although the rate and equilibrium constants, of the chemical reaction, were not explicitly determined, it was shown that attention must be paid to the chemical parameters for some electrochemical experiments. The rate of the following reaction will limit the rate at which the potential may be scanned in linear potential sweep experiments, and affect the results of potential and current step experiments. The equilibrium constant was shown to, probably, be neither large or small enough to ignore. The equilibrium constant must be accurately known, in order to be able to explicitly define the tribromide concentration, in the region of the electrode, during the course of an electrochemical experiment. Without this knowledge, precise experiments on the electrochemical behavior of the bromide species will not be possible.

CHAPTER 6

MIXED CHLORO-BROMOALUMINATE MOLTEN SALT SYSTEMS

In the previous chapters, the bromide system was studied for the purpose of gaining an understanding of the chemical and electrochemical behavior of the bromide species in molten salt systems. With this knowledge, characterization of the electrochemistry occurring in the mixed chloro-bromoaluminate molten salt system was possible.

Two possible methods of making a mixed melt exist. In the first method, either the organic or inorganic species may be added to the melt by itself. In the second method, a chloride and bromide melt can be combined in different proportions. These methods must be assumed to be different from one another until proven otherwise.

Addition of MEIB to a Chloride melt

Figure 41 shows a series of CVs of a chloride melt to which different amounts of MEIB have been added. In the initial CV (no added MEIB), the only couple observed is the oxidation of the chloride to trichloride. Upon the initial addition of MEIB, two new couples appear. The peak potentials of the two waves are comparable to those found for the bromide and the tribromide in the pure bromide system. As the concentration of the bromide is increased, by the addition of MEIB, the peak currents of the two new couples are seen to increase, indicating they are due to the bromide species.

As shown in Chapter 4, the first wave is due to the oxidation of bromide to bromine. The second oxidative process in the mixed melt system is still due to the oxidation of the chloride to trichloride. As in the pure bromide system, the second new wave (the third wave present in the mixed system) is due to the oxidation of the product formed when the bromine formed in the first oxidation reacts with another anion.

In the case of the mixed systems, the bromine can react with the chloride anion as well as the bromide anion, to form not only Br_3^- , but also Br_2Cl^- . The third wave, in the mixed melt system, is due to the oxidation of the Br_2Cl^- and Br_3^- . In the second oxidative process, the chloride is oxidized directly to trichloride without an intermediate chemical reaction, so the possibility of forming the species BrCl_2^- is minimized.

Upon the initial addition of bromide to the chloride melt, the current due to the oxidation of the chloride to trichloride increased 36.9%, and the width of the wave decreased noticeably. There are three possible explanations for the increase in the current. First, if another species was oxidized at the same potential as the chloride, the concentration of the species being reduced would be greater, and thus the current would increase. Second, if the added bromide increased the rate of the electrode kinetics for the oxidation of chloride to chloride, the flux, and thus the observed current, would increase. Third, if the rate at which the chloride diffuses to the surface of the electrode increases, the current will increase.

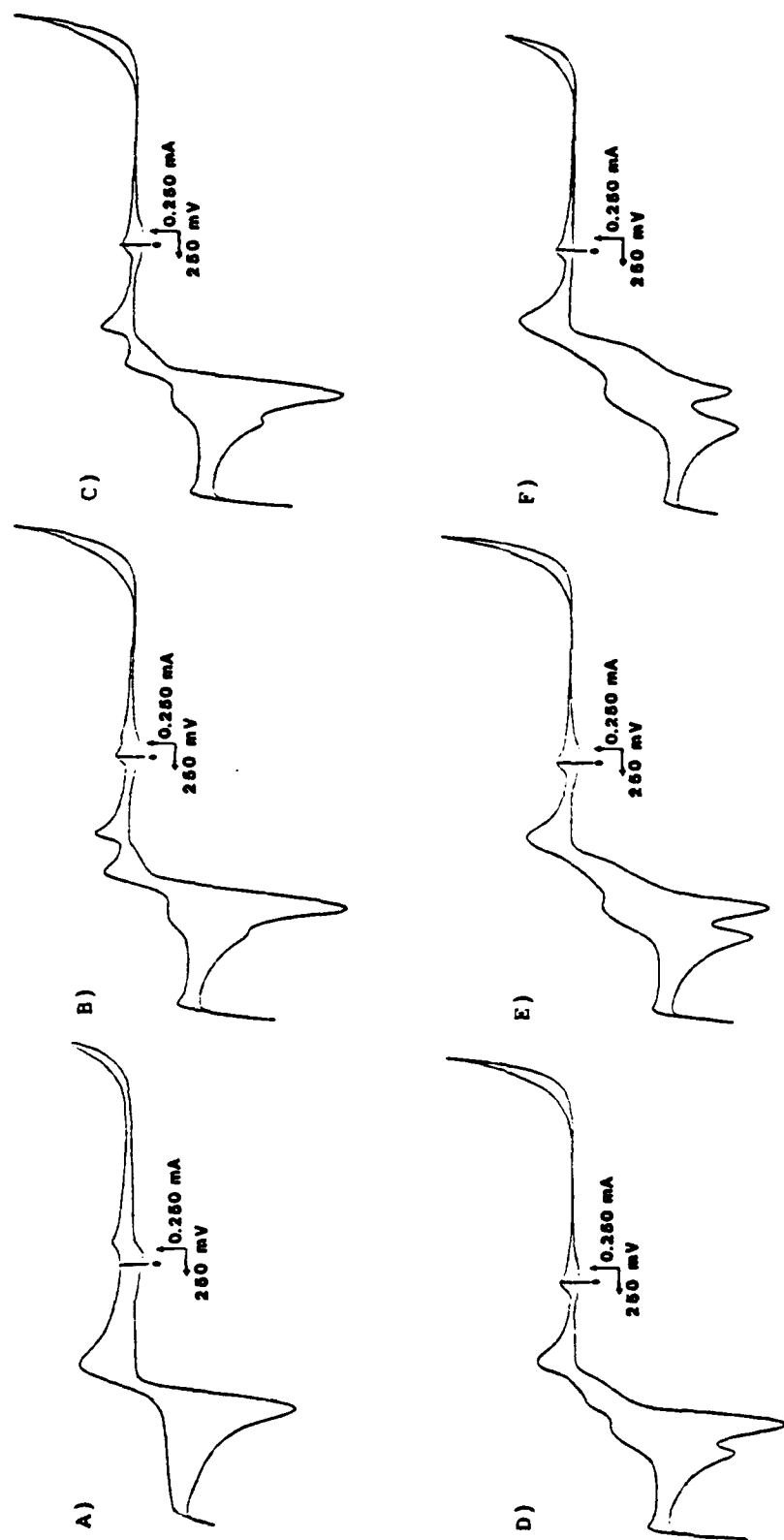


Figure 41. The CVs of A) an $N = 0.4800$ chloride melt, and B)-F) sequential additions of MEIB.

If the current increase was due to the addition of a second species, which was also oxidized at the same potential as the chloride, the current would increase upon further additions of MEIB. Not only is this not the case, but the current is seen to decrease with increasing MEIB addition. The subsequent decrease in the peak current is due to the reaction of the chloride with the bromine formed in the first oxidative process, which effectively decreased the chloride concentration in the region of the electrode.

The narrowing of the chloride oxidation wave also argues against a second electroactive species causing the increase in the peak current. It is unlikely that a species would have exactly the same oxidation potential as the chloride. Reasonably, one would expect the oxidation potentials of the chloride and the other species to vary by, at least, a few millivolts. This difference in oxidation potentials would cause the waves to become broader, instead of the narrower waves which are actually observed.

The increase in the peak current, of the second oxidation wave in the mixed system, could also be explained by an alteration in the electrode kinetics for the oxidation of the chloride. If the rate of electron transfer, from the electrode surface to the chloride ion, is increased, the rate at which chloride ions could be oxidized, and thus the current, would increase. It has been shown, though, that the rate of electron transfer in the chloride system is facile.⁴⁵ If the electron transfer is reasonably fast, a minor alteration in it should not affect the current to a large degree.

The most likely reason the peak current increases, when the MEIB is initially added, is because of an alteration in the diffusion of the chloride to the electrical double layer. If the packing of the solvation spheres around the chloride ions is altered, by the added bromide, the chloride could diffuse to the double layer faster. Faster diffusion (a larger diffusion coefficient) will increase the current due to Fick's first law (equation 15). The larger a diffusion coefficient, the faster the concentration gradient will decrease. The smaller concentration gradient results in a smaller chloride flux, and thus current.

Addition of Two Dissimilar Melts

When MEIB is added to a chloride melt, the apparent mole fraction of the inorganic species, decreases. The change in the composition might noticeably manifest itself in the electrochemistry of the system. A second method of making a mixed chloride-bromide melt is to combine two different melts of the same composition together in varying proportions. This method insures knowledge of the composition of the resulting melt.

Experimentally, an $N = 0.480$ chloride and an $N = 0.480$ bromide melt were made. A term, L , was created to indicate the percentage of the monohalide species which is chloride. An $L = 1.0$ indicates that all of the monohalide species is chloride. An $L = 0.0$ melt contains only bromide as the monohalide species.

Like the pure bromide system, any mixed melt with $L < 0.5$ was liquid only at elevated temperatures. Because of this, all of the experiments performed on the mixed melt system were run at 60°C , in order to maintain uniform conditions throughout the experiments. Figure 42 shows the CV of several melts as a function of L .

The CVs of the melt made by mixing two melts initially appear fundamentally different from those of the mixed system created by adding

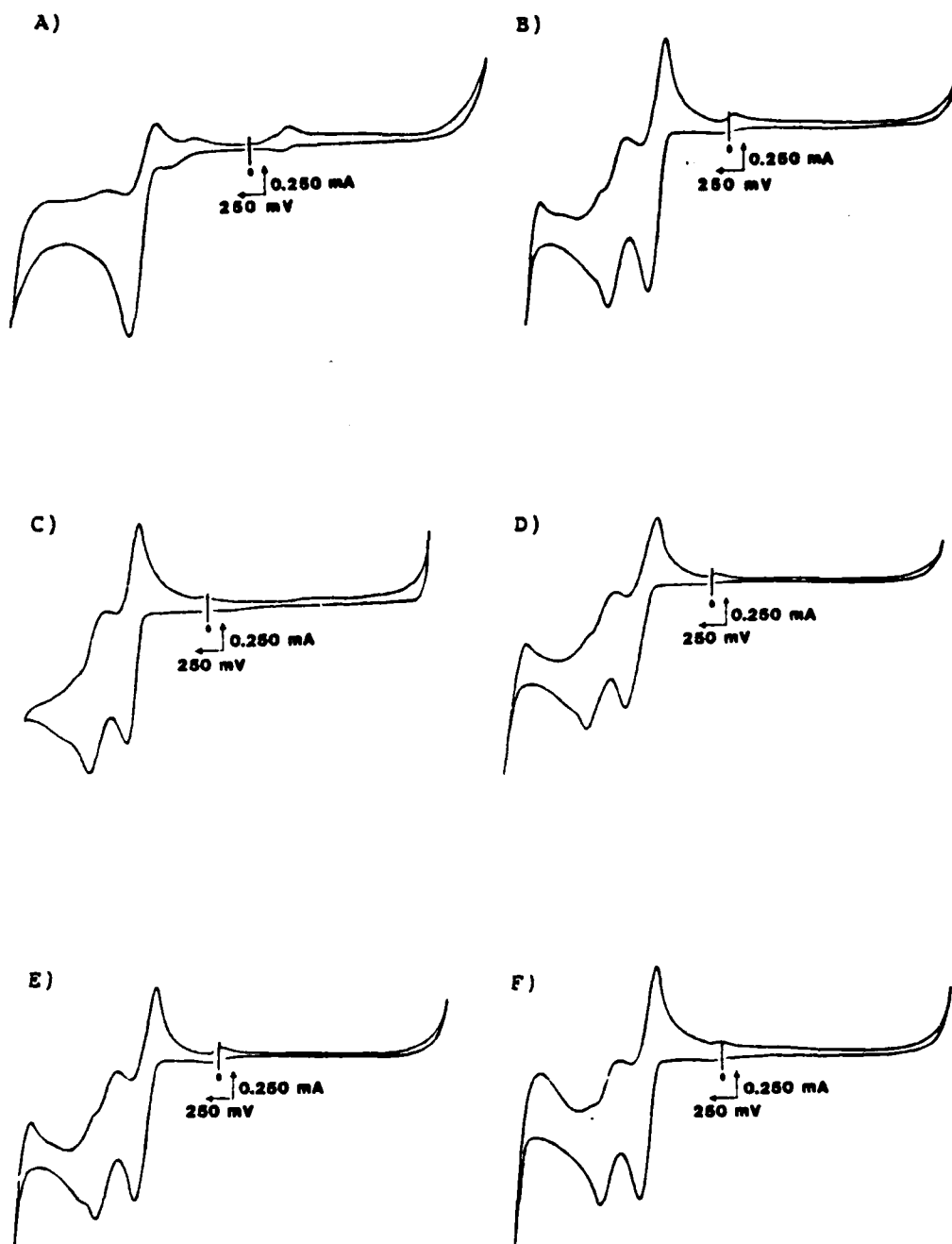


Figure 42. The CVs of an A) $L = 1.0$, B) $L = 0.8$, C) $L = 0.6$, D) $L = 0.4$, E) $L = 0.2$, and F) $L = 0.0$ mixed melt.

MEIB α phase. Throughout the range of mixtures, only two oxidation processes are observed, the peak currents of which remain fairly constant. There are two possible explanations for the differences between the two experiments.

First, the composition of composition was studied for the addition of two different melts. The composition was from $L = 0.10$ to $L = 0.90$. Even at the lowest composition of added bromide melt, the melts made from combining bromide and chloride melts have a much higher concentration of bromide ions than the melt made from adding MEIB to a chloride melt. The higher bromide concentration would tend to cause the waves for the oxidation of the chloride and trichloride to overlap, making them appear as a single oxidation. The high bromide concentration would also decrease the chloride concentration in the region of the electrode by the reaction of the chloride with the bromine formed by the oxidation of the bromide.

A second possible explanation for the differences observed between the two experiments is the presence of process equilibrating the bromide and chloride concentrations. In a method proposed by Dr. John W. Pong¹⁶, it can be seen that the free halides present in the mixed molten salt system are in exchange with the halides on the tetrahaloaluminate ion.

Figure 43 shows the ^{27}Al NMR of several melts as a function of L , for a melt made by combining a bromine and a chloride melt. It has been previously shown that the aluminum species observed in a basic melt is the tetrahaloaluminate¹⁷. It is apparent that there are five different tetrahaloaluminate species present in any mixed melt, corresponding to AlCl_4^- , AlCl_3Br , AlCl_2Br_2 , AlClBr_3 , and AlBr_4^- , with the tetrachloroaluminate shifted the farthest, and the tetrabromoaluminate shifted the least down field.

The temperature at which the two experiments were carried out varied. Figure 44 shows the ^{27}Al NMR spectra of an $L = 0.500$ melt at various temperatures. At 30 °C, the aluminum species appear well defined, indicating either no, or very little, exchange is occurring, on the NMR timescale (from Figure 44 it appears the exchange at room temperature is approximately 100 Hz). An appreciable rate of exchange, on the NMR timescale, begins only when the temperature is elevated.

The experiments where the bromide was added to a chloride melt were run at room temperature, while the experiments where the bromide and chloride melts were combined were run after holding the temperature at 60 - 100 °C for 20 hours. This would argue that the halides of the experiments where the bromide was added to the chloride melt had undergone very little exchange, while the halides of the experiments where the chloride and bromide melts were combined probably underwent exchange to completion.

The actual explanation for the differences observed for the two methods of making a melt appears to be a combination of the two explanations proposed above. Not only cause the experiments, where bromide additions were made to a chloride melt, were run at lower temperatures, and thus had very little exchange (on the NMR timescale), the lower bromide concentration allowed for the observation of the oxidation of the chloride to trichloride as a distinct process. On the other hand, the large bromide concentration and the equilibration of the halide composition, through the exchange mechanism, caused the oxidations

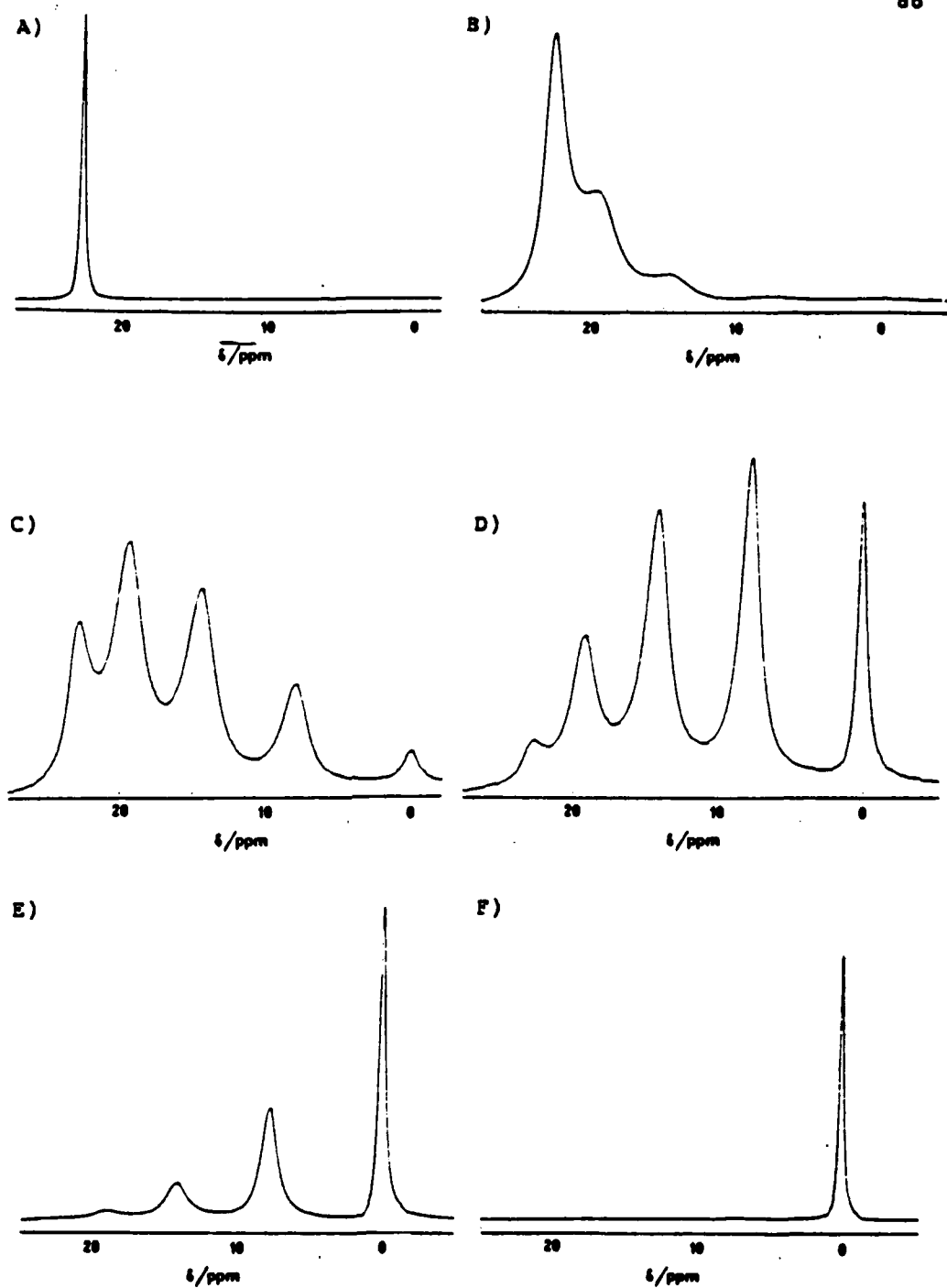


Figure 43. The ^{27}Al NMR of an A) $L = 1.0$, B) $L = 0.8$, C) $L = 0.6$, D) $L = 0.4$, E) $L = 0.2$, and F) $L = 0.0$ mixed melt.

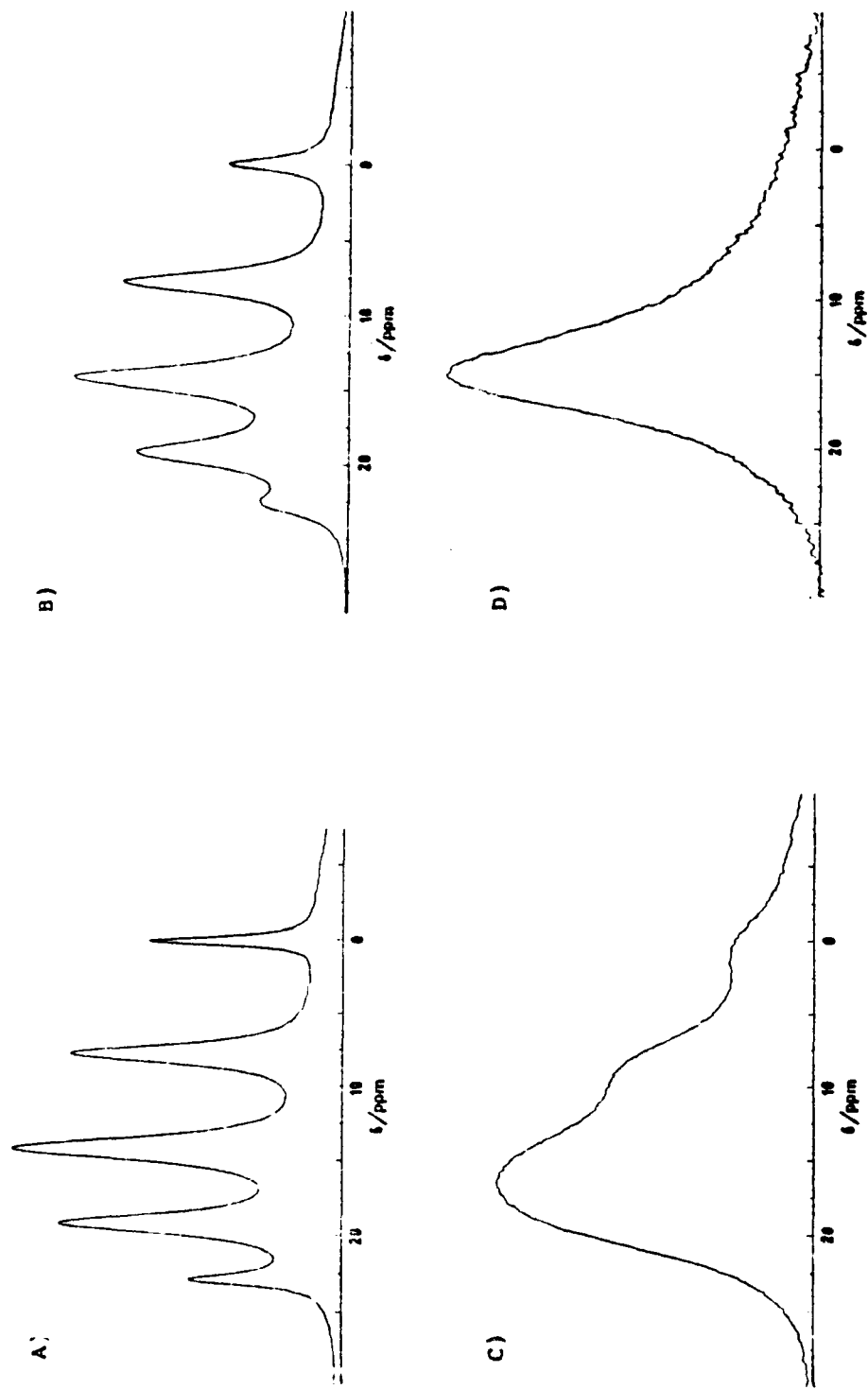


Figure 44. ^{27}Al NMR of an $L = 0.50$ mixed melt at A) 30°, B) 50°, C) 100°, and D) 150° celsius.

of bromide to bromine and chloride to trichloride to merge together, and to appear as one wave, for the experiments where the bromide and chloride melts were combined.

Summary

Because of the exchange process, the composition of the mixed melt system must be studied further. Although it was shown that exchange occurred, it was not determined what the equilibrium distributions of the products are. One of the driving factors for studying the molten salt mixtures for use as electrolytes, is the ability of the molten salts to withstand elevated temperatures. With the mixed melt system, it is apparent that at elevated temperatures, exchange will occur. As a result of the exchange process, free chloride will be present, which can subsequently be oxidized to chlorine. This chlorine can then chlorinate the imidazolium ring by the process described in Chapter 1. The importance of this chlorination process must be investigated further.

If the resulting melt is not heated, there appears to be a distinct difference between a melt made from combining a chloride and a bromide melt from a melt made from adding bromide to a chloride melt. If, on the other hand, the melt is to be used at an elevated temperature, or the melt is to be warmed during the preparation, there is no difference between the two methods of making the melt.

BIBLIOGRAPHY

1. Hurley, Frank H.; U.S. Patent 2,446,331 February 14, 1944.
2. Wier, Thomas P.; Hurley, Frank H.; U.S. Patent 2,446,349 February 29, 1944.
3. King, L. A.; Brown, A. D.; Frayer, F. H.; Proceedings of the OAR Research Applications Conference March 21, 1968.
4. Nardi, John C.; Hussey, Charles L.; King, Lowell A.; U.S. Patent 4,122,245 October 24, 1978.
5. Lawrence, Lovell Jr.; "Earth Satellites as Research Vehicles", Monograph #2, Journal of the Franklin Institute, Lancaster Press Inc., Lancaster PA. April 18, 1956, pp 89-99.
6. Donahue, Francis M.; FJSRL-TM-84-0002 1984 Frank J. Seiler Research Laboratory (AFSC), U. S. Air Force Academy.
7. Wilkes, John S.; Levisky, Joseph A.; Wilson, Robert A.; Hussey, Charles L.; Inorg. Chem. 1982 21 1263-1264.
8. Popov Alexander I.; Geske, David H.; J. Am. Chem. Soc. 1958 80 5346-5349.
9. Desbene-Monvernay, Annie; Berthelot, Jacques; Desbene, Paul-Louis; J. Chem. Ed. 1987 64 86-87.
10. Adanuvor, P. K.; White, R. E.; J. Electrochem. Soc. 1987 134 1450-1454.
11. Mastragostino, Marina; Valcher, Sergio; Electrochim. Acta 1983 28 501-505.
12. Eustace, Daniel J.; J. Electrochem. Soc. 1980 127 528-532.
13. Donahue, Francis M.; FJSRL-TM-84-0002 1984 Frank J. Seiler Research Laboratory (AFSC), U. S. Air Force Academy.
14. Reynolds, G. F.; Unpublished results 1985
15. Wilkes, John S.; Levisky, Joseph A.; FJSRL-TR-81-0001 1981 Frank J. Seiler Research Laboratory (AFSC), U.S. Air Force Academy.

16. Chattaway, Frederick Daniel; Hoyle, George; J. Am. Chem. Soc. 1923 45 654-662.
17. Alfa Catalog 1986 p552.
18. Buckles Robert E.; Popov, Alexander I.; Zelezny, William F.; Smith, Robert J.; J. Am. Chem. Soc. 1951 73 4525-4528.
19. Dymek, C. J. Jr.; Williams, J. L.; Groeger, D. J.; Auburn, J. J.; J. Electrochem. Soc. 1984 131 2887-2892.
20. Lipsztajn, M.; Osteryoung, R. A.; J. Electrochem. Soc. 1983 130 1968-1969.
21. Fannin, Armand A. Jr.; Floreani, Danilo A.; King, Lowell A.; Landers, John S.; Piersma, Bernard J.; Stech, Daniel J.; Vaughn, Robert L.; Wilkes John S.; Williams, John L.; J. Phys. Chem. 1984 88 2614-2621.
22. Sanders, John R.; Ward, John R.; Hussey, Charles L.; J. Electrochem. Soc. 1987 133 325-330.
23. Hussey, Charles L.; Sanders, John R.; J. Electrochem. Soc. 1987 134 1977-1980.
24. Bard, Allen J.; Faulkner, Larry R.; Electrochemical Methods; John Wiley & Sons:New York, 1980, p. 160.
25. Chrysosoulakis, Yannis; Pognet, Jean-Claude; Manoli, Georgia; Journal of Applied Electrochemistry 1987 17 857-867.
26. Bard, Allen J.; Faulkner, Larry R.; Electrochemical Methods; John Wiley & Sons:New York, 1980, p. 219.
27. Ibid. p. 223
28. Ibid. p. 225
29. Ibid. p. 91
30. Ibid. p. 105
31. Ibid. p. 106
32. Iwasita, T.; Giordano, M. C.; Electrochim. Acta 1969 14 1045-1059.
33. Bard, Allen J.; Faulkner, Larry R.; Electrochemical Methods; John Wiley & Sons:New York, 1980, p. 288.
34. Ibid. p. 143

35. Mastragostino, Marina; Valcher, Sergio; Lazzari, Paola;
J. Electroanal. Chem. 1981 125 189-198.
36. Lipsztajn, Marek; Osteryoung, Robert A.; Inorg. Chem. 1984
23 1735-1739.
37. Dieter, Kenneth M.; Dymek, Chester J. Jr.; Heimer, Norman
E.; Rovang, John W.; Wilkes, John S.; J. Am. Chem. Soc.
1988 110 2722-2726.
38. Bond, Alan M.; Henderson, Terry L. E.; Oldham, Keith B.;
J. Electroanal. Chem. 1985 191 75-90.
39. Nicholson, Richard S.; Anal. Chem. 1965 37 1351-1355.
40. Oldham, Keith B.; Anal. Chem. 1972 44 196-198.
41. Grenness, Morton; Oldham, Keith B.; Anal. Chem. 1972 44
1121-1129.
42. Goto, Masashi; Oldham, Keith B.; Anal. Chem. 1973 45
2043-2050.
43. Bard, Allen J.; Faulkner, Larry R.; Electrochemical Methods;
John Wiley & Sons: New York, 1980, p. 96.
44. Mastragostino, Marina; Gramellini, Carla; Electrochim. Acta
1985 30 373-380.
45. Wilkes, John S.; Private Communication 1988.
46. Rovang, John W.; Unpublished work, 1988.
47. Wilkes, John S.; Frye, James S.; Reynolds, G. Fredric;
Inorg. Chem. 1983 22 3870-3872.

APPENDIX 1

The mass balance equations of the chemical reaction are:

$$[\text{Br}^-] = [\text{Br}^-]' - [\text{Br}_3^-] \quad (\text{A1})$$

$$[\text{Br}_2] = [\text{Br}_2]' - [\text{Br}_3^-] \quad (\text{A2})$$

where $[\text{Br}^-]$, $[\text{Br}_3^-]$, and $[\text{Br}_2]$ are the equilibrium concentrations of the species and $[\text{Br}^-]'$, and $[\text{Br}_2]'$ are the initial concentrations. The equilibrium constant is given by the equation

$$K = \frac{[\text{Br}_3^-]}{[\text{Br}^-] [\text{Br}_2]} \quad (\text{A3})$$

Substituting equation A1 into equation A3 and rearranging gives:

$$[\text{Br}^-] = \frac{[\text{Br}^-]'}{(1 + K [\text{Br}_2])} \quad (\text{A4})$$

Similarly, equation A2 and equation A3 gives:

$$[\text{Br}_2] = \frac{[\text{Br}_2]'}{(1 + K [\text{Br}^-])} \quad (\text{A5})$$

Substituting equation A4 into equation A5 and rearranging gives:

$$K [\text{Br}^-]^2 + (1 + K [\text{Br}_2]' - K [\text{Br}^-]') [\text{Br}^-] - [\text{Br}^-]' = 0 \quad (\text{A6})$$

Solving the quadratic for $[\text{Br}^-]$ and rearranging gives:

$$[\text{Br}^-] = \frac{K([\text{Br}^-]' - [\text{Br}_2]') - 1}{2K} + \frac{[1 + 2K([\text{Br}^-]' + [\text{Br}_2]') + K^2([\text{Br}_2]' - [\text{Br}^-]')^2]^{\frac{1}{2}}}{2K} \quad (\text{A7})$$

Substituting equation A7 into equation A5 gives:

$$[\text{Br}_2] = \frac{[\text{Br}_2]'}{1 + \frac{K([\text{Br}^-]' - [\text{Br}_2]') - 1}{2}} + \frac{[1 + 2K([\text{Br}^-]' + [\text{Br}_2]') + K^2([\text{Br}_2]' - [\text{Br}^-]')^2]^{\frac{1}{2}}}{2} \quad (\text{A8})$$

Substituting equation A7 into equation A1 and rearranging gives:

$$[\text{Br}_3^-] = [\text{Br}^-]' - \frac{K([\text{Br}^-]' - [\text{Br}_2]') - 1}{2K} + \frac{[1 + 2K([\text{Br}^-]' + [\text{Br}_2]') + K^2([\text{Br}_2]' - [\text{Br}^-]')^2]^{\frac{1}{2}}}{2K} \quad (\text{A9})$$